

University of Alberta

**Development of a Non-viral Delivery System for siRNA in Treatment of
Lymphoma**

by

Basak Sahin

A thesis submitted to the Faculty of Graduate Studies and Research
in partial fulfillment of the requirements for the degree of

Master of Science

in

Biomedical Sciences

Biomedical Engineering

©Basak Sahin

Fall 2013

Edmonton, Alberta

Permission is hereby granted to the University of Alberta Libraries to reproduce single copies of this thesis and to lend or sell such copies for private, scholarly or scientific research purposes only. Where the thesis is converted to, or otherwise made available in digital form, the University of Alberta will advise potential users of the thesis of these terms.

The author reserves all other publication and other rights in association with the Copyright © in the thesis and, except as herein before provided, neither the thesis nor any substantial portion thereof may be printed or otherwise reproduced in any material form whatsoever without the author's prior written permission.

Acknowledgements

I would like to thank my committee members Drs. Michael Weinfeld, Afsaneh Lavasanifar, and Hasan Uludag.

The scholarships and awards that allowed me to complete this thesis was provided by the Womens and Children's Health Research Institute (WCHRI) Graduate Studentship, Faculty of Medicine & Dentistry (FoMD) 75th Anniversary Award and my supervisor's grants.

I would like to thank Dr. Hamidreza Aliabadi and Cezary Kucharski for their help in siRNA library screenings, and suggestions regarding several procedures used in this study; Perveen Mehdipoor for her help in all PCR related experiments; Drs. Remant Bahadur and Hamidreza Aliabadi for providing lipid-conjugated PEI; and Dr. Hilal Gul-Uludag for her helpful suggestions about this thesis.

I thank all the members of the Uludag Lab for their kindness, assistance, and friendship: Hilal Gul-Uludag, Hamidreza Aliabadi, Perveen Mehdipoor, Cezary Kucharski, Breanne Landry, Laura Rose, Juliana Valencia Serna, Rahul Agrawal.

I also thank the community and residence of International House Alberta for their support, friendship and kindness as well as providing a productive and encouraging environment through my thesis writing process.

Lastly and most importantly, I would like to thank Dr. Hasan Uludag for all his time and effort to assist and guide me through my masters and thesis. I am very grateful.

Table of Contents:

1. Scope	1
2. Introduction	3
2.1. Hematopoiesis and cancers of blood cells	3
2.1.1. Non-Hodgkin Lymphomas	6
2.1.2. Current therapies for lymphoma	8
2.1.3. Cutaneous T-cell lymphoma (CTCL)	11
2.1.4. CTCL cell lines	15
2.2. RNA interference (RNAi)	16
2.3. Current therapies using RNAi and delivery methods	18
2.3.1. Viral vectors	19
2.3.2. Non-viral vectors	21
2.3.3. Nanoparticles	22
2.3.4. Lipid based delivery systems for siRNA	23
2.3.5. Polymer based delivery systems for siRNA	25
2.3.5.1. Polyethylenimine (PEI)	27
2.3.5.2. Hydrophobic lipid substitution on PEI	28
2.3.6. siRNA for treatment of leukemia and lymphoma	29
2.4. GFP as a reporter gene	31
3. Materials and Methods	33
3.1. Cell lines	34
3.2. Cell culture	35
3.3. Engineered PEI Polymers	35
3.4. siRNA Complex formation	37
3.5. GFP silencing	40
3.6. Flow cytometry analysis	40
3.7. Cytotoxicity assays	41
3.7.1. AlamarBlue® assay	42
3.7.2. Trypan Blue Assay and Cell Counting	42
3.7.3. FlowTACS™ Apoptosis Detection	43

3.7.4. FITC Annexin V Apoptosis Detection	43
3.8. Statistical Analysis	44
4. Results and Discussion	46
Part I: GFP Silencing with Lipid-modified PEI	46
4.1. FAM-labelled siRNA uptake	46
4.2. Polymer library screening	48
4.3. Time course response to GFP siRNA	52
4.4. Response to Multiple anti-GFP siRNA Treatments	55
4.5. FAM-labelled siRNA uptake in Jurkat cells	58
4.6. GFP silencing in Jurkat cells	60
4.7. Effect of complex formation volume	62
4.8. Effect of continuous shaking	64
4.9. Effect of centrifugation	67
4.10. Effect of Extent of Lipid Substitution	71
4.11. Polymer Toxicity	73
Part II: Endogenous Gene Silencing	76
4.12. Screening Select Targets for Silencing	76
4.12.1. Cell Viabilities Based on AlamarBlue® Assay	78
4.12.2. Cell Viabilities Based on Trypan Blue Assay	81
4.13. PI3K dose response	82
4.14. Silencing PI3K for Apoptosis Induction	84
4.15. Silencing CDK18 Over 9 Days	86
4.16. CDK18 silencing over 3 days and apoptosis	87
5. Conclusions and Future	92
6. References	96

List of Tables:

Table 1 Estimated new cases and deaths for cancers by sex, Canada, 2011

Table 2 Types of non-Hodgkin lymphomas.

Table 3 Characteristic primary gene aberrations in select B- and T-cell lymphoma subtypes.

Table 4 Cancer related genes mapped to the chromosomal areas with high rates of chromosomal irregularities in CTCL.

Table 5 Non-viral delivery methods for siRNA.

Table 6 Examples of the studies using RNAi for treatment of leukemia and lymphomas

Table 7 Table of lipid substituted PEI showing the lipid substitution ratios per PEI backbone.

Table 8 Preparation of siRNA-Polymer complexes, concentrations, volumes and amounts for 25nM siRNA concentration in tissue culture medium and siRNA:polymer ratios 1:4 and 1:8.

Table 9 Information about the cytotoxic siRNAs used.

Table 10 Names, symbols and functions of the endogenous genes targeted in Hut78 cells.

List of Figures:

Figure 1 Differentiation of hematopoietic stem cells into mature blood cells.

Figure 2 Schematic diagram of silencing with RNAi. Mechanism.

Figure 3 Schematic diagram of a viral vector.

Figure 4 Schematic diagrams of liposomes with different attributes.

Figure 5 Chemical structure of linear polyethylenimine (PEI), branched PEI, poly(lactic-co-glycolic acid) (PLGA), chitosan, and β -cyclodextrin.

Figure 6 X-ray crystal structure of Aequorea GFP (PDB code 1W7S) in two projections.

Figure 7 Guideline for method development.

Figure 8 GFP positive Hut78 cells, with phase contrast and with green fluorescence filter.

Figure 9 The structure of branched 2 kD PEI.

Figure 10 Lipids used for substitution to PEI adapted from.

Figure 11 A schematic representation of preparation of siRNA-Polymer complexes

Figure 12 Overlaid histograms for GFP silencing in Hut78 cells.

Figure 13 FAM-labeled siRNA uptake by Hut78 cells.

Figure 14 Percentage of Hut78 cells outside the main GFP peak and percent decrease in mean GFP fluorescence 72 hours after treatment with anti-GFP siRNA complexes.

Figure 15 Correlation between the percentage of silenced Hut78 cells and mean GFP fluorescence.

Figure 16 Percentage of Hut78 cells outside the main GFP peak and percent decrease in mean GFP fluorescence 24, 48 and 72 hours after treatment with anti-GFP siRNA complexes.

Figure 17 Effect of repeated treatments of cell with siRNA:polymer complexes.

Figure 18 FAM-labeled siRNA uptake by Jurkat cells.

Figure 19 Percentage of Jurkat cells silenced and percent GFP silencing 72 hours after treatment with anti-GFP siRNA complexes.

Figure 20 Effect of complex formation volume.

Figure 21 Effect of shaking.

Figure 22 Effect of centrifugation I.

Figure 23 Effect of centrifugation II.

Figure 24 Effect of the extent of lipid substitution.

Figure 25 Polymer toxicity.

Figure 26 Percentage of viable Hut78 cells after treatment with selected siRNAs and 2PEI-CA1-4, 2PEI-LA1-4 and Lipofectamine®RNAiMAX complexes at siRNA:carrier ratio 1:4.

Figure 27 Percentage of viable Hut78 cells after treatment with selected siRNA complexes at siRNA:polymer ratio 1:4.

Figure 28 Percentage of viable Hut78 cells after treatment with PI3K siRNA.

Figure 29 Percentage of apoptotic Hut78 cells after treatment with PI3K siRNA.

Figure 30 Percentage of viable Hut78 cells after treatment with CDK18 siRNA.

Figure 31 Percentage of viable Hut78 cells after treatment with CDK18 siRNA.

Figure 32 Percentage of early apoptotic and apoptotic Hut78 cells after treatment with CDK18 siRNA.

List of Abbreviations:

AGO	:	Argonaute
ALCL	:	Anaplastic large cell lymphoma
ALL	:	Acute Lymphoblastic Leukemia
ALP	:	Alkaline phosphatase
AML	:	Acute Myelogenous Leukemia
CA	:	Caprylic Acid
CCP	:	Cell membrane permanent peptide
CD	:	Cyclodextrin
CDK	:	Cyclin dependent kinase
CLL	:	Chronic Lymphocytic Leukemia
CLP	:	Common Lymphoid Progenitor
CML	:	Chronic Myelogenous Leukemia
CMP	:	Common Myeloid Progenitor
csiRNA	:	Control siRNA
CTCL	:	Cutaneous T-cell Lymphoma
CXCR	:	Chemokine receptor
DLBL	:	Diffuse large B-cell lymphoma
DMSO	:	Dimethyl sulfoxide
DNA	:	Deoxyribonucleic Acid
DOPC	:	Dioleylphosphatidyl choline
DOPE	:	Dioleylphosphatidyl ethanolamine
DOTAP	:	1,2-dioleoyl-3-trimethylammonium-propane
DOTMA	:	N-[1-(2,3-dioleoyloxy) Propyl]- N,N,N trimethyl ammonium chloride
EBV	:	Epstein-Barr Virus
ECM	:	Extra Cellular Matrix
FAM	:	Carboxyfluorescein
FBS	:	Fetal bovine serum
FDA	:	Food and Drug Administration
FITC	:	Fluorescein isothiocyanate
FLT	:	Fms-related tyrosine kinase
FR	:	Folate receptor
GFP	:	Green fluorescent protein
GFP	:	Green Fluorescent Protein
GlcN	:	D-glucosamine
GlcNAc	:	N-acetyl(-D-glucosamine)
HA	:	Hyaluronic acid
HBSS	:	Hank's balanced salt solution
HL	:	Hodgkin Lymphoma

HRS	:	Hodgkin and Reed-Sternberg
HSC	:	Hematopoietic Stem Cell
IL	:	Interleukin
KSP	:	Kinesin spindle protein
LA	:	Linoleic Acid
LCP	:	Lipid-calcium-phosphate
LPD	:	Lipid-protamine-DNA
LT-HSC	:	Late Hematopoietic Stem Cell
MA	:	Myristic Acid
MAP	:	Mitogen activated protein
MCL	:	Mantle cell lymphoma
MF	:	Mycosis fungoides
miRNA	:	Micro RNA
MoMLV	:	Moloney murine leukemia virus
MPP	:	Multipotent Progenitor
mRNA	:	Messenger RNA
MSCV	:	Mouse stem cell virus
MTT	:	3-(4,5-Dimethylthiazol-2-yl)-2,5-diphenyltetrazolium bromide
NHL	:	Non-hodgkin Lymphoma
NK	:	Natural Killer
NP	:	Nanoparticle
OA	:	Oleic Acid
PA	:	Palmitic Acid
pDNA	:	Plasmid DNA
PEG	:	Polyethylene Glycol
PEI	:	Polyethylenimine
PI	:	Propidium iodide
PI3K	:	Phosphatidylinositol-4,5-biphosphate-3-kinase
PLGA	:	Poly(Lactic-co-glycolic acid)
PLL	:	Poly-L-Lysine
PS	:	Phosphatidyl serine
RISC	:	RNA induced silencing complex
RNA	:	Ribonucleic Acid
RNAi	:	RNA interference
RPS	:	Ribosomal protein S
SA	:	Stearic Acid
siRNA	:	short interfering RNA
SL	:	Stealth liposome
SLN	:	Solid lipid NP

SLNP	:	Solid lipid NP
SNALP	:	Stable nucleic acid lipid particle
SS	:	Sézary Syndrome
STAT	:	Signal transducer and activator of transcription
TCR	:	T-cell receptor
TdT	:	Terminal deoxynucleotide transferase
TfR	:	Transferrin receptor
TNF	:	Tumor necrosis factor
UV	:	Ultra violet

1. Scope

The focus of this thesis is to develop an effective non-viral, polymer-based carrier and to identify suitable gene targets that would reduce cell growth specifically in lymphoma cells upon down-regulation with short interfering RNA (siRNA).

This thesis consists of two main parts; for the first part, GFP expressing Hut78 cells (a human cutaneous T-cell lymphoma model) have been used to identify a suitable carrier for siRNA delivery by using an anti-GFP siRNA as a model siRNA. GFP was used as a target initially due to the ease of quantification of its silencing by flow cytometry and the ability to detect minor changes. Several polymer conjugates composed 2 kDa Polyethylenimines (PEI) and lipids such as Caprylic acid (CA, C8:0), Myristic acid (MA, C14:0), Palmitic acid (PA, C16:0), Stearic acid (SA, C18:0), Oleic acid (OA, C18:1) and Linoleic acid (LA, C18:2) at different levels of substitutions have been investigated for siRNA delivery. They have been evaluated against commercial reagents as well as the 25 kDa PEI, which is considered to be a generally effective carrier accompanied with a high cytotoxicity due to its disruptive effect on the cell membrane. The main idea was to find a lipid that when conjugated to non-toxic but also ineffective 2 kDa PEI would increase the silencing efficiency to a level comparable, or ideally superior to, 25 kDa PEI while keeping the toxicity relatively lower.

After selecting the most appropriate carrier for siRNA delivery in Hut78 cells, several strategies such as changing the complex formation conditions, shaking or centrifuging the cells with the complexes to increase the chances of encounter with the complexes were explored to increase the efficiency and optimize the method for GFP silencing. As the treatment is aimed to be used in a more generalized group of leukemia and lymphomas, a cell line similar to Hut78 cells, namely Jurkat (Adult T-cell Leukemia/Lymphoma) that also belongs to the same group of Cutaneous T-cell and NK-cell lymphomas, was used to compare the efficiency of the method in these cells.

The toxicity of the most promising carriers was investigated using cell viability assays. The in-house carriers were also compared to 2 kDa PEI and 25 kDa PEI, alongside Lipofectamine® RNAiMAX, in terms of their toxicity as a response to increasing doses

and concentration of the carrier. 2 kDa PEI was considered the non-toxic control, while 25 kDa PEI was considered a highly toxic control, and Lipofectamine®RNAiMAX was used as a commercial control.

Following the optimization of the method with GFP-expressing cells, for the second part of the thesis, I explored several therapeutic siRNAs that were obtained from commercial siRNA libraries, the literature search and using promising siRNAs available in the Uludag Lab. The siRNAs were delivered to wild-type Hut78 cells to identify suitable gene targets whose silencing would result in decreased cell viability and an inhibition of cell growth. For this purpose, several lymphoma or cancer related genes were screened. The possible targets were further investigated using more extensive dose-response ‘validation’ studies. Finally, apoptosis assays were performed on the targets that have promising results from the dose response studies.

2. Introduction

2.1. Hematopoiesis and cancers of blood cells

Blood is one of the most rapidly replaced tissues in the body. The undifferentiated **hematopoietic stem cell (HSC)** found in the bone marrow gives rise to all of the different types of blood cells (**Figure 1**). The multi/pluripotent and most primitive stem cell in the bone marrow is called **long term HSC (LT-HSC)**, and does not proliferate under normal conditions but can respond to various factors such as stress, blood loss or low oxygen environment. LT-HSC gives rise to a short-term version called **short term HSC (ST-HSC)**, which in turn gives rise to **multipotent progenitors (MPP)**. MPPs then give rise to two different types of progenitor cells, **common myeloid progenitor (CMP)** and **common lymphoid progenitor (CLP)** cells [1].

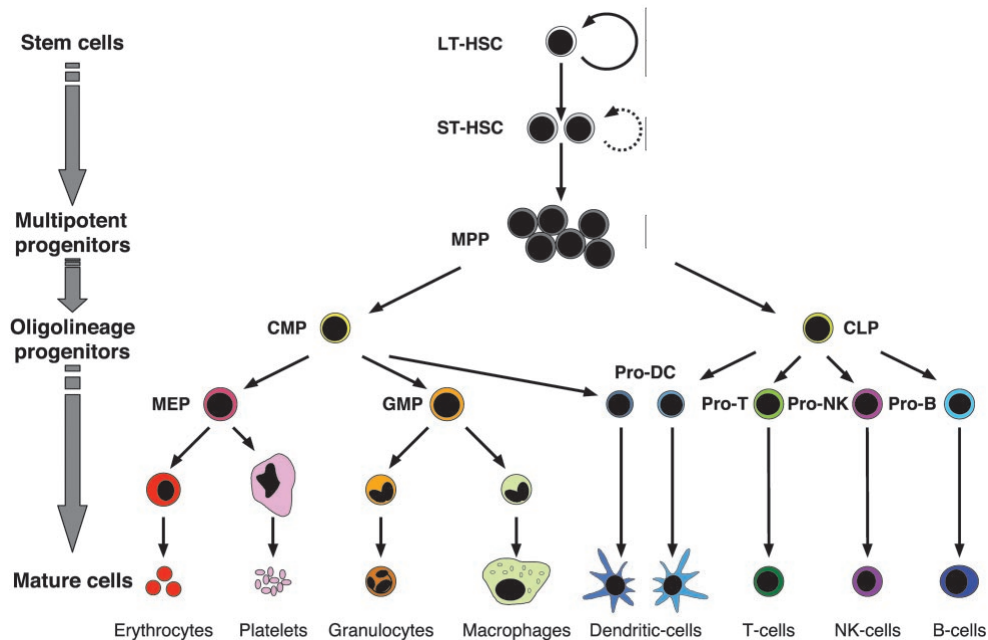


Figure 1 Differentiation of hematopoietic stem cells into mature blood cells, Reproduced with permission from: Passegué E. et al, PNAS, 2003 [2] Copyright © 2003 National Academy of Sciences, U.S.A.

The progeny of CMP and CLP differentiates into mature circulating blood cells. The myeloid lineage gives rise to erythrocytes, platelets, granulocytes and macrophages, while the lymphoid lineage gives rise to T-cells, B-cells and Natural Killer (NK) cells.

Dendritic cells can originate from both lineages. Circulating blood cells, the majority of which cannot proliferate, have varying life-spans, such as polymorphonuclear cells that only live for a few days, erythrocytes that survive for months and lymphocytes that survive for days to years [1].

A genetic change, such as genetic rearrangements, changes in the gene expression or epigenetic changes, in a single cell that produces progeny and that continues to proliferate unchecked and/or does not die as programmed is a major cause of blood cancers, such as leukemia, lymphoma, and myeloma [3,4]. This means that the original malignant cell is the multi/pluripotent tumor stem or progenitor cell with the capacity to differentiate into multiple types of stem cells [2]. The stage of maturation arrest (differentiation) of the cells and the nature of the genetic change determine the nature and growth rate of the blood cancers [2]. The genetic change can cause either cell proliferation or cell death and the nature of this change determines the type of cancer, whether leukemia or lymphoma. However, even if the genetic lesion occurs in the stem cells, sometimes the effect of the gene is not manifested until the gene promoter is activated during the maturation. Thus, the growth characteristics of the tumor are determined by the stage of the maturation of the affected cell [2]. The types of blood cancers can be summarized as follows:

Leukemia is the cancer of cells in the blood system. According to their origin, myelogenous leukemias develop from abnormal myeloid cells and lymphocytic leukemias develop from abnormal lymphoid cells. Also according to the course of disease, acute leukemia starts suddenly, developing within days or weeks, while chronic leukemias develop slowly over months or years. The four main types of leukemia are:

- acute lymphoblastic leukemia (ALL)
- acute myelogenous leukemia (AML)
- chronic lymphocytic leukemia (CLL)
- chronic myelogenous leukemia (CML)

Lymphoma is the cancer of cells in the lymphatic system such as lymph nodes,

spleen, thymus and tissues. Two main types of lymphoma are Hodgkin and non-Hodgkin lymphomas that are differentiated via the presence of a single cell type, called the Hodgkin and Reed-Sternberg (HRS) cells present in the Hodgkin lymphoma [5]. There are about 30 different non-Hodgkin lymphomas, which are going to be explained in the following section in detail.

Myeloma is clonal proliferation of malignant plasma cells that overpopulate bone marrow and cause anemia, spread to solid part of bone and cause pain or fractures, or cause mineral imbalance [6]. The disease is called multiple myeloma because it affects many bones.

Table 1 Estimated new cases (on the left) and estimated deaths (on the right) for cancers by sex, Canada, 2011 (Canadian Cancer Statistics, 2011)

	New Cases				Deaths		
	Total*	M	F		Total*	M	F
All Cancers	177,800	93,000	84,800	All Cancers	75,000	39,900	35,100
Prostate	25,500	25,500	—	Lung	20,600	11,300	9,300
Lung	25,300	13,200	12,200	Colorectal	8,900	5,000	3,900
Breast	23,600	190	23,400	Breast	5,100	55	5,100
Colorectal [†]	22,200	12,500	9,700	Prostate	4,100	4,100	—
Non-Hodgkin Lymphoma	7,700	4,200	3,400	Pancreas	3,800	1,900	1,950
Bladder [‡]	7,200	5,400	1,800	Non-Hodgkin Lymphoma	3,000	1,700	1,350
Thyroid	5,700	1,200	4,500	Leukemia	2,500	1,450	980
Melanoma	5,500	3,100	2,500	Bladder	1,850	1,300	520
Kidney	5,100	3,100	1,950	Esophagus	1,850	1,450	410
Leukemia	5,000	3,000	2,100	Stomach	1,800	1,150	680
Body of Uterus	4,700	—	4,700	Brain	1,800	1,050	750
Pancreas	4,100	2,000	2,100	Ovary	1,750	—	1,750
Oral	3,600	2,400	1,200	Kidney	1,650	1,050	580
Stomach	2,900	1,900	1,000	Multiple Myeloma	1,350	730	640
Brain	2,700	1,550	1,150	Oral	1,150	760	370
Ovary	2,600	—	2,600	Melanoma	950	590	360
Multiple Myeloma	2,300	1,300	1,000	Liver	810	640	170
Liver	1,950	1,500	460	Body of Uterus	750	—	750
Esophagus	1,750	1,350	410	Larynx	490	390	95
Cervix	1,300	—	1,300	Cervix	350	—	350
Larynx	1,150	930	210	All Other Cancers	10,400	5,300	5,000
Testis	970	970	—				
Hodgkin Lymphoma	920	510	420				
All Other Cancers	14,000	7,300	6,800				
Non-Melanoma Skin	74,100	40,700	33,300				

According to the statistics of the Canadian Cancer Society (2011), non-Hodgkin

lymphoma is the 5th most common cancer among all the cancer types, while leukemia is 10th, myeloma is 17th and Hodgkin lymphoma is 23rd. However, non-Hodgkin falls to 6th place while leukemia rises to 7th place and myeloma to 14th place in terms of death caused by the cancer type as seen in **Table 1**.

2.1.1. Non-Hodgkin Lymphomas

Non-Hodgkin Lymphoma (NHL), being the most common and the one causing the most number of deaths of all blood cancers, has several subtypes. According to the general subtype, there are B-cell, T-cell and NK-cell neoplasms that are further divided according to their maturation stage as precursor and peripheral neoplasms [7]. Although some types are very rare and their classification is complicated, the classification of non-Hodgkin lymphomas can be summarized as seen in **Table 2**.

Cytogenetics has played a crucial role in providing substantial insight into the genetic mechanisms and aided the classification of lymphoma as well as establishment of some distinct subtypes such as mantle cell lymphoma. Majority of NHLs have a number of clonal and relatively complex chromosome abnormalities that are seen with high frequencies in most of the same lymphoma subtype. However, this genetic alteration-lymphoma subtype association is not absolute so other characteristics such as morphology and immunology also have important effect in the classification of the lymphoma [8]. Some of the known genetic rearrangements of some lymphoma subtypes are given in **Table 3**.

As seen in **Table 3**, there are several mutations that appear in more than one NHL subtype, as well as several others that are specific to one subtype only. Immunoglobulin genes such as IgH, IgK, IgL are some of the rearrangements that can be considered common as well as BCL genes, especially BCL2 that is seen in many of the subtypes. P53 mutation is seen in more than one subtype, but unlike many other cancer types, it is not one of the main mutations. There are many unidentified chromosome abnormalities that have the potential to help understand lymphoma better upon identification [8-10].

Table 2 Types of non-Hodgkin lymphomas, adapted from: Harris NL et al. 1994 [7]. Note that the highlighted Sezary syndrome is the origin of the cell model used in this thesis research.

B-cell Neoplasms

Precursor B-cell neoplasm:

Precursor B-lymphoblastic leukemia/lymphoma

Peripheral B-cell neoplasms

1. B-cell chronic lymphocytic leukemia / prolymphocytic leukemia / small lymphocytic lymphoma
2. Lymphoplasmacytoid lymphoma / immunocytoma
3. Mantle cell lymphoma
4. Follicle center lymphoma, follicular
5. Marginal zone B-cell lymphoma
6. Splenic marginal zone lymphoma (i / - villous lymphocytes)
7. Hairy cell leukemia
8. Plasmacytoma / plasmacell myeloma
9. Diffuse Large B-cell lymphoma
10. Burkitt's lymphoma
11. High-grade B-cell lymphoma, Burkitt-like

T-cell and Putative NK-Cell Neoplasms

Precursor T-cell neoplasm:

Precursor T-lymphoblastic lymphoma/leukemia

Peripheral T-cell and NK-cell neoplasms

1. T-cell chronic lymphocytic leukemia / prolymphocytic leukemia
2. Large granular lymphocyte leukemia T-cell type / NK-cell type
3. Mycosis fungoides / **Sezary syndrome** (CTCL)
4. Peripheral T-cell lymphomas, unspecified
 - medium-sized cell,
 - mixed medium and large cell,
 - large cell,
 - lymphoepithelioid cell
 - Hepatosplenic $\gamma\delta$ T-cell lymphoma
 - Subcutaneous panniculitic T-cell lymphoma
5. Angioimmunoblastic T-cell lymphoma
6. Angiocentric lymphoma
7. Intestinal T-cell lymphoma
8. Adult T-cell lymphoma/leukemia
9. Anaplastic large cell lymphoma CD30⁺, T- and null- cell types
10. Anaplastic large-cell lymphoma, Hodgkin's-like

Table 3 Characteristic primary gene aberrations in select B- and T-cell lymphoma subtypes.
Adapted from: Dave et al, 2011 [8,9,10]

Lymphoma Subtype (other subtypes sometimes containing the abnormality)	Gene abnormalities
CLL/SLL (mantle cell lymphoma)	IgH, ATM, TP53
Splenic marginal zone	IgK, CDK6
Extranodal MALT	BIRC3 (API2), MALT1, FOXP1, IgH, BCL10
Nodal marginal zone	IgH, BCL3
Follicular (diffuse large cell)	IgH, BCL2, IgK, IgL
Mantle cell	CCND1, IgH
Diffuse large cell (follicular)	BCL6, IgH, CD10, IRF4, MUM1, STAT3
Burkitt (diffuse large cell)	MYC, IgH, IgK, IgL
Anaplastic large cell	ALK, NPM
Mycosis fungoides / Sezary syndrome	TP53, CDKN2B, CDKN2A, PTEN, STAT3, STAT5, BCL2, TCR
Other T-cell lymphomas	TCR

2.1.2. Current therapies for lymphoma

The fact that there are so many subtypes and each subtype has its own growth characteristics makes the treatment of NHL complicated. In treatment of lymphoma, there are numerous issues to be taken into account. The clinical behavior of lymphoma, similar to leukemia, strongly depends on the stage of maturation arrest of the tumor lineage. The stage of maturation arrest determines the degree of differentiation, which is directly related to the rate of cell proliferation and cell death [2]. The more differentiated the cancerous cells are the slower the cells proliferate, meaning the life span of the patient is longer if the cancerous cells are differentiated and shorter if they are more primitive [2]. Therefore, accurate diagnosis of the cancer subtype plays an important role in the determination of the required therapy.

Chemotherapy is the leading mode of treatment in blood cancers, often accompanied by radiation therapy or several other drugs that are newly emerging as the research in the area progresses. The radiation therapy used in treatment of cancer also is subjected to many changes with the novel methods of delivery of the ionizing radiation that improves

the efficiency of the treatment and decreases the involvement of the nearby healthy tissue. In addition, radioimmunotherapy, a treatment that combines radiation therapy with immunotherapy, is used to treat some types of NHL [11].

The newly developed drugs **according to their action mechanism** include:

Bcr-Abl tyrosine kinase inhibitors:

- imatinib mesylate (Gleevec®)
- dasatinib (Sprycel®)
- nilotinib (Tasigna®)

Histone deacetylase inhibitors (HDACs):

- vorinostat (Zolinza®)

Hypomethylating or demethylating agents:

- azacitidine (Vidaza®)
- decitabine (Dacogen®)

Immunomodulators:

- lenalidomide (Revlimid®)
- thalidomide (Thalomid®)

Monoclonal antibodies:

- rituximab (Rituxan®)

Antibody-drug conjugates:

- brentuximab vedotin (Adcetris®)

Proteasome inhibitors:

- bortezomib (Velcade®) [11]

Several drugs are used to treat people with lymphoma, and a number of potential new therapies are under study in clinical trials. Many of these new drugs are used to treat several types of blood cancer. Some of the **FDA approved drugs** for lymphoma and the respective lymphoma types they are recommended include:

Bendamustine (Treanda®)

- Chronic Lymphoid Leukemia and indolent B-cell Non-Hodgkin Lymphoma

Brentuximab vedotin (Adcetris®)

- Hodgkin Lymphoma, Systemic Anaplastic Large Cell Lymphoma

Denileukin diftitox (Ontak®)

- Cutaneous T-cell Lymphoma

Ibritumomab tiuxetan (Zevalin®)

- Follicular Non-Hodgkin Lymphoma, Follicular B-cell Non-Hodgkin Lymphoma

Pralatrexate (Folotyn®)

- Peripheral T-cell lymphoma, Cutaneous T-cell lymphoma

Rituximab (Rituxan®)

- Follicular, CD20⁺, B-cell Non-Hodgkin Lymphoma, Chronic Lymphoid Leukemia

Romidepsin (Istodax®)

- Peripheral T-cell lymphoma, Cutaneous T-cell lymphoma

Vorinostat (Zolinza®)

- Cutaneous T-cell lymphoma [11]

Some other non-drug therapies for lymphoma include:

Immunotherapy: Immune cells with capability to recognize and kill cancer cells are produced in the laboratory and given to patients to treat cancer. It is usually used in combination with another therapy such as chemotherapy. It includes (i) **monoclonal antibody therapy**, where laboratory-produced proteins targeting cancer specific cell surface antigens are infused (ii) **cancer vaccines**, designed to induce immune response against cancer cells present in the patient after treatment and (iii) **donor lymphocyte infusion**, where a donor's lymphocytes are infused to a patient with relapsed cancer after stem cell transplantation [11].

Gene therapy: Several agents are used to alter the expression of oncogenes and synthesis of corresponding proteins participating in malignancy. Rather than nullifying the effect of the oncoprotein by an external agent, its synthesis could be altered by gene therapy. Instead of protein replacement therapy, for example for a missing tumor-suppressor, a functional gene is delivered to code for the missing protein. As the oncoproteins and missing tumor-suppressors are responsible for development of cancerous features, the prevention of the synthesis of oncoproteins and/or reactivation or reintroduction of the tumor suppressors can cure the cancerous state or cause the death of the cancerous cells. In another approach, **gene transfer therapy**, the patients' T-cells are removed, genetically engineered and re-infused after chemotherapy to stop or slow down the remission of the disease [11].

Stem cell transplantation: when the bone marrow of the patient is impaired due to the blood cancer and/or the treatment, stem cells are transplanted into the patient to restore the function of the bone marrow. The stem cell transplantations are mainly either (i) autologous, where patient's own stem cells are collected, frozen and then thawed to be returned to the patient after intensive chemotherapy, or (ii) allogeneic, where a matching donor's stem cells are transplanted into the patient [11].

2.1.3. Cutaneous T-cell lymphoma (CTCL)

Cutaneous T-cell lymphoma (CTCL) is a subtype of peripheral T-cell lymphomas, and is characterized by the clonal accumulation of T-lymphocytic neoplasms in the skin. The malignant T-cells are usually mostly CD4⁺ with the immunophenotype of T-helper cells with only about 5% of the cases being CD8⁺. According to the World Health Organization, there are 13 subtypes of CTCL, the most common two being mycosis fungoides (MF) and Sézary syndrome (SS) [12,13] (the latter is the source of cell model for this thesis research)

In early clinical stages, CTCL cells are present within the epidermis, due to the expression of homing factors, such as the cutaneous lymphocyte antigen and chemokine receptors (e.g. CXCRs). The infiltration to the basal layer and adjacent Langerhans cells takes place as the disease progresses, thus neoplastic cells are detected within dermal layers with a consequent loss of epidermotropism [12].

Mycosis fungoides presents as patches and/or thin plaques containing small or medium sized T-cells. The lesions can persist for years before progression and peripheral blood and lymph node involvement and metastasis may occur in advanced stages [13].

Sézary syndrome is characterized by circulating, atypical, malignant T lymphocytes with cerebriform nuclei (Sézary cells), erythroderma and, often, lymphadenopathy. Severe itching, part of the lower eyelid turning outwards, hair loss, and abnormal thickening of the palms and sole are common associated features [12].

Molecular cytogenetic analysis of MF and SS show that they have similar chromosomal abnormalities such as loss of 1p, loss of 17p, gain of 4q/4, loss of 10q/10, gain of 18 and gain of 17q/17 where p is the short and q designates the long arm of the chromosomes [14]. **Table 4** shows some of the genes that are mapped on these chromosome regions.

Table 4 Cancer related genes mapped to the chromosomal areas with high rates of chromosomal irregularities in CTCL [14].

Chromosome regions with CTCT irregularities:	Cancer related genes mapped around the irregularities:
1p (loss)	BRCD2, MOM1/PLASG2, CDC2L1, DAN, TNFR2, ID2, P73, P18, TAL-1, BCL10 and MTS1/SA1/TFS1
17p (loss)	p53
4q/4 (gain)	hPTTG, TBC1D1, FGFR3, WHSC1/MMSET, AF4, TEK, KIT and PDGFRA,
10q/10 (loss)	PTEN, LGI1, DMBT1, MXI1 and FAS
18 (gain)	BCL2
17q/17 (gain)	HER-2, NIK, NME1, RPS6KB1, PRKCA and STAT3

As seen in **Table 4** there are several genes that has been mapped in the areas with high mutation rates; however, their involvement with MF and SS has not all been clarified. Some of the related genes such as p53 have been seen in various tumors including leukemia and lymphomas [14]. Also amplification of the PDGFRA and KIT oncogenes has been found in gliomas and B-cell lymphoma, deletion of PTEN and lower expression of FAS protein have been found in tumor-stage MF. Loss of MXI1 has also been detected in desmoplastic melanoma. High-level amplification of the HER-2 and RPS6KB1 genes has been detected in breast cancer and constitutive expression and activation of STAT3 have been detected in Hodgkin and CTCL cell lines [14].

Most authorities consider MF and SS as separate entities, while some argue that SS is a variant of MF or that SS is the leukemic stage or late development of MF due to the common occurrence of complex rearrangements in MF and SS. The difficulty in karyotype interpretation and identification of possible recurrent abnormalities is one of the reasons behind lack of knowledge in MF and SS. Also skin specimens from affected individuals do not produce good quality metaphases suitable for chromosome analysis, while cytogenetic studies of peripheral blood is hard, as in MF the involvement of peripheral blood does not occur or occurs very late into the disease, limiting our knowledge of MF and SS [13].

The diagnosis of CTCL is based on medical history, clinical examination and cutaneous histopathology, including immunohistology. Molecular biology diagnostic techniques are available but are not used routinely in most parts of the world [12].

The life expectancy of patients diagnosed with MF can vary from 10 to 15 years depending on the extent of the disease while SS is more aggressive with a 3-year survival from the diagnosis [12].

Several therapeutic choices are available based on the stage of the disease. Treatment must protect immune function to prevent immune collapse as the neoplastic T-cells usually expend at the cost of normal T-cells causing the patient to become immune compromised. The decision to apply skin directed or systemic therapy depends on extensive skin and blood involvement [12].

Skin-directed therapies include:

Steroids: topical corticosteroids are used to induce the clearing of skin lesions in early stages. They inhibit lymphocyte adhesion to other cells and endothelium resulting in cell death [15].

Nitrogen mustard (mechlorethamine): used topically as first-line treatment of early stage MF cutaneous toxicities may occur. They are non-specific DNA alkylating agents that alkylates and cross-links DNA during all phases of the cell cycle, resulting in disruption of DNA function, cell cycle arrest, and apoptosis [12].

Carmustine: topical chemotherapy that has been employed for early stage MF, cutaneous toxicities may occur more than nitrogen mustard. Carmustine is another non-specific DNA alkylating agent like nitrogen mustard [12].

Retinoids: vitamin A derivatives that have important effects on cell growth, terminal differentiation, and apoptosis. Approved by FDA for early stage MF, unlikely to cause irritation. Remission occurs 24-27 months [12].

Phototherapy: UV light therapy for early stage CTCL with high remission rates, Long-term exposure causes increased risk for chronic photo-damage and non-melanoma skin cancer. UV light disrupts and cross-links the DNA resulting in apoptosis [16].

Photodynamic therapy: exposure of tumor cells to a photosensitizing drug and to subsequent irradiation with light. Targets only limited parts of the body; the action mechanism is like phototherapy only difference is the inclusion of photosensitizing agents [16].

Radiation: localized radiation penetrating to the dermis, causing DNA damage. Remission rates range from 40% to 98%; however, relapse rates are high when the treatment is used as the sole modality. Some may suffer from delayed chronic skin damage with non-healing ulcerations and poikiloderma [12].

Systemic therapies include:

Interferon: one of the most widely used first-line treatments and probably the most effective single agent in the treatment of CTCL. Interferons boost the immune system to clear the cancer. Overall response rates range from 29% to 74% of patients, with median durations of 4–42 months. Initially, almost all patients develop temporary flu-like symptoms. Chronic side effects can include anorexia, fatigue, depression, alopecia, cytopenia, and impaired liver function [11,12].

Retinoids: overall response rate range from 44% to 67% and complete response rates from 21% to 35%. Retinoids are strongly teratogenic, side effects include skin and mucous membrane dryness, headaches, hypertriglyceridemia, hypercholesterolemia, central hypothyroidism, and leukopenia [12].

Chemotherapy: used in advanced, refractory, and aggressive forms of CTCL, associated with high response rates but short-lived durations. Options involve single-agent or multi-agent chemotherapy including with steroids, methotrexate, chlorambucil, vincristine, doxorubicin, PEGylated liposomal encapsulated doxorubicin, Caelyx, cyclophosphamide, etoposide, gemcitabine, nucleoside analogs, and alkylators. Can cause grade 0-4 toxicities and side effects, most frequent being mild anemia and lymphopenia [12].

Extracorporeal photopheresis: Circulating mononuclear cells are separated by a leukapheresis- based method, activated via psoralen, to make the cancerous white blood cells in the blood more sensitive to the effects of UVA light, and re-infused to the patient to give a systemic anti-tumor response. May cause catheter-related infection and hypotension caused by volume shifts [17].

Finally, the experimental therapies include **vaccination and virus-mediated therapies:** viruses such as measles virus are used for their selective infection of lymphocytes expressing a surface receptor such as CD46 are used to eliminate CTCL by inducing cell lysis. It is also possible to use adenoviruses to mediate gene transfer such as interferon genes or other therapeutic genes [12].

2.1.4. CTCL cell lines

In this study, an established CTCL cell line called **Hut78** was used as the cancer model. There are several established CTCL cell lines, including MyLa, SeAx, HH, PNO, SZ-4, MJ and Hut78 [18,19], and the sources of these cell lines are given below:

- MyLa: 82 year old Caucasian male with MF [20]
- SeAx: 66 year old female with SS [21]
- HH: 61 year old Caucasian male with aggressive CTCL [22]
- PNO: 50 year old female CTCL with [23]
- SZ-4: 66 year old black female with SS [24]
- MJ: 50 year old Caucasian male with MF (HTLV positive) [25]
- Hut78: 53 year old Caucasian male with SS [26]

All of these cell lines grow in suspension and have varying genetic backgrounds. Hut78 cell line was used in this study due to its frequent use in the literature as a CTCL model. Another cell line, Jurkat, from a 14-year old boy with ALL [27] was also used to determine the applicability of the treatment method to other T-cell malignancies as these two cell lines are frequently used together due to their similarities.

2.2. RNA interference (RNAi)

RNAi is a natural method of post-transcriptional gene silencing that is involved in several cellular processes. For the regulation of expression, the cell incorporates regulatory RNA molecules, called microRNAs (miRNA) that are encoded in the genome, into a complex called **RNA Induced Silencing Complex (RISC)** that facilitates cleavage of messenger RNAs (mRNAs) in the cytoplasm complementary to the miRNA incorporated. RISC is also involved in the defense mechanism of the cell against double stranded RNA viruses. If the genetic material of the virus is a double stranded RNA molecule, it is incorporated into RISC. This stops the viral proteins from being produced, again at a translational level, by cleaving the mRNA sequences that are complementary to the RNA segment incorporated into the RISC complex coming from the double stranded viral RNA [28].

There are several ways to induce RNAi; (i) by delivering synthetic RNA molecules in the form of long double stranded RNAs, (ii) short double stranded hairpin RNAs that are going to be cleaved in the cell by **Dicer** or (iii) by delivering short double stranded RNA ready to be incorporated into RISC directly. The latter, short interfering RNA (siRNA), is a synthetic exogenous short (21-23 nucleotides in length with a characteristic and highly specific structure of 2-3 nucleotide 3' overhangs and 5' phosphate and 3' hydroxyl groups) RNA duplex designed to use the RNAi mechanism to achieve specific gene silencing. siRNA usually has a **sense** or **guide** strand that has complementary and a **anti-sense** or **passenger** strand that has identical sequence to the targeted mRNA molecule. When siRNA is introduced to the cytosol of the cell, it is incorporated into RISC where it is unwound to have a single stranded RNA, the guide strand in the complex and the passenger strand is degraded. The single stranded RNA in the RISC then binds to its target mRNA, that has complementary sequence to the short RNA in the RISC, found in the cytosol. The cleavage of the mRNA at the central location of the complementary binding is facilitated by the endonuclease found in the RISC, namely argonaute (AGO) (summarized in **Figure 2**) [29]. This process silences the gene corresponding to the mRNA and that the siRNA is targeted against at the translational or post-transcriptional level. In other words, the gene is transcribed into mRNA but cannot be translated into protein as it is cleaved by the RISC coupled with the siRNA.

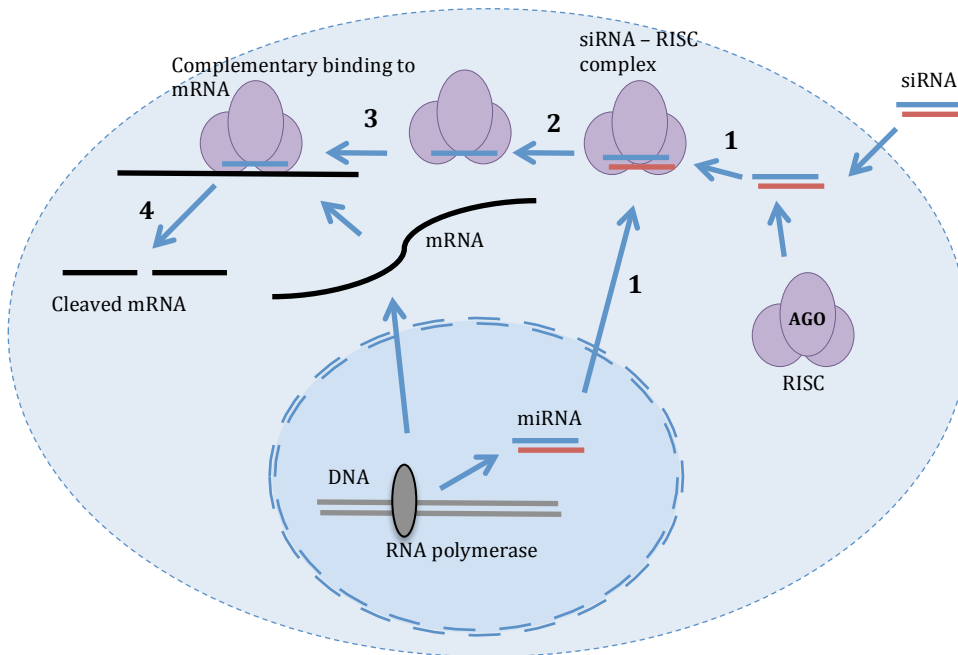


Figure 2 Schematic diagram of silencing with RNAi. mechanism. The double stranded RNA moiety enters the cytosol from outside the cell in the case of siRNA and from the nucleus in the case of miRNA, and then recognized and included into RISC (1). The passenger strand is then unwound and degraded (2) and the guide strand forms complementary binding with the target mRNA (3). Then the mRNA is cleaved by the endonuclease AGO, found in RISC (4) and degraded, thus achieving gene silencing at a post-transcriptional level.

RNAi is a powerful therapeutic tool that holds great potential in treatment of many diseases including cancer since it is a very specific gene silencing process. The specificity of the siRNA therapy, which could be down to a single nucleotide differences, and its applicability to any target, as long as the sequence of the target is available, makes it a substantially better therapeutic candidate for the treatment of cancer as compared to the conventional drug therapy [30].

As discussed in previous sections, cancer cells are often characterized by genetic alterations such as down-regulating important tumor suppressor genes or up-regulating oncogenes causing uncontrolled proliferation. RNAi is a very powerful tool to uncover the key genes whose deregulation leads to cancer and understand the roles of the deregulated genes [29]. Uncovering the key genes and understanding their roles is very important in developing new therapies for cancer. However, the applicability of the RNAi

is not limited in this respect. As cancer cells depend on aberrant expression of specific genes to achieve the state of increased proliferation, silencing of such genes with RNAi via intracellular delivery of siRNA has the potential to cause apoptosis. This makes siRNA a very suitable therapeutic against cancer [29].

Also it must not be forgotten that cancer cells usually have several deregulated pathways that drive cancer, such as oncogenesis, apoptosis, cell cycle regulation, cell senescence, tumor-host interaction, and resistance to conventional therapies. Therefore, the blockage of a single gene may not be sufficient to control the cancer, but silencing of several deregulated genes involved in different pathways might be necessary. Another major benefit of RNAi therapy is that siRNA can be potentially used to silence several genes involved in tumorigenesis at once [29]. Also, in case of drug-resistant strains of cancers, it is possible to reverse the resistance using siRNA therapy [31].

Another superiority of siRNA is due to its relatively non-toxic nature, since most of the toxicity comes from the delivery agent. This is unlike the current therapies such as chemotherapy or radiotherapy, that are very destructive and painful on the patient both in the short and long-term. The most common therapy for cancer, chemotherapy, destroys each and every fast dividing cell in the body such as blood-forming cells in the bone marrow; hair follicles; and cells in the mouth, digestive tract, and reproductive system causing severe side effects. siRNA on the other hand, due to its high selectivity, spares the normal cells and only targets the cancer cells [29].

2.3. Current therapies using RNAi and delivery methods

There are several difficulties that must be overcome to use siRNA therapy in clinic. One such difficulty is the delivery of the siRNA into the cell, the main challenge towards the use of siRNA [32]. The siRNA to be efficient needs to reach the cytoplasm in sufficient amounts for sustainable silencing. However, siRNAs are highly unstable in serum due to the presence of RNAses, and are also unable to enter the cells due to their large size (13 kDa) and highly polyanionic nature [29,33,34]. They are subjected to dilution at each cell

division, which requires repetitive dosing for long-term effects [35]. Potential toxicities due to siRNA include (i) saturation of RISC to enable miRNA pathways, (ii) stimulation of immune response, and (iii) silencing of unintended targets due to partial complementarity [29].

Another aspect to consider for using siRNA is the route of delivery. In case of systemic delivery with intravenous injection, the molecules are diluted in the body, taken up by the phagocytes, aggregate with serum proteins and are filtered in the kidneys. They also need to reach the target tissue by passing through biological barriers such as the endothelium lining the blood vessels, and the dense network of extracellular matrix (ECM) and macrophages found in the ECM. Even after reaching the cell, the siRNA needs to be internalized, escape the endosome to reach the cytoplasm before getting degraded by the low pH and lysosomal enzymes, and be freed from the carrier [29,34,36].

All these obstacles made it clear that siRNA needs to be protected from both biochemical and mechanical interactions and guided to its target. DNA transfection techniques gave rise to early approaches to protect siRNA. These approaches can be **mechanical**, enhancing the permeability of biological barriers via sonoporation or electroporation; **chemical** or **biological**, transporting the genetic cargo through biological systems via the involvement of a vector [29]. The ideal gene delivery system should be specifically targeting, biodegradable, non-toxic, non-inflammatory, non-immunogenic and stable for storage. It should also have a large capacity for genetic material, efficient transfection and the capacity to be produced in high concentrations at low cost [40]. Delivery systems used for siRNA delivery can be broadly classified as viral and non-viral vectors.

2.3.1. Viral vectors

The most efficient delivery is achieved via viral vectors; however, their usage is limited due to several issues associated with the vector. The first viral vectors to be used were retroviral vectors based on the mouse stem cell virus (MSCV) and the Moloney murine leukemia virus (MoMLV) [37-39]. The surface molecules and G-glycoproteins found on

the surface of the retroviruses allow them to infect a number of cell types, including primary cells. Another source of retroviral vectors is lentiviruses, which can infect non-dividing cells unlike MoMLV and MSCV that require cell division for expression [37]. Adenoviruses are also used for siRNA delivery, as they do not require cell division for expression and can infect many cell types. The adenoviruses used for gene transfer are generally replication defective recombinant viral particles [37].

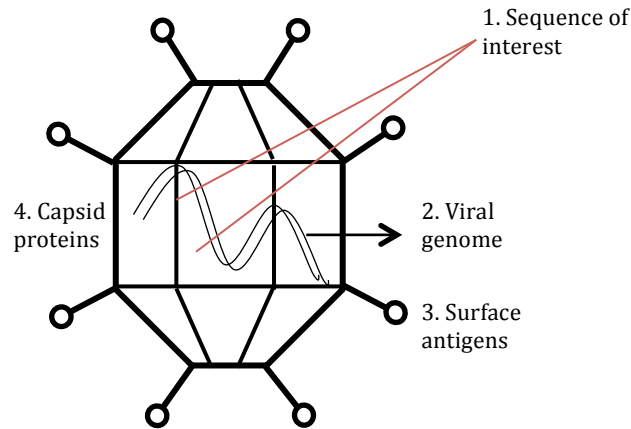


Figure 3 Schematic diagram of a viral vector. The target sequence to be delivered (1) is packaged into the genome of the virus (2) via recombination. The surface antigens of the virus (3) direct the viral particle to the target tissue or cell, while the capsid proteins (4) protect the cargo.

There are other viruses used for gene therapy; however, there are several issues keeping the viral based delivery agents from going into clinical trials. One of these issues is that they have been held responsible for the death of at least one patient, leading to the suspension of clinical trials [37]. Also the need for the existence of a packaging cell line for the desired genetic component to be integrated -packaged- into the viral particle, and the complexity associated with it is a drawback in usage of viral vectors. Concerns about the safety of using viruses, meaning the possibility of recombination with a pre-existing latent virus to produce replicating viral particles, their toxicity, immunogenic nature and lack of cell-specific targeting also limit their use. Moreover, the transfection via viral vectors is limited to first-pass organs such as lungs, liver and spleen as they are rapidly cleared from the circulation [37].

2.3.2. Non-viral vectors

There are several non-viral delivery methods for siRNA (**Table 3**). The delivery method can simply be conjugation of a ligand directly to siRNA or a chemical alteration of siRNA such as methylation, resulting in higher stability and targeting. The delivery method can alternatively involve the use of a carrier that can be organic or inorganic based. The formulation can have a size in the ‘micro’ or ‘nano’ scale, identifying it as microparticle or nanoparticle [29]. Leaving chemical modifications of siRNAs aside, lipid and polymer based constructs that are sized in the nano-scale can be considered as ‘nanoparticle’ delivery systems collectively. The general characteristics and some general information about different nanoparticles can be summarized as follows:

Table 5 Non-viral delivery methods for siRNA, adapted from Miele E et al, Int. J Nanomedicine, 2012 [29]

<p><u>Direct chemical modifications of siRNAs (<10 nm)</u></p> <ul style="list-style-type: none"> ➤ Sense and antisense strand <ul style="list-style-type: none"> ○ 2’-OH-Methyl ○ Phosphorothioate backbone linkage ○ Other 2’-Sugar modification (eg, fluorine, hydrogen) ➤ 3’ or 5’ modification in the sense strand <ul style="list-style-type: none"> • Ligands conjugated include: <ul style="list-style-type: none"> ○ PEG ○ Sugar molecules (e.g., cyclodextrin) ○ Hyaluronic acid (HA) ○ Cell permeant peptides (CCPs) ○ Cholesterol ○ Lipids (bile and long chain fatty acids) ○ Mipomersen [2’O-(2-Methoxyethyl)] ○ Folate receptor (FR) ○ Tranferrin receptor (TfR) ○ Aptamers ○ Antibodies 	<p><u>Liposomes</u></p> <ul style="list-style-type: none"> ➤ Cationic lipids <ul style="list-style-type: none"> • DOTMA (N-[1-(2,3-dioleoyloxy) Propyl]- N,N,N trimethyl ammonium chloride) • DOTAP (1,2-dioleoyl-3-trimethylammonium- propane) ➤ Neutral nano-liposomes <ul style="list-style-type: none"> • DOPC (1,2-dioleoyl sn-glycero-3-phosphatidylcholine)
<ul style="list-style-type: none"> ➤ Inorganic Nanoparticles (NPs): Gold NPs ➤ Organic NPs: SNALP (Stable nucleic acid lipid particle) and SLNP (solid lipid nanoparticle) ➤ Liposomes SLNP 	<p><u>Polymers</u></p> <ul style="list-style-type: none"> ➤ Cationic polymers <ul style="list-style-type: none"> ○ Poly-L-Lysine (PLL) ○ Polyethylenimine (PEI) ○ Cyclodextrin-based polycation ○ Chitosan ○ Atelocollagen ○ Cationic polypeptides

2.3.3. Nanoparticles

Dramatic progress has been made in the area of nanotechnology in the last years, making the use of nanotechnology very promising to overcome the drug delivery obstacles in molecular medicine. Nanoparticles are fruits of nanotechnology that offer the opportunity to change the current treatments dramatically, as they have tunable size, shape, surface, and biological behavior. The ability to manipulate matter on a nanometric scale made the fabrication of uniquely tailored devices with any desired physicochemical property possible, giving them enormous therapeutic and diagnostic potential [29]. Nanoparticles also have a size range of 1-100 nm giving them enhanced permeability across biological barriers and enormous surface area to volume ratio meaning there is plenty of space on the particle for transport, chemical reactions, and interaction with biological systems. The size also gives the particles an inherent passive targeting for cancer due to vasodilation effect around the tumorous tissue [29].

Nanoparticles can enable scientists to improve drug stability and carrier capacity, target the cargo to site of interest, send the cargo through the epithelial and endothelial barriers, and even do combination therapies by packing more than one drug in the particle [29].

Nanoparticles can be classified broadly as organic and inorganic according to the origin of the materials, and can be further divided according to their size, shape, surface, structure, and chemical behavior. The cargo can be adsorbed, dissolved or dispersed inside or attached outside the nanoparticles, and it can be released by diffusion, swelling, erosion or degradation. The particles can be passively or actively targeted, meaning their target depends on the particle size and route of administration or they are functionalized with ligands or antibodies to actively recognize the target respectively. Furthermore, the nanoparticles can be designed to be stimuli responsive, such as pH, light or temperature sensitive, using appropriate materials [29]. As discussed, nanoparticles hold great potential, and can be used to overcome the challenges concerning the therapeutic use of siRNA. Two most widely used nanoparticles for siRNA delivery are lipid and polymer based as follows:

2.3.4. Lipid based delivery systems for siRNA:

Lipids are amphiphilic molecules that have both polar and non-polar characteristics at two sides of the molecules causing them to readily assemble into micelles or bilayers. The double characteristic nature and self-assembly makes lipids promising vectors. Liposomes have been used in clinical trials in drug delivery [29] and an extensive range of lipids has also been developed for siRNA delivery [41]. Cationic lipids were used in the form of liposomes for their self-assembling nature. Helper lipids (co-lipids) such as cholesterol, dioleoylphosphatidyl choline (DOPC) or dioleoylphosphatidyl ethanolamine (DOPE) and other neutral lipids are often used together with cationic lipids to improve the efficiency of the liposomes or give them additional characteristics or stability [41].

Liposomes: are spherical vesicles made of lipid bilayer, the main material of cell membrane. They are usually made of planar lipid bilayers via sonication to form spherical particles, where the charged or polar hydrophilic moieties arrange to face the outer and inner aqueous environment and the non-polar hydrophobic fatty acid chains arrange between two layers of polar heads to form a lipophilic layer, as seen in **Figure 4**.

Liposomes have been used extensively for the delivery of genetic materials since 1980s, and there are several commercially available cationic liposome/lipid based systems such as DOTAP, Lipofectin, RNAifect, Oligofectamine, Lipofectamine® and TransIT TKO. PEGylation, which is a way to improve pharmacokinetics of several agents in vivo, have been applied to liposomes to form ‘stealth’ liposomes (SL). PEGylated liposomes are a clinically approved delivery system for doxorubicin, and therefore represent a viable option for delivering siRNA in humans [41]. However the use of liposomes for siRNA delivery is still limited due to low stability and toxicity to the cells. Even though the stability and delivery efficiency of lipoplexes can be enhanced by increasing the overall positive charge via increased cationic lipid ratio, the increase in the amount of cationic lipids also cause an increase in the cytotoxicity [42].

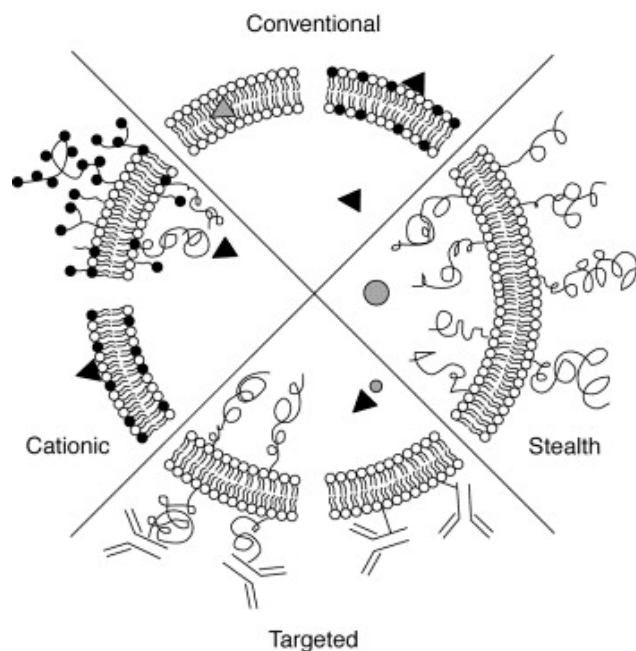


Figure 4 Schematic diagrams of liposomes with different attributes. The conventional liposome only consists of phospholipids and is usually neutral or negatively charged, the stealth liposome is coated to increase serum stability with agents like PEG, the targeted liposome includes antibodies or ligands and the cationic liposome can be either anchored with other moieties to give a positive charge or includes positively charged lipids to give an overall positive charge to the liposome. Reproduced with permission from Storm G et al, PSTT, 1998 [43] Copyright © 1998, Elsevier.

For the use of liposomes in siRNA delivery, it is still necessary to overcome some of the issues related with stability, efficiency and encapsulation. Some of the solutions proposed to overcome the issues related with stability, efficiency and encapsulation are; the usage of pentavalent cationic lipids, lipidoids and pH responsive lipids or assembly of different nanostructures such as **lipid-protamine-DNA (LPD)**, **lipid-calcium-phosphate (LCP)**, **solid lipid nanoparticles (SLN)** and **stable nucleic acid-lipid particles (SNALP)** based on lipids [42]. Although it is still not perfect, lipid based nanoparticles hold potential to be used as efficient non-viral delivery systems for siRNA in the future.

2.3.5. Polymer based delivery systems for siRNA:

Polymer-based systems provide several advantages for delivery of therapeutic drugs and therapeutic delivery of nucleic acids. The first polymer used for gene delivery was diethylaminoethyl-modified dextran in 1965, and the area has been growing exponentially since then [44].

There are several polymers used in drug-delivery, they can be either of natural origin such as collagen, chitosan, elastin, or synthetic such as poly-L-lysine (PLL) or polyethyleneimine (PEI). The choice of the polymer determines the characteristics of the carrier such as the rate of clearance from blood, the rate of release, targeting and size. Although the natural source polymers can be manipulated to a point via partial degradation, crosslinking and such, the degree of manipulation is limited compared to their synthetic counterparts, which can be freely manipulated and tailored to the need for the specific application [39,40]. One advantage of natural polymers to synthetic polymers is that they are more biocompatible and they are better biodegradable as the enzymes for their degradation is readily available [45]. However, this advantage can also be a disadvantage in terms of immunogenicity as not only the enzymes but also antibodies against the natural source polymers are also available in the body.

The assembly of polymer-based nucleic acid nanoparticles is generally driven by charge interactions, making the preparation of particles easier such as simply mixing the polymer with the nucleic acid. Some examples of the polymers used in nucleic acid delivery are polyethylenimine (PEI), Poly-L-Lysine (PLL), poly(lactic-co-glycolic acid) (PLGA), chitosan, and β -cyclodextrin, whose chemical structures are seen in **Figure 5** [46].

Chitosan is a copolymer of N-acetyl-D-glucosamine (GlcNAc) and D-glucosamine (GlcN) and is a highly abundant natural polymer. It is non-allergenic, biocompatible, biodegradable and its cationic nature makes it a potent vector for siRNA. Chitosan is a commonly used polymer for plasmid DNA (pDNA) but its use in siRNA is yet to gain momentum. Some difficulties associated with chitosan is the low solubility and inefficient endosomal buffering resulting in the degradation of the siRNA as the endosomal pH drops [46].

Cyclodextrin (CD) is a group of naturally occurring cyclic oligosaccharides. CD containing polymers are non-immunogenic making them suitable targets for delivery of therapeutics. Also unique geometric and structural characteristics of CD having a hydrophilic outer surface and hydrophobic inner cavity made it a target for delivery of insoluble molecules. Like chitosan, although applied in pDNA delivery, CD has not been extensively studied for siRNA delivery. One major drawback of CD based nanoparticles is their inability to achieve endosomal escape [46].

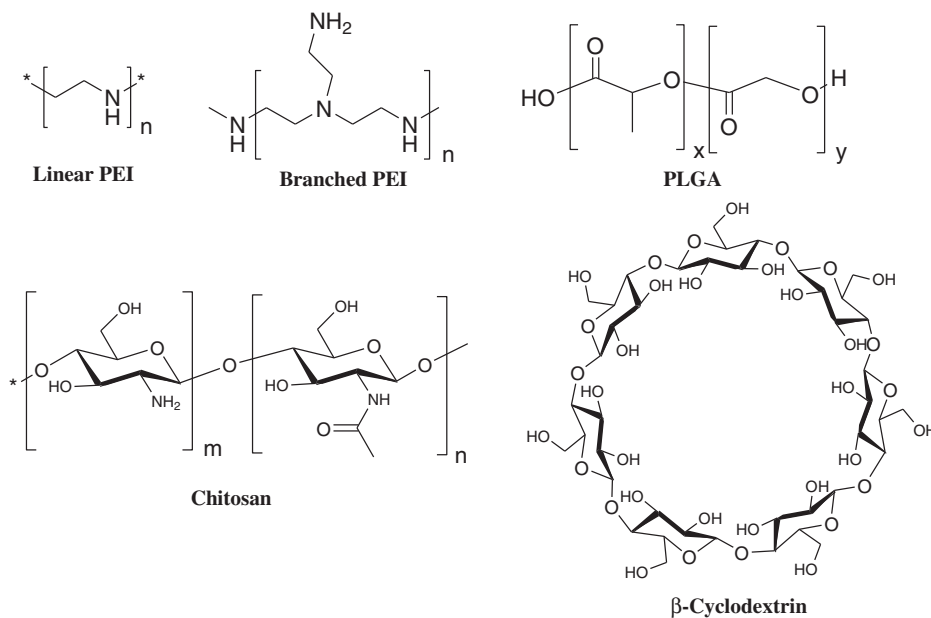


Figure 5 Chemical structure of linear polyethylenimine (PEI), branched PEI, poly(lactic-co-glycolic acid) (PLGA), chitosan, and β -cyclodextrin. Reproduced with permission from Singha K et al, *Nucleic Acid Therapeutics*, 2011 [46] Copyright © 2011, Mary Ann Liebert, Inc., publishers.

PLL is a synthetic polymer of L-lysine, and is one of the oldest polymers that have been studied for nucleic acid delivery. Even now it is one of the most commonly used polymers alongside PEI. Its highly cationic nature makes it a suitable carrier for siRNA due to high electrostatic interaction and it can be synthesized at any given molecular weight and be easily modified or anchored with other molecules to tailor the characteristics. However PLL, especially the high molecular weight versions, has low transfection efficiency due to its high toxicity. PLL has been modified in several ways

and a biodegradable version of it by adding glycolic acid into the polymer (PLGA) has been synthesized to decrease its cytotoxicity [47].

PLGA is a copolymer of glycolic acid (GA) and lactic acid (LA) linked together via ester linkages. The degradation of PLGA occurs via hydrolysis of the ester bonds to give the original monomers and the rate of degradation and some other characteristics can be tailored by changing the GA/LA ratio. Their small particle size, favorable safety profile, and sustained-release characteristics caused them to be studied extensively in the biomedical research. However, the loading and encapsulation efficiency of PLGA is quite low as siRNA escapes from the carrier as it is very small, hydrophobic, and the phosphate groups in the siRNA backbone repel the anionic groups in PLGA. As a result, the practical applicability of PLGA for siRNA delivery is limited [46].

2.3.5.1. Polyethylenimine (PEI)

PEI consists of the monomer ethylenimine, polymerized either in a linear fashion (giving primarily secondary amines with terminal primary amines) or in a branched fashion (giving a mixture of primary, secondary and tertiary amines). A detailed chemical structure for PEIs is given in **Figure 9** in the materials and methods section. It is highly cationic due to the existence of several amino groups and has been considered the gold standard for plasmid DNA (pDNA) delivery [48,49]. However, the small size of siRNA causing weak electrostatic interactions, and hence dissociation of PEI/siRNA complexes at the anionic cell surface may reduce the efficiency of PEI for siRNA delivery [46]. Also the toxicity of high molecular weight PEI (>10 kDa) is a main concern for its use in nucleic acid delivery [50]. However, PEI is still a very extensively studied polymer due to the availability of linear and branched PEI in a wide range of molecular weights.

PEI has a very useful property owing to its high content of protonable amino groups that cause a “proton sponge effect” to aid endosomal escape. The amino groups of endocytosed PEI could get protonated by the hydrogen ions pumped into the endosome, resulting in elevated osmotic pressure and subsequent flow of other species (including

water) into the endosome. This ultimately causes the endosome to swell and eventually rupture to release the genetic cargo into the cytosol [51].

However, not all PEIs are suitable for nucleic acid delivery; the high molecular weight PEIs (>10 kDa, and in particular 25 kDa) is effective in delivery of the nucleic acids but they are accompanied with high toxicity. On the other hand, the low molecular weight PEI (<5 kDa and in particular 2 kDa PEI) has negligible cytotoxicity but also demonstrate very low transfection efficiency [46]. Several methods have been tried to increase the efficiency of the PEI while decreasing the toxicity, such as incorporating low and high molecular weight PEI together to form a blend, or crosslinking the PEI with degradable disulfide bonds [46].

Polyethylene glycol (PEG) is also used to coat not only PEI but most cationic carriers to overcome the intrinsic drawbacks associated with the carrier, such as low solubility, cytotoxicity and low transfection efficiency. PEGylation prevents the nanocarriers from attracting serum proteins and blood cells due to its nature stopping them from changing their physiochemical properties [40]. However, stabilization via PEGylation also reduces the ability of the nanoparticles to interact with cells [39].

2.3.5.2 Hydrophobic lipid substitution on PEI

Another approach to increasing the efficiency of PEI is synthesizing “cell interactive polymers” that target cells via interaction with the cell membrane. Incorporating targeting molecules such as aptamers, peptides, antibodies, proteins, or ligands are ways of targeting the carrier to specific cells but are usually specific to one cell type or another. Introduction of hydrophobic character into the PEI, on the other hand, is a non-specific way of cell membrane targeting, as the target is the hydrophobic cell membrane itself, and can be applied for a more general approach to enhance cell permeability. One issue with using hydrophobic groups in carriers is the reduction of the positive charges in the carriers. If the positive charge density of the carrier is too low, not only the polyplex formation with the anionic siRNA will be hindered, resulting in unstable particles but

also the proton sponge effect will be weak, i.e., unable to induce endosomal escape [46] (that is of course the lipid group has no endosolytic activity). Hence, there should be a balance between the induced hydrophobic character and the reduced positive charge.

In the Uludag group, the non-toxic, low molecular weight (2 kDa) PEI has been modified using several conventional fatty acids to introduce a hydrophobic character to the polymer [52,53]. Several lipids were covalently bound to the PEI backbone through the modification of primary amine groups at different ratios (the full list of lipids and ratios used is given in **Table 7** in the **Materials and Methods** section). The “gold standard” for the pDNA delivery, 25 kDa PEI, has been routinely used to compare the toxicity and efficiency of the resulting constructs [46,48,49]. The two different PEIs, 2PEI and 25PEI were chosen in this study due to several reasons. One of the reasons is the cytotoxicity, 2PEI was chosen due to its negligible cytotoxicity, and so as the toxicity might increase due to modifications, it is best if the starting product is non-toxic. If a higher molecular weight PEI was used, as the toxicity increases with size (amount of cationic groups) the end product’s toxicity would also be high. 25PEI, on the other hand, is very toxic [46], so any construct that has similar or more cytotoxicity than 25PEI does not serve the purpose. Another reason is their efficiency, 25PEI has as noted before high efficiency, while 2PEI is not efficient at all [46], so if the constructs are as efficient as or more efficient than 25PEI, then they can be considered successful.

2.3.6 siRNA for treatment of leukemia and lymphoma

As explained in the previous sections, there are several methods for delivering siRNA into cells and siRNAs have been explored for treatment of leukemia and lymphomas. There are two main routes of using siRNA as a therapeutic tool; (i) to silence cancer related genes in order to induce apoptosis (or prevent cell growth in general), or (ii) to silence genes conferring drug resistance to cancer cells in order to sensitize the cells to the chemotherapy drugs. In this thesis, the former and **direct** method has been studied; however, there are several studies focusing on the latter **indirect** method. Some examples

of the studies using siRNA for treatment of leukemia and lymphomas are summarized in **Table 6A (Direct Method) and 6B (Indirect Method)**.

As seen in **Table 6**, Lipofectamine® 2000 is the most widely used transfection agent, followed by nucleofection, electroporation and lentiviral vectors that are not suitable for use in clinic. It is also seen that while a large variety of gene targets are used for the treatment of leukemia and lymphomas, STAT family, survivin, BCR-ABL are the most frequently used targets.

Table 6A. Examples of the studies using siRNA for treatment of leukemia and lymphomas (Direct Method)

Targeted gene(s)	Delivery method(s) / Transfection agent(s)	Target disease(s)	Source
Survivin	Direct plasmid addition	NHL	Congmin G et al, Leukemia & lymphoma, 2006 [72]
LMP1	Lipofectamine®2000	EBV+ lymphoma	Mei YP et al, Cancer lett, 2006 [73]
Bcl11b	Nucleofection/ Lipofectamine®2000	T-ALL/ lymphoma	Grabarczyk P et al, Oncogene, 2007 [69]
WT1	Lipofectamine®2000	AML, CML, ALL	Glienke W et al, Leukemia, 2007 [74]
BCR-ABL	Quantum dots	CML	Zhao Y et al, J nanosci and nanotech, 2010 [75]
STAT3	Lentiviral vector	CML	Ma LD et al, Leukemia & lymphoma, 2010 [76]
ROR1, FOMD	TransIT-TKO®	CLL	Choudhury A et al, Brit J Haematol, 2010 [77]
FLT	sc-29528	AML	Wang CM et al, J Int Med Res, 2011 [78]
Plk1	Lentiviral vector	CTCL	Nihal M et al, Cell cycle, 2011 [18]
ALK	PEI polymeric carriers	ALCL*	Zhao N et al, J of Nanobiotechnology, 2011 [79]
AGO2	Lipofectamine®2000	AML, CML	Naoghare PK et al, Basic Clin Pharmacol Toxicol, 2011 [80]
Notch3	Electroporation	T-ALL	Xiang J et al, Clin Lymphoma Myeloma Leuk, 2012 [81]
E2A	Nucleofection	CLL	Kardava L et al, International Immunology, 2012[82]
TAK1	Nucleofection	MCL**	Buglio D et al, Blood, 2012 [83]
EZH2	Nucleofection	B-ALL	Chen J et al, Exp Biol and Med, 2012 [84]
STAT3	INTERFERin™	AML	Kang SH et al, Pone, 2012 [85]
STAT3, STAT5A, STAT5B	Dharmafect-I, HiPerFect and Electroporation	CML	Kaymaz BT et al, Ann Hematol, 2013 [86]

Table 6B. Examples of the studies using siRNA for treatment of leukemia and lymphomas (Indirect Method)

Targeted gene(s)	Delivery method	Drug used	Target disease	Source
Bfl1	Lentiviral vector	Rituximab	B-cell lymphoma	Brien G et al, Oncogene, 2007 [87]
Survivin	Lipofectamine® 2000	Nutlin-3	ALL	Zhu N et al, Mol Cancer Ther, 2008 [88]
SPARC, Fyn	Not specified	Imatinib	CML	Fenouille N et al, Cancer Res, 2010 [89]
Aurora-A kinase	Nucleofection	Cytosine arabinoside	AML	Cheong JW et al, Cancer lett, 2010 [90]
BCR-ABL	DOTAP®	Nilotinib	CML	Koldehoff M et al, Haematol, 2010 [91]
Mcl-1	Nucleofection	ABT-737	MCL**	Touzeau C et al, Clin Cancer Res, 2011 [92]
Survivin ⁺	Electroporation, transductin	YM155	ALL	Tyner JW et al, Leukemia, 2012 [93]
CDC7	Lipofectamine® 2000	Rituximab	DLBL***	Hou Y et al, J Cancer Res Clin Oncol, 2012 [94]
APAF1	TransIT-TKO®	Bortezomib	ALL	Ottoson-Wadlund A et al, Mol Pharmacol, 2013 [95]

*Anaplastic large cell lymphoma, **Mantle cell lymphoma, ***Diffuse large B-cell lymphoma,

⁺Also used directly to induce apoptosis

2.4. GFP as a reporter gene

Fluorescent bioimaging is extensively used in the fields of biochemistry, biotechnology, cell and developmental biology to image single molecules, intact organelles, live cells or even whole organisms. However, the labeling of the cellular parts or molecules with small molecular fluorescent tags is a cumbersome and tedious protocol. GFP-like proteins have been extensively used in this area for their auto-fluorescent nature, and hence their ability to form internal chromophore without requiring accessory cofactors, enzymes or substrates other than molecular oxygen making possible chromophore formation in live organisms, tissues and cells [54].

Green Fluorescent Protein (GFP) was discovered several decades ago (1971) in jellyfish *Aequorea victoria* and *Renilla reniformis* sea pansy. Since its discovery, GFP has become the most extensively studied and widely used cell biology protein and the GFP-like protein family is a fast growing family consisting of several naturally occurring mutant

versions of GFP with superior properties. GFP-like family not only includes the enhanced versions of GFP, but also GFP-like proteins that have different colors such as red, green and blue and even dual colored ones [54].

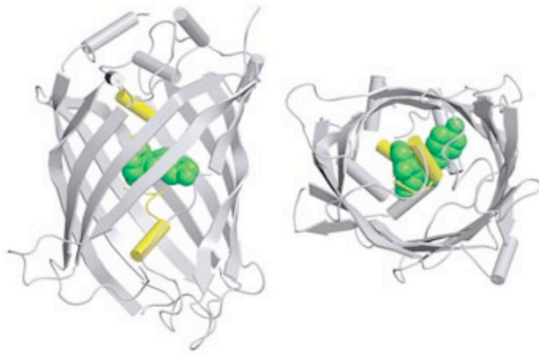


Figure 6 X-ray crystal structure of Aequorea GFP (PDB code 1W7S) in two projections. Adapted from Stepanenko OV et al, Current Protein and Peptide Science, 2008 [54].

In this study, GFP was used as a reporter gene whose silencing using anti-GFP siRNA can be easily observed and measured due to the decrease in the amount of fluorescence with the decrease in the amount of protein. The details of the measurements will be discussed in detail in the Materials and Methods section.

3. Materials and Methods

PEIs of all molecular weights, Trypan Blue and formaldehyde (37%) were purchased from Sigma Aldrich (St Louis, MO). RPMI 1640 medium, penicillin (10000 U/mL), streptomycin (10 mg/mL), Ultra pure water, AlamarBlue®, CyQUANT® Cell Proliferation Assay Kit, scrambled control siRNA as well as cytotoxic siRNAs were purchased from Life Technologies (Burlington, ON). Fetal Bovine Serum (FBS) was purchased from PAA Laboratories Inc. (Etobicoke, ON). Anhydrous dimethylsulfoxide (DMSO) was purchased from Fisher scientific (Ottawa, ON). FlowTACS™ Apoptosis Detection Kit was purchased from Trevigen (Gaithersburg, MD). FITC Annexin V Apoptosis Detection kit was purchased from BD Biosciences (Franklin Lakes, NJ). GFP siRNA (GFP-22) was purchased from Qiagen (Toronto, ON). Clear HBSS for non-sterile purposes was prepared in house.

Lipid modified PEIs were generously synthesized by the members of the Uludag Lab using published procedures [52,53]: PEI-CA-1, PEI-CA-10, PEI-CA-20, PEI-MA-1, PEI-MA-10, PEI-MA-20, PEI-PA-1, PEI-PA-10, PEI-PA-20, PEI-SA-1, PEI-SA-10, PEI-OA-1, PEI-OA-10, PEI-OA-20, PEI-LA-1, PEI-LA-10, PEI-LA-20 were synthesized by Dr. Artphop Neamnark, PEI-LAVH and PEI-LA1.2 was synthesized by Dr. Hamidreza Aliabadi and Dr. Vanessa Incani, PEI-CA 4-2, PEI-CA 1-3, PEI-CA 1-4, PEI-LA 4-3, PEI-LA 4-4, and PEI-LA 1-4 were synthesized by Mr. Jeremy Fife (undergraduate student, U. of Alberta; the level of substitutions are summarized in following sections). The materials for the lipid modified PEI synthesis, caproyl chloride (C8; >99%), linoleyl chloride (C18:2 9Z,12Z;99%), myristoyl chloride (C14; 97%), palmitoyl chloride (C16; 98%) and octanoyl chloride (C18:2 9Z,12Z; 99%), were purchased from Sigma Aldrich (St Louis, MO). Stearoyl chloride (C18; >98.5%) was obtained from Fluka (St Louis, MO).

Wild-type and GFP-expressing Hut78 cells were generously given to us by Dr. Xiaoyan Jiang (Senior Scientist, Terry Fox Laboratory, BC Cancer Agency, 675 West 10th Avenue, Vancouver BC, Canada V5Z 1L3). Wild-type and GFP-expressing Jurkat cells were generously given to us by Dr. Olaf Kutsch, (Associate Professor, Centre for AIDS

Research, University of Alabama at Birmingham, Birmingham, Alabama, United States of America). The GFP gene is genomic (stable integration) in both cell lines.

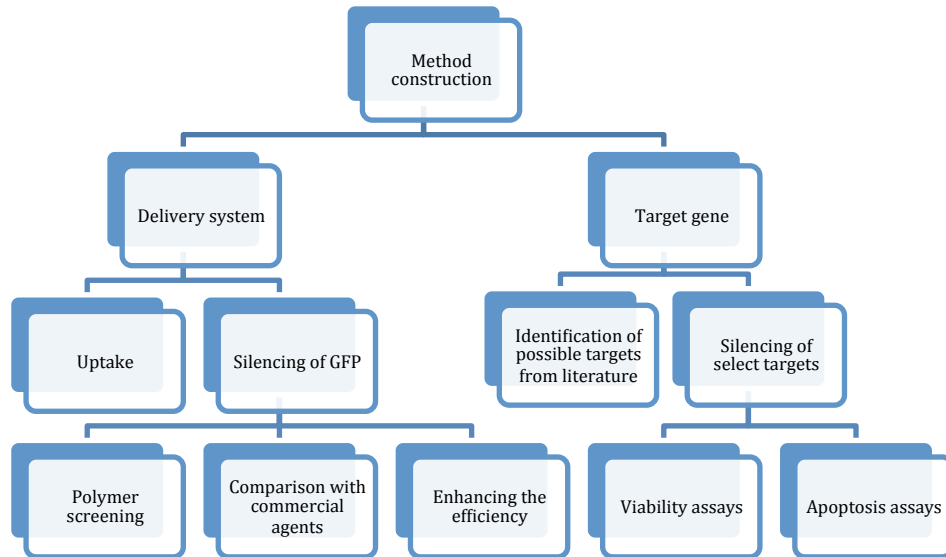


Figure 7 Design for the method construction explained in a flow chart showing the two main aspects –development of a delivery system and selection of a target gene- covered in this study.

3.1. Cell lines

In this study, Hut78 cells were used as a model of cutaneous T-cell lymphoma. They are originally skin-associated memory T-cells, and in the cancerous state they constitute a group of NHLs. They mainly affect the skin but can also involve the blood, lymph nodes and/or internal organs in patients with advanced disease. They form skin patches, plaques or tumor nodules, which are in fact solid tumors. They produce IL-2 and TNF-alpha and have IL-2, CXCR4 and T-cell receptors, and CD4 antigen on cell surface [26,55-57]. Another cell line used in this study to compare the efficiency of the delivery system in other cell lines was Jurkat ALL cell line. Jurkat cells are closely related to Hut78 cells and have similar characteristics. They also produce IL-2 and have IL-2, CXCR4 and T-cell receptors and CD4 antigen [57-60]. Both the Hut78 and Jurkat cells used in this study grow in suspension, which makes transfection more challenging [60].

For the optimization of the transfection method the retrovirally engineered GFP (Green Fluorescent Protein) expressing counterparts of the same cell lines (GFP expressing Hut78 and GFP expressing Jurkat cell lines) were used (**Figure 8**).

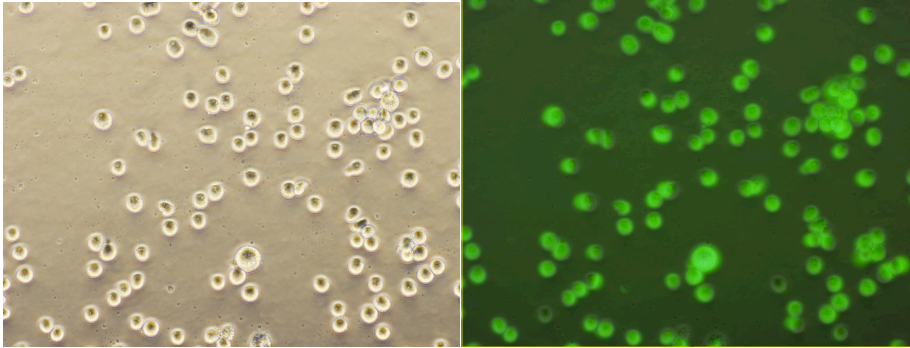


Figure 8 GFP positive Hut78 cells, with phase contrast and with green fluorescence filter.

3.2. Cell culture

Hut78 cells were cultured in RPMI-1640 media + 10% FBS (v/v) + 100 U/mL (1%) Penicillin + 100U/mL (1%) streptomycin, and were kept between 10^5 - 10^6 cells/ml concentration by routine subculturing. Subculturing of the cells was performed by simply sampling the cells and diluting in fresh media (10 to 25 fold dilution) without any trypsin mediated detachment as the cells grow in suspension. The cells were cultured for a maximum of 4-5 weeks for transfection for more reproducible results, since they start losing the GFP expression after 4-5 weeks of culture. For siRNA treatments, the cells were seeded at 0.5×10^5 cells/mL or 5000 cells/well for 96 well plates, 10000 cells/mL for 48 well plates, and 15000 cells/well for 24 well plates (unless otherwise specified), 24 hours prior to the treatment.

3.3. Engineered PEI Polymers

The synthesis of lipid-engineered 2 kD PEI polymers were performed in the Uludag Lab using published procedures [52,53]. The structure of PEI is shown in **Figure 9**. The lipids

and lipid anchored PEI polymers used in this study have been schematically summarized in **Figure 10** and **Table 7** respectively.

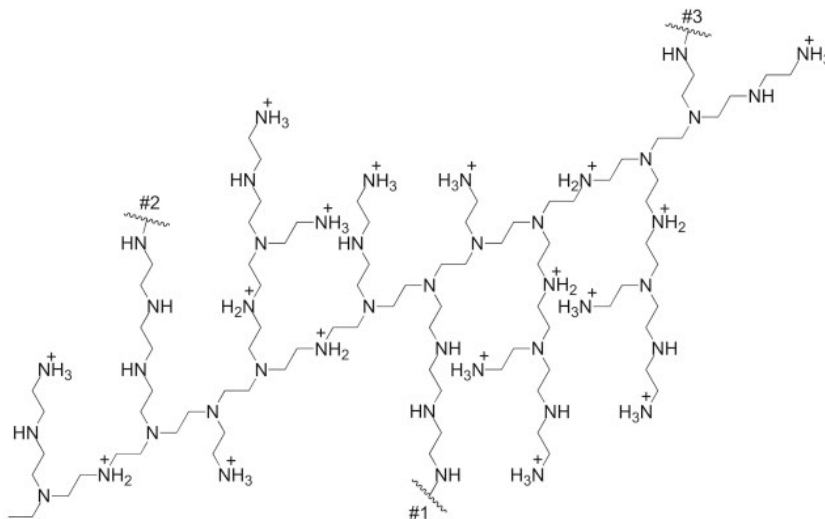


Figure 9 The structure of branched 2 kD PEI. #1, #2 and #3 represent sites of typical lipid substitutions (see Figure 10 for specific lipid substituents). Reproduced with permission from: Sun C. et al, *Biomaterials*, 2013 [61] Copyright © 2013, with permission from Elsevier.

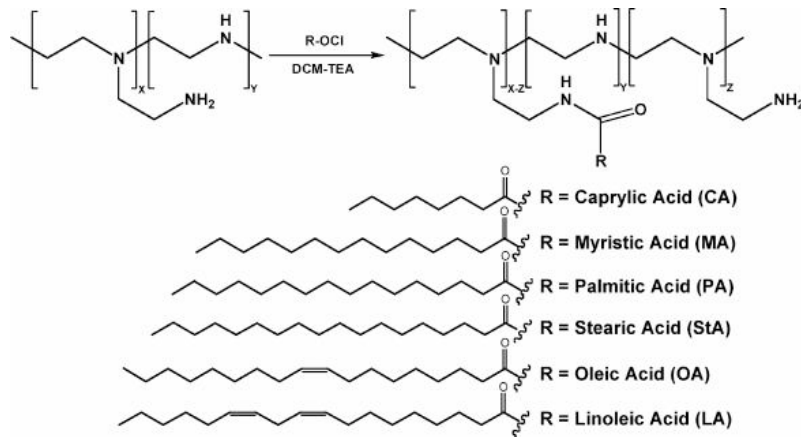


Figure 10 Lipids used for substitution to PEI. Reproduced with permission from Neanmark A. et al, *Molecular Pharmaceutics*, 2009 [52] Copyright © 2009 American Chemical Society.

Table 7 Table of lipid substituted PEI showing the lipid substitution ratios per PEI backbone. Polymers with * was previously described in: Neanmark A. et al, Molecular Pharmaceutics, 2009 [52].

Polymer Designation	Substituent	Lipid/PEI backbone
* PEI-CA-1	Caprylic acid	1.1
* PEI-CA-10	Caprylic acid	2.4
* PEI-CA-20	Caprylic acid	6.9
* PEI-CA-4-2	Caprylic acid	2.5
* PEI-CA 1-3	Caprylic acid	3.3
* PEI-CA-1-4	Caprylic acid	6.0
* PEI-MA-1	Myristic acid	0.6
* PEI-MA-10	Myristic acid	1.7
* PEI-MA-20	Myristic acid	1.5
* PEI-PA-1	Palmitic acid	0.6
* PEI-PA-10	Palmitic acid	0.8
* PEI-PA-20	Palmitic acid	1.1
* PEI-SA-1	Stearic acid	0.5
* PEI-SA-10	Stearic acid	3.6
* PEI-OA-1	Oleic acid	1.0
* PEI-OA-10	Oleic acid	1.7
* PEI-OA-20	Oleic acid	2.5
* PEI-LA-1	Linoleic acid	1.0
* PEI-LA-10	Linoleic acid	1.8
* PEI-LA-20	Linoleic acid	3.2
PEI-LA1.2	Linoleic acid	1.2
PEI-LA-4-3	Linoleic acid	1.3
PEI-LA-4-4	Linoleic acid	1.7
PEI-LAVH	Linoleic acid	2.1
PEI-LA-1-4	Linoleic acid	2.6

3.4. siRNA Complex formation

siRNA/PEI complexes were formed by incubating siRNAs with polymers at room temperature for 30 minutes in the presence of salt (150 mM NaCl) solution. The siRNA used were GFP siRNA as the treatment, scrambled siRNA as the control and other specific siRNAs as additional treatments.

First, both siRNA solution (in RNase free water; stored at -20°C) and polymer (in nuclease free ultra pure water from Life Technologies (Burlington, ON); stored at $+4^{\circ}\text{C}$) solutions were allowed to equilibrate to room temperature. Then they were vortexed at low setting to obtain a homogeneous solution, as the materials tend to settle. siRNAs were added to 150 mM NaCl solution at the desired volume (e.g., $10\ \mu\text{L}$ per well \times no of wells + $5\ \mu\text{L}$ extra volume) in eppendorf tubes and polymers were added to this solution, followed by a brief vortex to mix the siRNA and polymers thoroughly. The formed complexes were added to the cell media at $10\ \mu\text{L}/\text{well}$ at the end of the 30-minute incubation time (**Figure 11**).

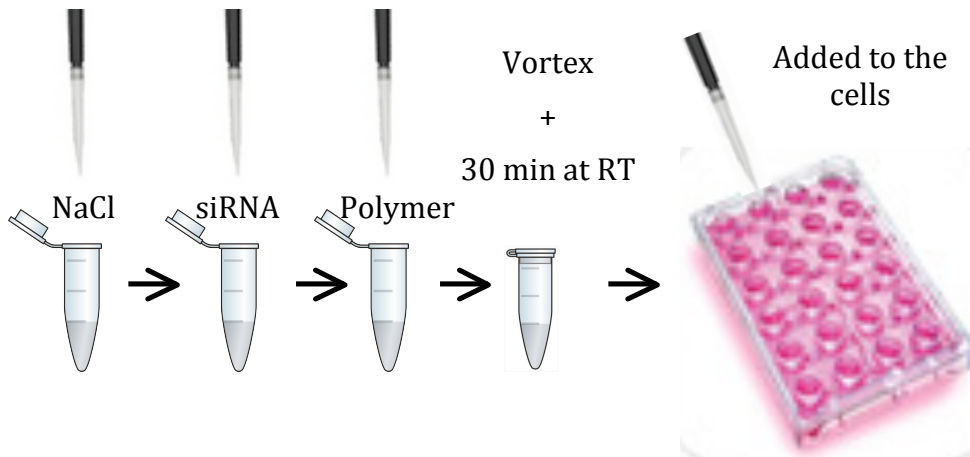


Figure 11 A schematic representation of preparation of siRNA-Polymer complexes

Table 8 below shows a typical complex preparation for a study that involved 16 study groups. In part **A**, the calculations for the siRNA added to the medium is given, in this case, the final siRNA concentration is set to be $25\ \text{nM}$, in a well containing $0.3\ \text{mL}$ medium. The amount of complex solution added to each well is set to be $10\ \mu\text{L}$, so the complex formation volume is set to be $35\ \mu\text{L}$ for triplicate samples, including an extra $5\ \mu\text{L}$ to account for the volume errors. To satisfy these conditions with an initial siRNA solution with concentration $10\ \mu\text{M}$, the siRNA amount added to form complexes is calculated to be $2.63\ \mu\text{L}$. In part **B**, the polymer amount added to the complex formation medium to give a 4 or 8 siRNA:polymer weight ratio from a stock solution of $1\ \mu\text{g}/\text{mL}$ is calculated to be 1.47 and $2.95\ \mu\text{L}$ respectively. In Part **C**, the study groups and reagent

amounts are summarized, and the amount of 150 nM NaCl added to obtain a final volume of 35 μ L complex formation volume is calculated.

Table 8 Preparation of siRNA-Polymer complexes, concentrations, volumes and amounts for 25 nM siRNA concentration in tissue culture medium and siRNA:polymer ratios 1:4 and 1:8. A. Calculations for the siRNA amount added to the complexation medium. B. Calculations for the polymer amount added to the complexation medium. C. Experimental groups and summary of reagent amounts added to the complexation medium.

A	siRNA stock solution	10000 nmol/L	0.14000 / μ L			
	Amount added	5.26E-06 L	2.63 μ L			
	Amount of complex sol. added to well	1.00E-05 L	10 μ L			
	Total amount of complex solution	7.00E-05 L	35 μ L			
	Medium Volume	3.00E-04 L	0.3 mL			
	Concentration in complex solution	751 nmol/L	0.0105 μ g/ μ L			
	Concentration in wells	25 nmol/L	0.351 μ g/mL			
B	Polymer-Working Concentration	1 μ g/ μ L	1 μ g/ μ L			
	Amount added	1.47 μ L	2.95 μ L			
	Amount of complex soln. added to well	10 μ L	10 μ L			
	Total amt. of complex solution	35 μ L	35 μ L			
	Medium Volume	0.3 mL	0.3 mL			
	Concentration in complex solution	0.042 μ g/ μ L	0.084 μ g/ μ L			
	Final Concentration in Medium (weight)	0.42 μ g	0.84 μ g			
	Final Concentration in Medium (weight)	1.40 μ g/mL	2.80 μ g/mL			
	Final Concentration in Medium (molar)	0.21 nmol	0.42 nmol			
	Final Concentration in Medium (molar)	7.01E-04 nmol/L	1.40E-03 nmol/L			
siRNA:polymer Ratio (weight)	4.00	8.00				
C	ratio 4	Group	NaCl	siRNA	Polymer	Total
	1	NT GFP Cells	35.0			35.00
	2	NT WT Cells	35.0			35.00
	3	PEI25-csiRNA	30.9	2.63	1.48	35.00
	4	PEI25-GFP-siRNA	30.9	2.63	1.48	35.00
	5	PEI-CA-csiRNA	30.9	2.63	1.48	35.00
	6	PEI-CA-GFP-siRNA	30.9	2.63	1.48	35.00
	7	PEI-LA-csiRNA	30.9	2.63	1.48	35.00
	8	PEI-LA-GFP-siRNA	30.9	2.63	1.48	35.00
	ratio 8					
	9	NT GFP Cells	35.0			35.00
	10	NT WT Cells	35.0			35.00
	11	PEI25-csiRNA	29.4	2.63	2.95	35.00
	12	PEI25-GFP-siRNA	29.4	2.63	2.95	35.00
	13	PEI-CA-csiRNA	29.4	2.63	2.95	35.00
	14	PEI-CA-GFP-siRNA	29.4	2.63	2.95	35.00
15	PEI-LA-csiRNA	29.4	2.63	2.95	35.00	
16	PEI-LA-GFP-siRNA	29.4	2.63	2.95	35.00	

3.5. GFP silencing:

The siRNA against GFP and the scrambled control siRNA were purchased from Qiagen (GFP-22 Cat #: 1022064, Qiagen). The silencing results in terms of decrease in GFP expression were analyzed using flow cytometer. The anti-GFP siRNA sequences were:

sense: GCA AGC UGA CCC UGA AGU UCA U

anti-sense: GAA CUU CAG GGU CAG CUU GCC G

The scrambled siRNA's sequence used as a negative control was not disclosed by the manufacturer (Silencer® Negative Control #1 siRNA, Cat #: AM4635, Ambion).

3.6. Flow cytometry analysis

After treatment of cells by incubation with the complexes, the cells were washed twice with Hank's Balanced Salt Solution (HBSS) and fixed with 3.7% formalin. The samples were analyzed for GFP expression using Beckman Coulter Cell Lab Quanta™ SC flow cytometer. The threshold for no expression was determined using wild type cells and the location and mean of the GFP peak was determined using the no treatment GFP expressing cells. The silencing of GFP with complexes of different polymers was analyzed relative to the scrambled siRNA containing counterparts. For clarity and precision, both the mean GFP fluorescence and the cell percentage that is out of the main GFP peak were analyzed (see **Figure 12**).

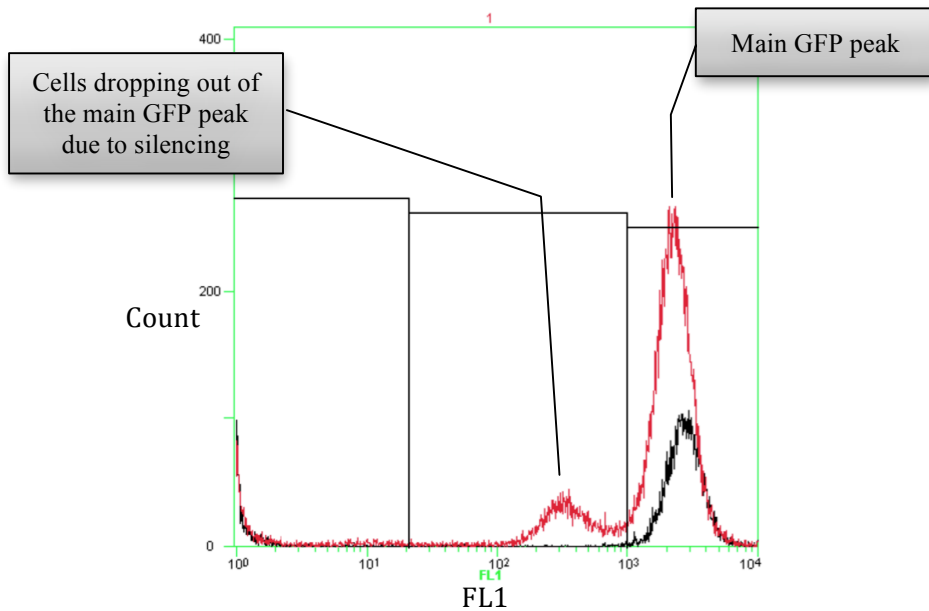


Figure 12 Overlaid histograms for GFP silencing in Hut78 cells. The black line represents the control (scrambled) siRNA treated GFP positive Hut78 cells and the red line represents anti-GFP siRNA treated GFP positive Hut78 cells.

3.7. Cytotoxicity assays

Hut78 cells grow strictly in suspension causing the handling of the cells such as centrifugation and the medium removal to interfere with the sensitivity of the cytotoxicity assays, hence several cell viability and apoptosis assays were performed on these cells to find the most sensitive assay that gives the best results.

Several siRNAs were explored for their ability to induce cytotoxicity in Hut78 cells. The potentially cytotoxic siRNAs used in this study are listed in **Table 9**.

Table 9 Information on cytotoxic siRNAs used

Gene name	Symbol	Source	Cat# / ID#
The kinesin spindle protein	KSP (KIF11)	Ambion	AM16708 / 14672
Cyclin-dependent kinase 18	CDK18 (PCTK3)	Ambion	AM16708 / 202296
Mitogen-activated protein kinase	MAP (ERK1-2)	Ambion	AM16708 / 143171
Ribosomal Protein S	RPS (RPS6KA5)	Ambion	AM16708 / 580
Fms-related tyrosine kinase 3	STK (FLT3)	Ambion	AM16708 / 425
Signal transducer and activator of transcription 3	STAT3-1	Qiagen	S100048363
	STAT3-2	Qiagen	S100048370
	STAT3-7	Qiagen	S102662338
	STAT3-8	Qiagen	S102662898
Phosphatidylinositol-4,5-bisphosphate 3-kinase	PI3K (PI3KCB)	Ambion	AM16708 / 144255
B-cell CLL/ lymphoma 11B	Bcl11b	Ambion	AM16708 / s224631

3.7.1. AlamarBlue® assay

AlamarBlue® assay was tried as an alternative to MTT assay for its success and sensitivity in suspension cells due to being water-soluble, thus bypassing the centrifugation and resolution steps, and avoiding any cell loss and variation introduced in these steps. For AlamarBlue® assay, cells were seeded onto non-tissue culture treated either 48 or 96 well plates (at volumes of 200 and 100 μ L respectively). After 72 hours of incubation with the complexes, AlamarBlue® solution was added at 5% (v/v) (5 μ L for 100 μ L medium in 96 well plates and 10 μ L for 200 μ L medium in 48 well plates) and was incubated at 37 °C for 2 hours. After the incubation time was complete, the fluorescence was read at 536 nm excitation and 604 nm emission using a fluorescence plate reader (Fluoroskan Ascent; Thermo Labsystems), and relative cell viability (%) was determined by normalizing to the absorbance of untreated or control siRNA treated cells.

3.7.2. Trypan Blue Assay and Cell Counting

Trypan Blue assay was performed as an alternative to mitochondrial reduction based viability assays MTT and AlamarBlue®. For this, 10 μ L of 0.4% Trypan Blue dye was mixed with 10 μ L of cell samples in a 0.5 mL eppendorf tube, and allowed to equilibrate for 1-2 minutes. 10 μ L of the Trypan blue-cell mix was loaded onto a hemocytometer and

counted for the amount of Trypan blue positive blue (dead) and Trypan blue negative clear (viable) cells. The % non-viable cells were calculated as number of Trypan blue positive cells divided by the total number of cells. Also, total and viable cell numbers in wells were calculated as follows:

Total Cell Number: (total count/number of squares counted) x 2 (dilution factor) x 10^4 x volume of wells,

Viable Cell Number: (viable cell count/number of squares counted) x 2 x 10^4 x volume of wells.

3.7.3. FlowTACS™ Apoptosis Detection

Trevigen's FlowTACS™ Apoptosis Detection Kit utilizes terminal deoxynucleotidyl transferase (TdT) to incorporate biotinylated nucleotides to the DNA that is fragmented during apoptosis, which is detected with streptavidin-FITC using a flowcytometer. The cells were seeded to 24 well plates at 300 μ L, a total of 6 wells per treatment group were used but 72 hours after the complex addition 3 wells were combined into a single eppendorf and the apoptosis assay was performed in duplicate. The assay was performed as instructed by the manufacturer (without the use of propidium iodide) and the FITC showing apoptosis was quantified using Beckman Coulter Cell Lab Quanta™ SC flow cytometer as mean fluorescence of FL1 (green) channel as well as percent gated. Relative apoptosis (%) were determined by normalizing to positive controls prepared as instructed in the instructions of the manufacturer.

3.7.4. FITC Annexin V Apoptosis Detection

BD Pharmingen's FITC Annexin V Apoptosis Detection kit detects the membrane phospholipid phosphatidylserine (PS) that is translocated from the inner to the outer leaflet of the plasma during apoptosis using FITC conjugated Annexin V for detection of apoptosis. Propidium iodide (PI) is additionally employed that is excluded from viable

cells but uptaken by dead cells. The cell staining by these markers is detected by flow cytometry. The cells were seeded to 24 well plates at 300 μ L, a total of 6 wells per treatment group was used but 2 wells were combined into a single eppendorf and the apoptosis assay was performed as triplicates. The assay was performed 24, 48 and 72 hours after complex addition as instructed by the manufacturer, and the FITC and PI showing apoptosis was quantified using BD LSR Fortessa™ cell analyzer. The relative early apoptotic cells (%) was determined as only FITC positive cells (FITC⁺, PI⁻), relative late apoptotic cells (%) was determined as both FITC and PI positive cells (FITC⁺, PI⁺), relative apoptotic cells (%) was determined as either PI or PI and FITC positive cells (PI⁺ or FITC⁺, PI⁺), and relative viable cells (%) was determined as both PI and FITC negative cells (FITC⁻, PI⁻).

3.8. Statistical Analysis

Several statistical tests were performed on the results for different purposes,

Percent of control: A qualitative measure of test compound activity

$$POC = \frac{x_i}{\bar{c}} \times 100$$

where x_i is the raw measurement on the i^{th} compound and \bar{c} is the mean of the measurements on the negative controls, meaning scrambled siRNA treated samples [62]. The critical value of POC was determined to be 80, meaning 80% cell viability respective to the control was considered to be a 'hit'.

z-score: is a simple normalizing score, this was applied in siRNA library screenings to identify targets whose reaction to the treatment is different than the general population. Specifically in this case the wells having lower cell viability than the rest of the plate, due to the given siRNA were identified using z-score calculated as:

$$Z = \frac{x_i - \bar{x}}{s_x}$$

where: x_i is the raw measurement on the i^{th} compound, and \bar{x} and s_x are the mean and the standard deviation, respectively, of all measurements within the plate [62]. The critical z-score was determined to be 1.96 (95% confidence or $p < 0.05$).

One sided t-test (T): With K replicates, for each compound a Student t statistic is

$$T = \frac{\bar{x} - cons}{s\sqrt{1/K}}$$

where \bar{x} and s are the arithmetic mean and the standard deviation, respectively, of the K replicate measurements, $cons$ is a constant typically equal to zero. T follows a T-distribution with K-1 degrees of freedom [62]. In our studies, the constant was determined as 1 as all the data was normalized to the control group, giving the control group the value of 1, and K as 3 as all the experiments were in triplicates. The critical T-score was determined to be 2.9 (95% confidence or $p < 0.05$).

Two sided t-test (t): Two sided t-test is used to determine if two sets of data are significantly different than each other. The t-test was applied to determine the significance of the difference between the control and treatment groups. t-score is calculated as:

$$t = \frac{\bar{x}_1 - \bar{x}_2}{S_{x_1x_2}\sqrt{2/n}}$$

$$\text{and: } S_{x_1x_2} = \sqrt{\frac{1}{2}(s_{x_1}^2 + s_{x_2}^2)}$$

where \bar{x}_1 and \bar{x}_2 are the means and s_{x_1} and s_{x_2} are the standard deviations of the two groups in question and $S_{x_1x_2}$ is the grand standard deviation [63]. For significance testing, the critical t-score was determined to be 4.3 (95% confidence or $p < 0.05$).

4. Results and Discussion

Part I: GFP Silencing with Lipid-modified PEI

4.1. FAM-labelled siRNA uptake

Two specific polymers have shown superior delivery efficiency in other cell lines [64]. These were 2PEI-CA20 (6.9 CAs/PEI) that has the shortest lipid, Caprylic Acid, modification and the highest substitution ratio, and 2PEI-LA (2.1 LAs/PEI) that has the longest lipid with two double bonds, Linoleic Acid, modification. These CA and LA modified PEI, PEI-CA and PEI-LA respectively, were inspected for their ability to deliver siRNA into wild-type Hut78 cells using FAM-labeled non-silencing (scrambled) siRNA at siRNA:polymer weight ratios 1:2, 1:4 and 1:8. The FAM-labeled siRNA do not give any cell uptake in the absence of a carrier (not shown). The results are summarized in **Figure 13**. Two sided t-test was used to determine the significance of the differences.

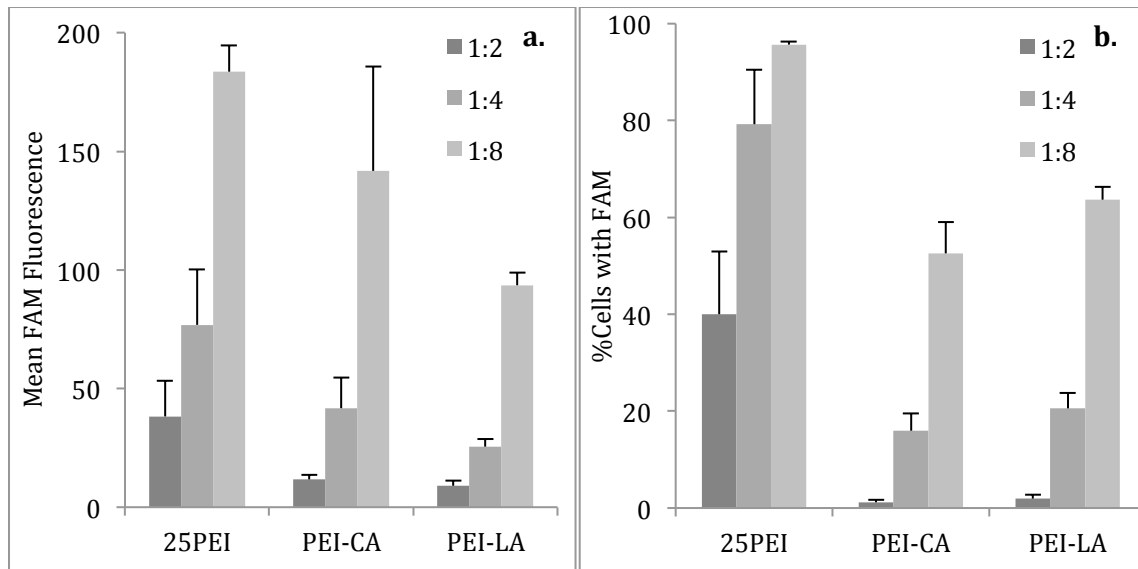


Figure 13 FAM-labeled siRNA uptake by Hut78 cells treated with 25PEI, PEI-CA, PEI-LA complexes at siRNA:polymer ratios 1:2, 1:4 and 1:8. The siRNA concentration in wells was 25 nM and polymer concentration in medium was 0.70 $\mu\text{g/mL}$ (1:2), 1.40 $\mu\text{g/mL}$ (1:4) and 2.80 $\mu\text{g/mL}$ (1:8). The samples were analyzed for FAM fluorescence using flow cytometer after 24 hours of incubation with the complexes. The data (mean \pm SD) is summarized in terms of mean FAM fluorescence per cell (a) and percentage of cells fluorescent with FAM (b).

According to **Figure 13**, 25PEI showed superior uptake at ratio 1:2, while PEI-CA and PEI-LA did not give any uptake at all. At ratio 1:4, again 25PEI gave the best uptake, and PEI-CA and PEI-LA gave some uptake, that was equivalent between these two lipid-substituted polymers, but significantly lower than 25PEI. At ratio 1:8, 25PEI again displayed the best uptake; PEI-CA and PEI-LA gave similar uptake at this ratio as well, which was still lower than the uptake by 25PEI. These conclusions were similar whether the uptake was quantitated based on mean siRNA uptake (**Fig. 13a**) or the percentage of cells positive for siRNA (**Fig. 13b**). Ratios higher than 1:8 were not attempted since that might lead to unspecified cell toxicities.

The delivery efficiencies of PEI-CA and PEI-LA were shown to be similar to each other while they were significantly lower than that of 25PEI. However, this does not necessarily mean that PEI-CA and PEI-LA were inferior to 25PEI as there are other factors that contribute to silencing efficiency (e.g., cytotoxicity on cells, ability for the siRNA to dissociate once inside the cells, etc.).

In addition, while 25PEI has shown $40.0 \pm 12.9\%$ uptake at 1:2 siRNA:polymer ratio, the lipid modified PEI, PEI-CA and PEI-LA showed almost no uptake suggesting that 1:2 siRNA:polymer ratio might be too low for PEI-CA and PEI-LA to mask the negative charge of the siRNA, while 25PEI succeeded to mask all the negative charges due to the length of the polycation, and hence having much higher amounts of positively charged moieties (amines).

The beneficial effect of LA might be attributed to (i) the hydrophobic chain length (C18) that increases the hydrophobicity of the particle causing better interaction with the cell membrane and (ii) presence of two double bonds, causing the hydrophobic tails of the lipids to be bent, and interfering with the packaging that results in a more flexible construct that can pass more freely through the cell membrane. The presence of double bonds in the membrane phospholipids cause an increase in the fluidity of the cell membrane, due to the more loose packing of the lipids in the bilayer. Similarly, the presence of the double bonds in the hydrophobic parts of the complexes has the same effect conferring flexibility and easier passage. So the double bond bearing LA introduces

fluidity to the complex and decreases the packaging as the bending of the tails interfere with the tight packaging meaning there is more “space” in the complex. The more empty space in the complexes means there is more disorder that enables solutes, which is the siRNA in this case, to penetrate into the cell membrane easier.

4.2. Polymer library screening

A select set of PEI polymers modified with several lipids, including Caprylic, Myristic, Palmitic, Stearic, Oleic and Linoleic Acids at different levels of substitutions were inspected for their ability to deliver and silence GFP in Hut78 cells at siRNA:polymer weight ratios 1:4 and 1:8. The silencing data for each polymer is shown in **Figure 14**; silencing efficiency was summarized as the percentage of cells with reduced GFP expression (**Figure 14a**) or the mean decrease in GFP fluorescence (**Figure 14b**). Note that the silencing data in **Figure 15** (mean GFP silencing) was obtained by normalizing the treatment groups against no treatment group. Some of the study groups gave negative silencing values, which implies that the GFP fluorescence in the treatment group was higher than the no treatment group (i.e., an indication of non-specific autofluorescence due to complex exposure). Two sided t-test was used to determine the significance of the differences.

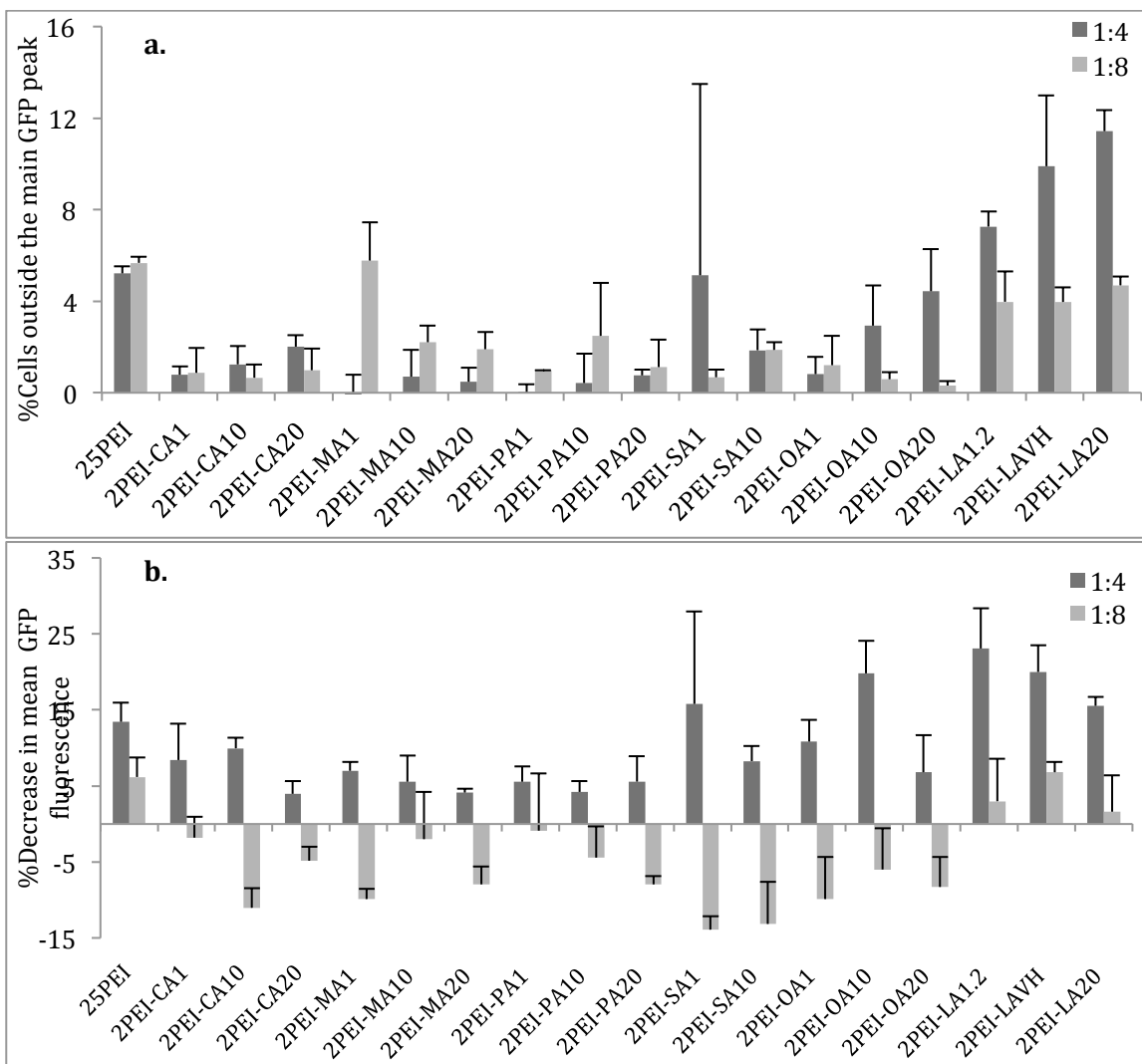


Figure 14 Percentage of Hut78 cells outside the main GFP peak (a) and percent decrease in mean GFP fluorescence (b) 72 hours after treatment with anti-GFP siRNA complexes at siRNA:polymer ratios 1:4 and 1:8. The siRNA concentration in wells was 25 nM and polymer concentration in medium was 1.40 $\mu\text{g}/\text{mL}$ (1:4) and 2.80 $\mu\text{g}/\text{mL}$ (1:8). The samples were analyzed for GFP expression using flow cytometry after 72 hours of incubation with the complexes. No control (scrambled) siRNA was used in this study, as the aim was to compare the polymers with each other rather than quantification of silencing.

Based on the data in **Figure 14**, 25PEI has shown superior silencing efficiency among the polymers at both ratios 1:4 and 1:8. PEI-CA constructs were not efficient in silencing in terms of cell percentage outside the main GFP peak, but were comparable to 25PEI in terms of mean GFP fluorescence at ratio 1:4, except for the highest CA substitution (PEI-

CA20). PEI-MA constructs were also inefficient in GFP silencing except for the lowest MA substitution at 1:8 ratio in terms of cell percentage outside the main GFP peak, which was comparable to 25PEI. PEI-PA constructs gave similarly insignificant silencing efficiency at every substitution ratio. The efficiency of lower lipid substitution ratio of PEI-SA was inconsistently high with a very high variation, while the higher substitution ratio was slightly better than PEI-MA and PEI-PA at ratio 1:4, but still significantly lower than that of 25PEI at both 1:4 and 1:8 ratios. PEI-OA constructs showed comparable silencing efficiency to 25PEI at ratio 1:4 except for the lowest OA substitution in terms of cell percentage outside the main GFP peak and except for the highest OA substitution in terms of reduction in mean GFP fluorescence. However they failed to show such efficiency at ratio 1:8. It is possible that this higher ratio, despite higher uptake, resulted in non-specific toxicity and prevented effective GFP silencing. The PEI-LA constructs have shown comparable or even higher efficiency to that of 25PEI at both ratios in terms of both cell percentage outside the main GFP peak and mean GFP silencing.

Figure 15 (a,b,c,d) explores the relationship between the silencing and the level of lipid substitution. In **Figure 15a**, it is seen that most PEI-lipid constructs show similar efficiency in general, while PEI-LA is the only construct that separates from the rest of the polymers and is comparable to or higher than 25PEI in all cases. Also PEI-LA has higher efficiency at ratio 1:4 in terms of cell percentage outside the main GFP peak (**Figure 15a**) (i.e., cell population displaying GFP silencing) and all polymers have higher efficiency at ratio 1:4 in terms of mean GFP fluorescence (**Figure 15c**). The negative silencing values were particularly noticeable with 1:8 siRNA:polymer ratio, indicating possible cytotoxicity at this ratio (**Figure 15b**). The cytotoxicity of the complexes causes the cells to have an autofluorescence at the FL1 channel of flow cytometry, the same channel used to quantify GFP expression, resulting in a noise that looks as if the GFP fluorescence has been increased.

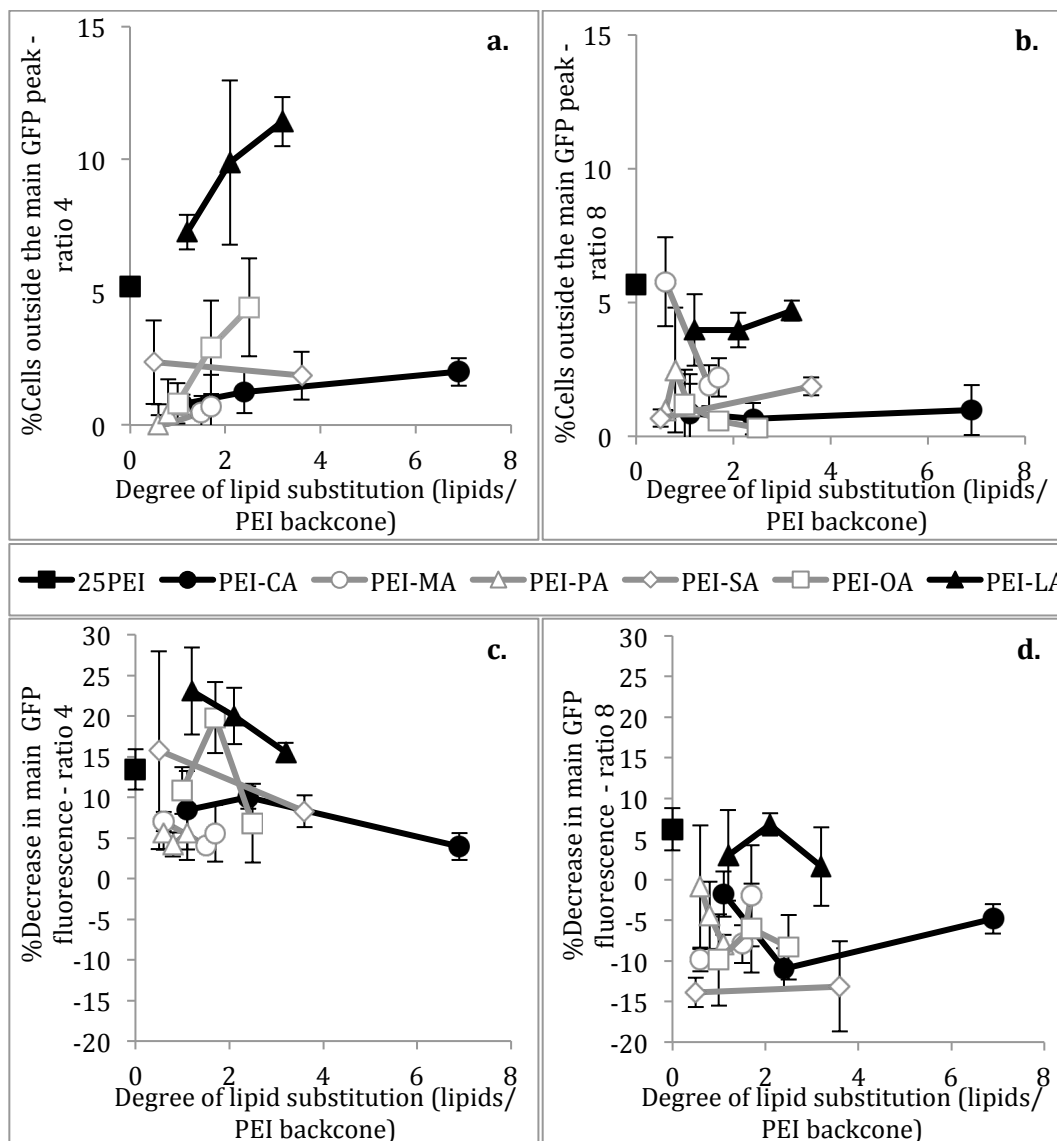


Figure 15 Correlation between the percentage of silenced Hut78 cells (a and b) and mean GFP fluorescence (c and d) and the polymer substitution ratios. The siRNA:polymer ratios were 1:4 (a and c) and 1:8 (b and d). The siRNA concentration in wells was 25 nM and polymer concentration in medium was 1.40 $\mu\text{g}/\text{mL}$ (1:4) and 2.80 $\mu\text{g}/\text{mL}$ (1:8). The original data is shown in Figure 14A and the extent of lipid substitutions were previously reported [52].

The fact that scrambled siRNA treated control group was omitted in this study to better calibrate the data was a significant shortcoming in hindsight. As the auto-fluorescence caused by each polymer was expected to be different, it is hard to draw a very solid conclusion such as absolute silencing values. However, we considered the silencing based on reduction in GFP-expression cell population more reliable and, based on this, the

Linoleic acid modified PEI (PEI-LA) have shown superior efficiency to others at both ratios, and therefore were chosen to be used in the future studies. The Caprylic acid modified PEI (PEI-CA) was also chosen to be used in the future studies alongside PEI-LA as it was the most stable polymer in terms of having low well-to-well variation, and had the highest rate of substitution as well as having superior efficiency in other cell lines used in the lab [64]. Using PEI-CA also served for the purpose of ‘modification’ control, where the specific effect of LA substitution was better revealed (i.e., compared to a generic substitution such as CA).

Stearic acid (PEI-SA) and Oleic acid (PEI-OA) modified PEI having the same length of hydrophobic tail as Linoleic acid (C18) modified PEI were not as efficient, implying that the extra double bond(s) in the Linoleic acid increases the silencing efficiency. Myristic acid (PEI-MA), Palmitic acid (PEI-PA) modified PEI, having intermediate lengths of hydrophobic tails (C14 and C16), showed very similar efficiency that is lower than PEI-SA, PEI-OA and PEI-LA suggesting that the length of the substituted lipid’s hydrophobic tail plays an important role as well. As a result, it can be concluded that there are two factors that have a positive effect on the efficiency of the carrier, the length of the substituted lipid’s hydrophobic tail, and the presence of double bonds in the hydrophobic moiety.

To further explore this concept, PEI constructs bearing longer lipids, or lipids with more double bonds can be used. Lipids like docosahexaenoic acid (C22:6) that has higher amounts of double bonds in the hydrophobic tail and longer than LA can be anchored to the PEI and tested for their efficiency.

4.3. Time course response to GFP siRNA

The GFP positive Hut78 cells were treated with anti-GFP siRNA complexed with 25PEI, PEI-CA20 and PEI-LA20 at siRNA:polymer weight ratios 1:4 and 1:8 and their efficiency was assessed at 24, 48 and 72 hours after complex addition. The results are shown in **Figure 16**. Due to the previously observed autofluorescence values, this study incorporated cells treated with scrambled siRNA complexes and all results with anti-GFP

treatments were normalized against the corresponding control treatments. Two sided *t*-test was used to determine the significance of the differences.

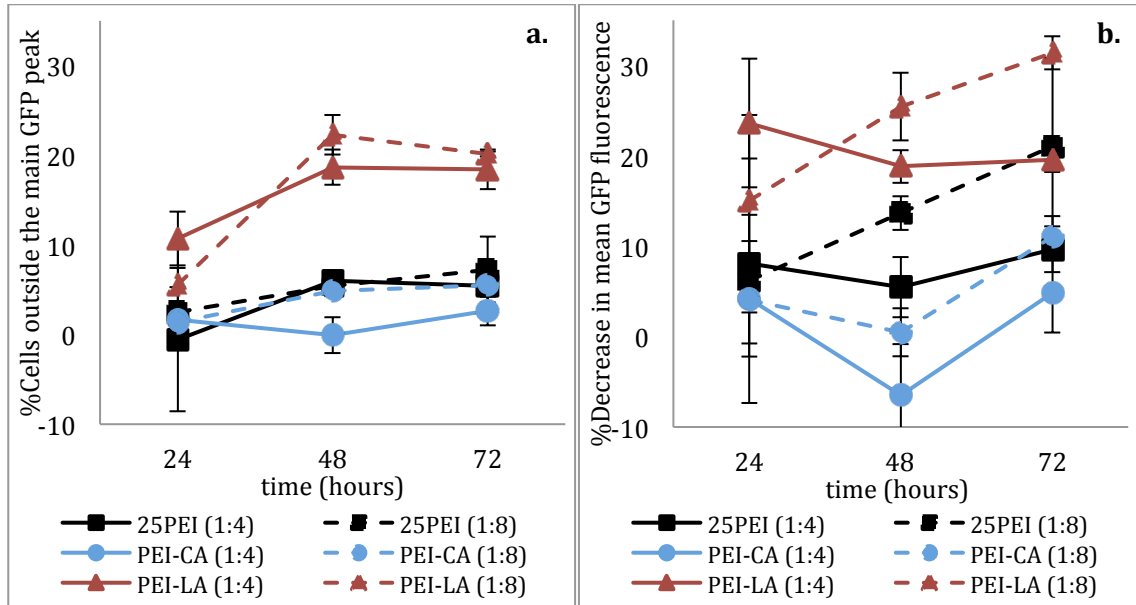


Figure 16 Percentage of Hut78 cells outside the main GFP peak (a) and percent decrease in mean GFP fluorescence (b) 24, 48 and 72 hours after treatment with anti-GFP siRNA complexes at siRNA:polymer ratios 1:4 and 1:8. The siRNA concentration in wells was 25 nM and polymer concentration in medium was 1.40 $\mu\text{g}/\text{mL}$ (1:4) and 2.80 $\mu\text{g}/\text{mL}$ (1:8). GFP fluorescence was measured by flow cytometry 24, 48 and 72 hours after the complex addition. The results were normalized to the control (scrambled siRNA treated) groups.

Based on percentage of silenced cells in **Figure 16a**, 25PEI and PEI-CA were not efficient after 24 hours, while PEI-LA was more efficient than both 25PEI and PEI-CA. The difference was significant (by two-tailed *t*-test) only at ratio 1:4. At 48 hours, 25PEI and PEI-CA, although slightly better than the previous time point except for PEI-CA at ratio 1:4, gave low silencing (approximately 5%), while PEI-LA gave significant silencing efficiency at $18.7 \pm 2.0\%$ and $22.3 \pm 2.2\%$ at ratios 1:4 and 1:8, respectively. At 72 hours, 25PEI and PEI-CA still gave low silencing, while PEI-LA gave significant efficiency similar to its efficiency at 48-hour time point at both ratios 1:4 and 1:8.

Based on the mean GFP silencing in **Figure 16b**, only PEI-LA at ratio 1:4 was significantly more efficient than 25PEI and PEI-CA at 24 hours, while PEI-LA at 1:8 was only slightly more efficient than both 25PEI and PEI-CA but not significantly. The 25PEI and PEI-CA were not efficient at 24 hours. At 48 hours, 25PEI at ratio 1:4 and PEI-CA at both ratios were not efficient while 25PEI at ratio 1:8, PEI-LA at ratios 1:4 and 1:8 gave significant efficiencies at $13.7\pm 1.8\%$, $18.8\pm 1.8\%$ and $25.4\pm 3.7\%$ respectively. At 72 hours, PEI-CA at ratio 1:4 was not efficient, PEI-CA at ratio 1:8 and 25PEI at ratio 1:4 ($11.1\pm 2.3\%$ and $9.6\pm 2.5\%$ respectively) had slight but not significantly increased silencing compared to 48 hours. 25PEI at ratio 1:8 showed relatively high variation in silencing efficiency to be significant ($21.3\pm 9.8\%$), but not significantly higher than that of PEI-CA at ratio 1:8 and 25PEI at ratio 1:4. PEI-LA, on the other hand, showed significant efficiency at both ratios 1:4 and 1:8 ($19.5\pm 1.3\%$ and $31.4\pm 1.8\%$ respectively). The efficiency of PEI-LA at ratio 1:4 remained constant in respect to the previous time point, while it was higher than the previous time point at ratio 1:8.

The results have shown that siRNA silencing is a dynamic process possibly due to the dynamics nature of GFP; i.e., GFP fluorescence drops as the protein is hydrolyzed and/or denatured and there is no or little new translation resulting in decreased level of GFP and in turn decreased fluorescence. It was concluded that assessment after 48 hours gives the best results in terms of percentage of cells silenced and assessment after 72 hours gives the best results in terms of decrease in the mean GFP fluorescence. While PEI-LA is significantly superior to both 25PEI and PEI-CA in terms of silencing efficiency, 25PEI and PEI-CA have similar efficiencies in terms of percentage of cells silenced, but 25PEI is slightly more efficient than PEI-CA in terms of mean GFP silencing.

The two siRNA:polymer ratios used (1:4 and 1:8) have shown similar efficiencies, except for the PEI-LA at 72 hours in terms of decrease in mean GFP silencing, suggesting that 1:4 siRNA:polymer ratio is enough to neutralize negative charge of the siRNA. PEI-LA has the least positive charge/mass ratio out of all three polymers, that might be the cause of the difference between 1:4 and 1:8 siRNA:polymer ratio at 72 hour time point. The results have shown that although 25PEI has higher delivery efficiency than both PEI-CA and PEI-LA at each ratio, the silencing efficiency of PEI-LA is significantly higher. Also

PEI-CA and PEI-LA had similar delivery efficiencies while PEI-LA was more efficient in terms of silencing. These findings suggest that the delivery efficiency does not necessarily determine the silencing efficiency of the complexes, but there might be additional factors that may play role in determining the silencing efficiency. The beneficial effect of the LA can be attributed to endosomal escape. Similar to the cell membrane case, where LA introduces fluidity to the membrane for easier passage, as the endosome is also a membrane, LA facilitates the passage of the siRNA into the cytosol by introducing fluidity to the endosomal membrane.

4.4. Response to Multiple anti-GFP siRNA Treatments

The siRNA induced silencing is expected to be a temporary process, so that when the silencer (siRNA) is removed, the gene expression is expected to return back to its former value. It is possible to have an additive effect or preserve the effect by applying several doses of the complexes over set intervals. It has been shown in other cell lines (leukemia) in the Uludag lab that the effect of siRNA induced silencing is seen most pronounced at day 3 and the effect is lost after 9 days [64]. For this study, the interval between the complex additions was chosen to be 3 days and the effect of single vs. repetitive doses were examined over a 9 day period. The results are summarized in **Figure 17**. Two sided t-test was used to determine the significance of the differences.

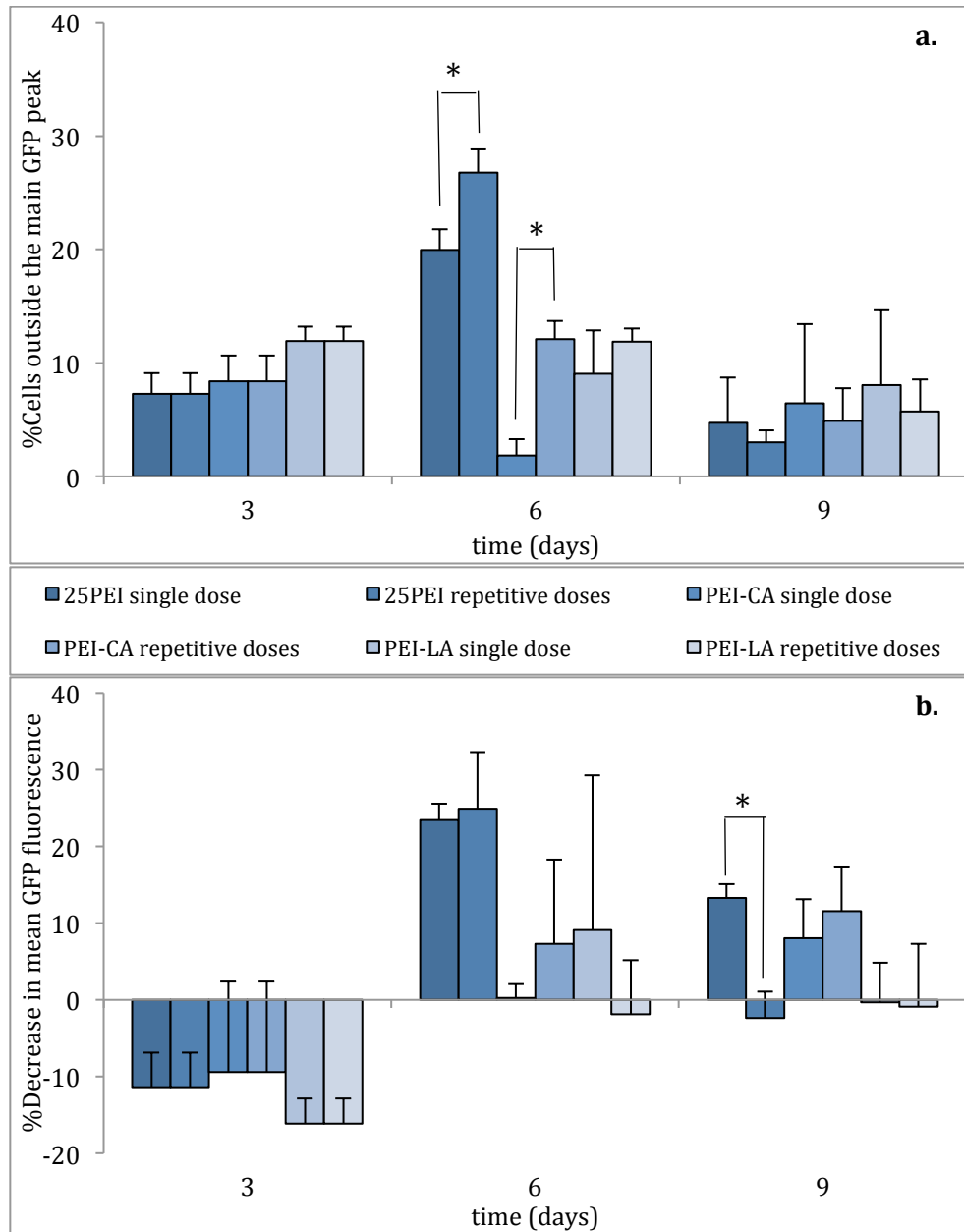


Figure 17 Effect of repeated treatments of cell with siRNA:polymer complexes in terms of percentage of cells silenced (a) and mean GFP silencing (b). The cells were harvested, the medium was removed and the cells were re-seeded before the addition of the complexes for repeat treatment groups. 25PEI, PEI-CA (2PEI-CA20) and PEI-LA (2PEI-LAVH) were used at siRNA:polymer weight ratio 1:4 and siRNA concentration in wells was 25 nM while polymer concentration in medium was 1.40 $\mu\text{g/mL}$.

Based on percentage of cells silenced in **Figure 17a**, all polymers (whether single dose over a 3 day period or repetitive doses every 3 days) showed similar efficiency at 7 to 12%, PEI-LA being the most efficient on day 3 ($11.9 \pm 1.3\%$). On day 6, 25PEI showed

increased efficiency than that of day 3 in both single ($19.9\pm 1.9\%$) and repetitive ($26.7\pm 2.1\%$) doses, repetitive dose being significantly ($p<0.05$) higher. On day 6, PEI-CA showed decreased effect on single dose ($1.8\pm 1.1\%$) and increased effect on repetitive dose ($12.1\pm 1.6\%$), repetitive dose being significantly ($p<0.05$) more efficient than single dose. PEI-LA, on the other hand, showed comparable efficiency in both single ($9.0\pm 3.8\%$) and repetitive doses ($11.9\pm 1.2\%$) that was similar to day 3 ($11.9\pm 1.3\%$). On day 9, all polymers, whether single (25PEI: $4.7\pm 4.0\%$, PEI-CA: $6.4\pm 7.0\%$, PEI-LA: $8.0\pm 6.6\%$) or repetitive (25PEI: $3.0\pm 1.0\%$, PEI-CA: $4.9\pm 2.9\%$, PEI-LA: $5.7\pm 2.8\%$) doses, showed decreased silencing effects, which was considered minimal compared to the background. The efficiencies and response for all polymers were very similar. The data was not normalized using control siRNA treated groups, as the aim was to evaluate the additive effect rather than actual silencing, resulting in underestimation of the values.

Based on the mean GFP silencing in **Figure 17b**, none of the polymers were efficient on day 3 – note that all values were negative for this time point indicating significant autofluorescence due to complex exposure, as no control siRNA group was used to calibrate the data. On day 6, 25PEI showed increased efficiency at both the single ($23.5\pm 2.1\%$) and repetitive ($24.9\pm 7.4\%$) doses. The efficiency of PEI-CA and PEI-LA were also higher compared to day 3, but it was similar between the single (PEI-CA: $0.3\pm 1.8\%$, PEI-LA: $9.1\pm 20.1\%$) and repetitive (PEI-CA: $7.3\pm 11.0\%$, PEI-LA: $-1.9\pm 7.1\%$) doses with high variation in some groups. On day 9, the efficiency of 25PEI dropped compared to day 6 the repetitive ($-2.4\pm 3.5\%$) dose being significantly lower than the single ($13.3\pm 1.8\%$) dose, while the efficiency of PEI-CA and PEI-LA were comparable to day 6 and similar between single (PEI-CA: $0.3\pm 1.8\%$, PEI-LA: $9.1\pm 20.1\%$) and repetitive (CA: $0.3\pm 1.8\%$, LA: $9.1\pm 20.1\%$) doses.

The significant differences between single dose and repetitive dose groups was seen on 6th day in the cells treated with 25PEI and PEI-CA in terms of cell percentage outside the main GFP peak, though the differences had disappeared on 9th day, presumably due to the toxicity of the complexes. All single dose effect was lost on day 9 supporting the idea that siRNA induced silencing is temporary. Meaning as the repetitive treatment has failed to

be efficient; the primary silencing achieved by the first dose of treatment has been lost at the end of 9 days.

The effect of the treatment did not change significantly in PEI-LA treated groups over the 9 days whether the treatment was single or repetitive. The reason could be the mode of internalization of the complexes or the effect of the polymer on the cells. The increase in the efficiency of 25PEI on day 6 in both study groups could be due to the fact that each polymer has a different way and rate of action, causing the effect of siRNA to be seen at different time points.

4.5. FAM-labelled siRNA Uptake in Jurkat cells

The two selected polymers PEI-CA and PEI-LA (2PEI-CA20 and 2PEI-LAVH; **Table 7**) were inspected for their ability to deliver siRNA into wild-type Jurkat cells to compare the efficiencies of polymers in a different cell line. Jurkat cells were selected because these two cell lines are frequently used together due to their similarities (eg. surface antigens, chemokines produced, group of T-cell malignancies). FAM-labeled non-silencing siRNA was delivered to Jurkat cells at siRNA:polymer weight ratios 1:2, 1:4 and 1:8. The results are summarized in **Figure 18**. Two sided t-test was used to determine the significance of the differences.

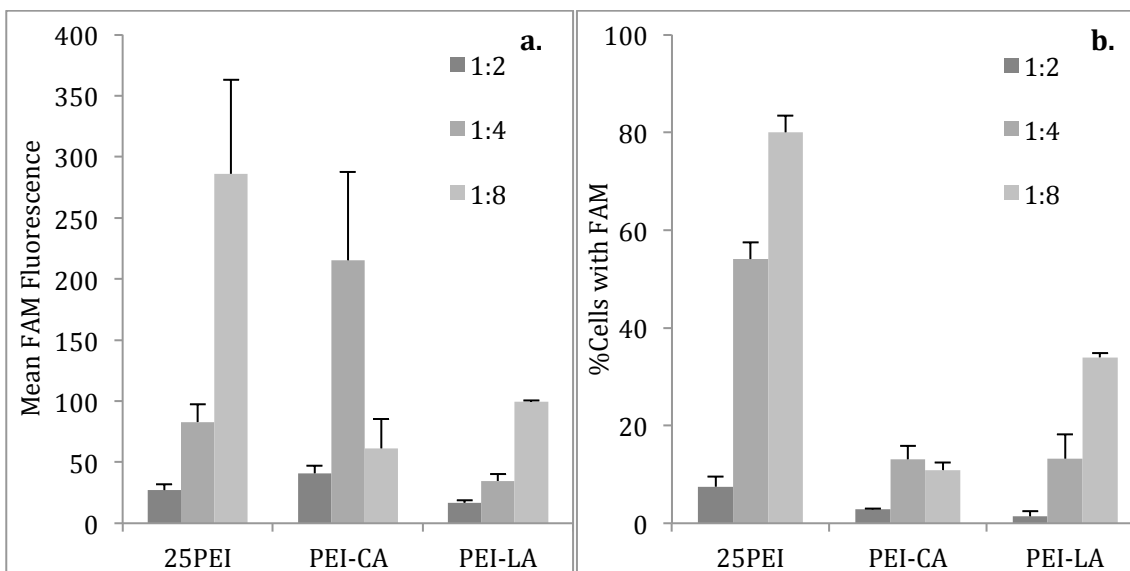


Figure 18 FAM-labeled siRNA uptake by Jurkat cells treated with 25PEI, PEI-CA, PEI-LA complexes at siRNA:polymer ratios 1:2, 1:4 and 1:8. The siRNA concentration in wells was 25 nM and polymer concentration was 0.70 $\mu\text{g/mL}$ (1:2), 1.40 $\mu\text{g/mL}$ (1:4) and 2.80 $\mu\text{g/mL}$ (1:8). The samples were analyzed for FAM fluorescence using flow cytometry after 24 hours of incubation with the complexes. The data (mean \pm SD) is shown in terms of mean FAM fluorescence (a) and percentage of cells fluorescent with FAM (b).

At siRNA:polymer ratio of 1:2, none of the polymers gave significant uptake. At ratio 1:4, 25PEI gave the best result in terms of cell percentage displaying uptake ($54.1 \pm 3.5\%$), which was not very pronounced in terms of mean siRNA uptake (mean fluorescence of 82.9 ± 14.4), but still significant, while PEI-CA was the best in terms of mean siRNA uptake (mean fluorescence of 215.1 ± 72.7), which was not very pronounced in terms of cell percentage displaying uptake ($13.1 \pm 2.8\%$). The siRNA delivery by the PEI-LA was minimal and not significant at this ratio (39.8 ± 8.7 for mean fluorescence and $13.2 \pm 5.0\%$ for percentage). At ratio 1:8, 25PEI was again the best in terms of both mean fluorescence (288.1 ± 76.9) and cell percentage ($80.0 \pm 3.4\%$). The PEI-CA lost efficiency at this ratio as compared to ratio of 1:4 in terms of mean fluorescence (61.3 ± 23.9) and stayed constant in terms of cell percentage ($10.9 \pm 1.6\%$). The PEI-LA gave better uptake than PEI-CA in terms of siRNA uptake (mean fluorescence of 99.3 ± 1.1), but it was significantly less than the 25PEI.

The delivery efficiencies of all polymers were significantly lower in Jurkat cells compared to Hut78 cells based on the uptake data shown in **Figure 13**. While 25PEI was still efficient –but not as efficient as in Hut78 cells- in Jurkat cells, (79.2±11.2% at ratio 1:4 and 95.7±0.6% at ratio 1:8 in Hut78 vs 54.1±3.5% at ratio 1:4 and 80.0±3.4% in Jurkat) PEI-CA and PEI-LA failed to deliver FAM-labelled siRNA with high efficiency (PEI-CA: 15.9±3.7 at ratio 1:4 and 52.9±6.5% at ratio 1:8 in Hut78 vs 13.1±2.8% at ratio 1:4 and 10.9±1.6% at ratio 1:8 in Jurkat / PEI-LA: 20.6±3.2% at ratio 1:4 and 63.7±2.7% at ratio 1:8 in Hut78 vs 13.2±5.0% at ratio 1:4 and 34.0±0.9% at ratio 1:8 in Jurkat) . Even the best efficiency seen at PEI-LA ratio 1:8 was much lower than that of 25PEI. However, we have shown that the delivery efficiency does not necessarily translate into silencing efficiency (explained in section 4.3), but other factors are involved. Hence, the polymers might still display silencing efficiencies in this cell type and we conducted a subsequent study to explore this issue.

4.6. GFP silencing in Jurkat cells

GFP positive Jurkat cells were treated with anti-GFP siRNA complexed with 25PEI, PEI-CA20 and PEI-LA20 at siRNA:polymer weight ratios 1:2, 1:4 and 1:8 and their efficiency was assessed at 72 hours after complex addition. The results are shown in **Figure 19**. Two sided t-test was used to determine the significance of the differences.

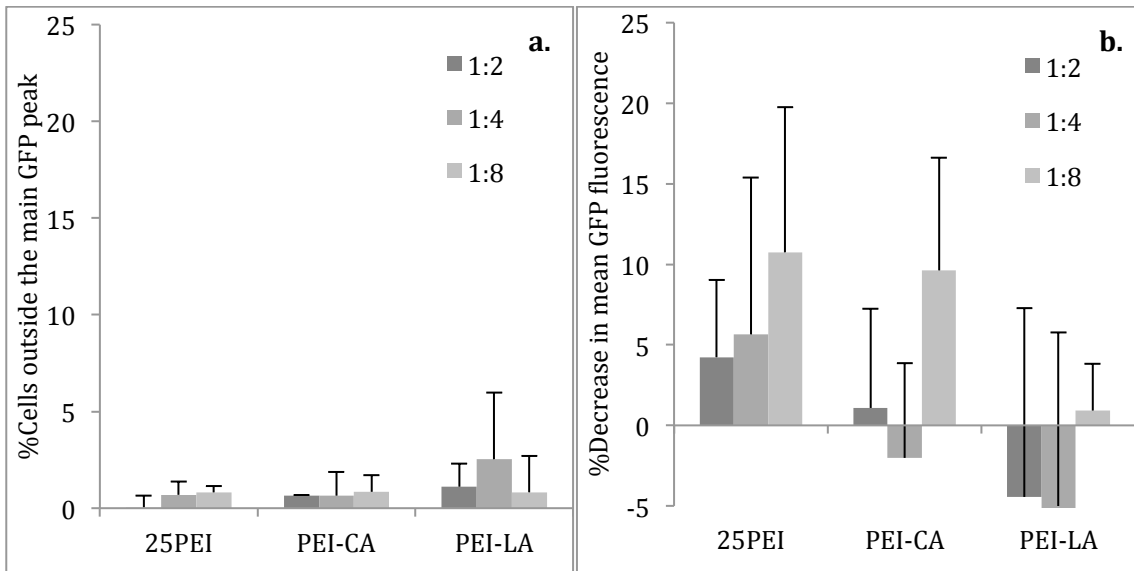


Figure 19 Percentage of Jurkat cells silenced (a) and percent GFP silencing (b) 72 hours after treatment with anti-GFP siRNA complexes at siRNA:polymer ratios 1:2, 1:4 and 1:8. The siRNA concentration in wells was 25 nM and polymer concentration in medium was 0.70 $\mu\text{g/mL}$ (1:2), 1.40 $\mu\text{g/mL}$ (1:4) and 2.80 $\mu\text{g/mL}$ (1:8). GFP fluorescence was measured by flow cytometry 72 hours after the complex addition. The results were normalized to the control (scrambled siRNA treated) groups.

Based on the percentage of cell silenced in **Figure 19**, none of the polymers were effective in GFP silencing at any of the ratios used (maximum values being 2.5% for percentage of cells silenced and 10.7% for mean GFP silencing). Based on the mean GFP silencing, some study groups gave a certain degree of silencing, but the large variation in these groups did not indicate a strong silencing effect (e.g., 25PEI at ratio 1:8: $10.7 \pm 9.0\%$ and PEI-CA at ratio 1:8: $9.6 \pm 7.0\%$). Although the PEI-CA and PEI-LA polymers have superior efficiency to 25PEI in Hut78 cells, neither modified nor unmodified (25 kDa) PEI was efficient in Jurkat cells. The difference in the efficiencies of the polymers in these two cell lines (the best efficiency seen in Hut78 was $22.3 \pm 2.2\%$ at ratio 1:4 with PEI-LA while the best efficiency seen in Jurkat was $10.7 \pm 9.0\%$ at ratio 1:8 with 25PEI) can be due to low delivery efficiency (see sections 4.1 and 4.5) as well as other cellular differences in processing the siRNA complexes. Jurkat (adult lymphoid leukemia) cells are very similar cells to Hut78 (T-cell Lymphoma) cells but Hut78 cells are more differentiated. It is possible that as Hut78 is more differentiated, the RISC pathway may be activated in Hut78 but not activated or less active in Jurkat cells causing the cells to be

not as responsive to siRNA treatment meaning delivery of higher amounts of siRNA may solve the problem or to the method used in this study meaning delivery of naked siRNA (i.e by means of electroporation) might be a better approach.

4.7. Effect of complex formation volume

It was previously suggested that increasing the volume of the complex formation would change the dynamics of complexation, resulting in smaller carriers that have higher delivery efficiency [65]. To test this hypothesis, the volume in which the polymer and siRNA is mixed was increased from 0.035 mL to 0.3 mL by adding media to the complexation medium. Also two similar LA modified constructs, PEI-LA1.2 (1.2 LA/2PEI) and PEI-LAVH (2.1 A/2PEI) that have given similar efficiencies in the polymer library screen, were tested against each other for their efficiency under these conditions. GFP positive Hut78 cells were treated with anti-GFP siRNA complexed with PEI-CA20, PEI-LA1.2 and PEI-LAVH at siRNA:polymer weight ratios 1:2, 1:4 and 1:8 and their efficiency was assessed at 72 hours after complex addition. The results are summarized in **Figure 20**. Two sided t-test was used to determine the significance of the differences.

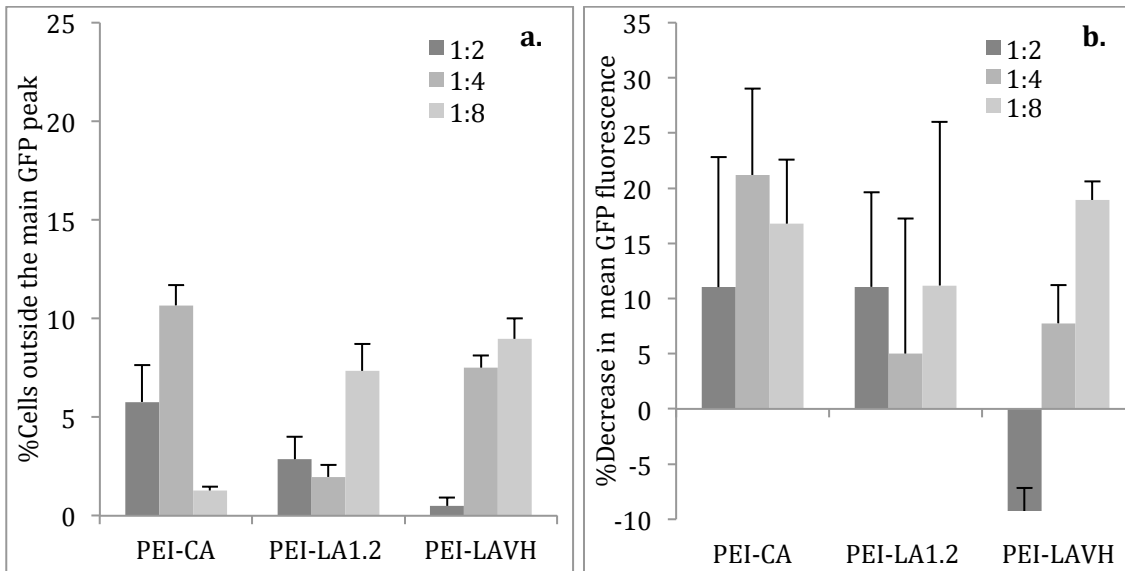


Figure 20 Effect of Complex Formation Volume: Percentage of Hut78 cells outside the main GFP peak (a) and percent decrease in mean GFP fluorescence (b) 72 hours after treatment with anti-GFP siRNA complexes at siRNA:polymer ratios 1:4 and 1:8. The final volume of the solution was 0.3 mL. The siRNA concentration in wells was 25 nM and polymer concentration in medium was 0.70 $\mu\text{g}/\text{mL}$ (1:2), 1.40 $\mu\text{g}/\text{mL}$ (1:4) and 2.80 $\mu\text{g}/\text{mL}$ (1:8). The results were normalized to the control (scrambled siRNA treated) groups.

Based on the percentage of cells silenced in **Figure 20a**, PEI-CA was more efficient than the LA-substituted polymers at ratio 1:2 ($5.8 \pm 1.9\%$ for PEI-CA and $2.9 \pm 1.3\%$ and $0.5 \pm 0.4\%$ for PEI-LA1.2 and PEI-LAVH respectively). At ratio 1:4, PEI-CA was most effective with only $10.7 \pm 1.0\%$ efficiency, while PEI-LAVH had slightly lower efficiency ($7.5 \pm 0.6\%$) than the PEI-CA and PEI-LA1.2 was not efficient ($2.0 \pm 0.6\%$) at all. At ratio 1:8, PEI-CA lost all its efficiency displayed at lower ratios ($1.3 \pm 0.2\%$), while PEI-LA1.2 and PEI-LAVH had similar efficiency ($7.3 \pm 1.4\%$ and $9.0 \pm 1.1\%$ respectively) that was significant but lower than 10%.

Based on the mean GFP silencing in **Figure 20b**, none of the polymers gave significant silencing efficiency at the ratio 1:2, since the variation was very high in PEI-CA and PEI-LA1.2 groups. At the ratio 1:4, PEI-CA had the best efficiency (21.2 ± 7.8); however, none of the results were significant. At the ratio 1:8, only PEI-LAVH had a significant efficiency of $18.9 \pm 1.7\%$, while PEI-CA and PEI-LA1.2 were inefficient in GFP silencing.

We compared these results (where complexes were prepared in 0.3 mL medium) to previous results where the silencing was undertaken with complexes prepared in a small (35 μ l) volume. It appears that the efficiency of the polymers when complexed in large volume was lower than when complexed in small volume. It was observed that the toxicity of the complexes were higher (based on counts from flow cytometry; see Appendix 1), which could be a cause of high variation as well as low efficiency. If the polyplexes are smaller as hypothesized, it is possible that more polymer is being internalized due to size effect, hence increasing the toxicity. It is possible that such a low toxicity might give lower silencing efficiency.

4.8. Effect of continuous shaking

As increasing the volume of the complexation mixture failed to increase the efficiency of the complexes, we next investigated the effect of shaking on silencing. The cells were shaken constantly (~200 rpm) with the complexes under cell incubation conditions to increase the chances of encounter between the cells and the complexes. Jurkat cells were included in this study to see if the shaking could generate similar responses in both cell lines. GFP positive Hut78 and Jurkat cells were treated with anti-GFP siRNA complexed with 25PEI, PEI-CA20, and PEI-LAVH at siRNA:polymer weight ratios 1:2, 1:4 and 1:8 and their efficiency was assessed at 72 hours after complex addition. The results are summarized in **Figure 21**. Two sided t-test was used to determine the significance of the differences.

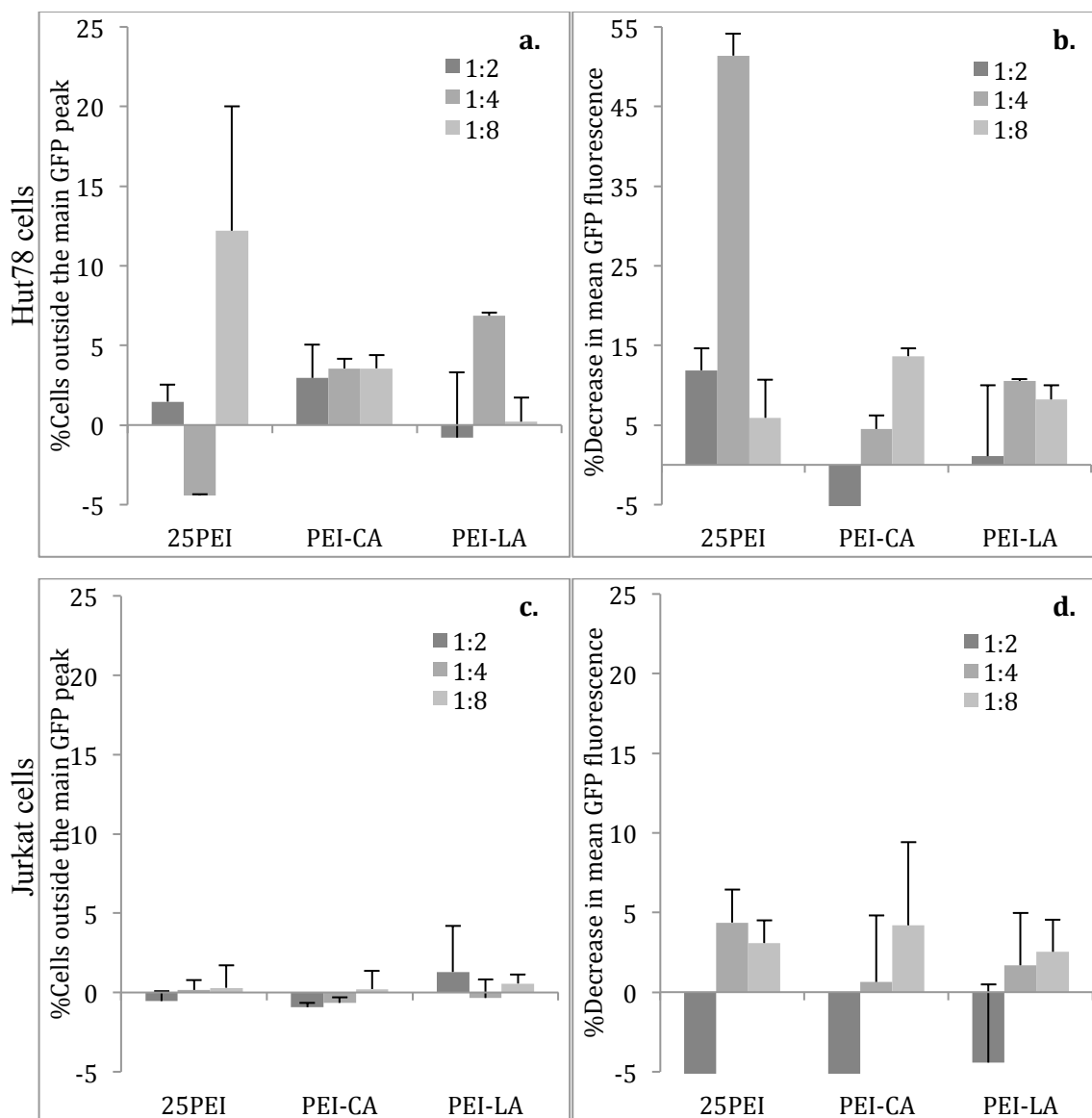


Figure 21 Effect of Shaking: Percentage of Hut78 and Jurkat cells outside the main GFP peak (a and c, respectively) and percent decrease in mean GFP fluorescence (b and d, respectively) 72 hours after treatment with anti-GFP siRNA complexes at siRNA:polymer ratios 1:2, 1:4 and 1:8. The siRNA concentration in wells was 25 nM and polymer concentration in medium was 0.70 $\mu\text{g}/\text{mL}$ (1:2), 1.40 $\mu\text{g}/\text{mL}$ (1:4) and 2.80 $\mu\text{g}/\text{mL}$ (1:8). GFP fluorescence was measured by flow cytometry 72 hours after the complex addition. The results were normalized to the control (scrambled siRNA treated) groups.

Based on the percentage of Hut78 cells silenced in **Figure 21a**, none of the polymers were efficient at the ratio of 1:2. At the ratio 1:4, 25PEI and PEI-CA were inefficient

while PEI-LA was minimally efficient in silencing ($6.8\pm 0.2\%$). At the ratio 1:8, none of the polymers were efficient the best result was seen in 25PEI (12.2 ± 7.8), but it was not significant (against the background of 5%) due to high variance.

Based on the mean GFP silencing in Hut78 cells in **Figure 21b**, none of the polymers were efficient at the ratio of 1:2. At the ratio 1:4, 25PEI gave very high efficiency of around $51.3\pm 2.7\%$, while PEI-CA was inefficient and PEI-LA was minimally efficient ($10.5\pm 0.3\%$). At the ratio 1:8, PEI-CA and PEI-LA gave some silencing ($13.7\pm 1.0\%$ and $8.2\pm 1.8\%$ respectively), while 25PEI did not give significant silencing.

The results from the Jurkat cells (**Figure 21c** and **21d**) did not indicate any silencing effect by the polymers at any of the ratios. This is consistent with previous results in section 4.6 where no silencing effect was seen in Jurkat cells without centrifugation.

For Hut78 cells, the only positive effect of shaking was seen on 25PEI at the ratio 1:4, all other groups have maintained or lost efficiency. Such a high silencing efficiency was not seen before. I speculate that the increased effect of 25PEI at ratio 1:4 may be a result of 25PEI particles not aggregating, resulting in better distribution and silencing. The toxicity of the complexes were observed to be higher, (based on cell counts from flow cytometry; see Appendix 2), so it is possible that the constant stress exerted on the cells might have caused the increase in toxicity and in turn the decrease in the efficiency.

4.9. Effect of centrifugation

As both increasing the volume of the complexation mixture and subjecting cells to constant agitation failed to increase the efficiency of the complexes, the cells were alternatively centrifuged with the complexes to force the cells and the complexes to settle down to the same level and increase the chances of encounter between the cells and complexes. Only Hut78 cells were used for this experiment given the lack of success with Jurkat cells. The centrifugal force (G) and duration (min) were used as two variables to investigate the effect of centrifugation. The G-forces used were 0 (no centrifugation), 100, 200 and 300 and for each G-force, the centrifugation was performed for 5, 10 and 15 minute durations. The centrifugation was also performed before and after complex addition, to see if the effect is due to settling of the cells or due to getting the complexes and cells to the same level. GFP positive Hut78 cells were treated with anti-GFP siRNA complexed with 25PEI, PEI-CA20, and PEI-LAVH at siRNA:polymer weight ratio 1:4 and their efficiency was assessed at 72 hours after complex addition. The results are summarized in **Figure 22** for centrifugation before and after complex addition, and **Figure 23** for G-force and time dependent effect of centrifugation. Two sided t-test was used to determine the significance of the differences.

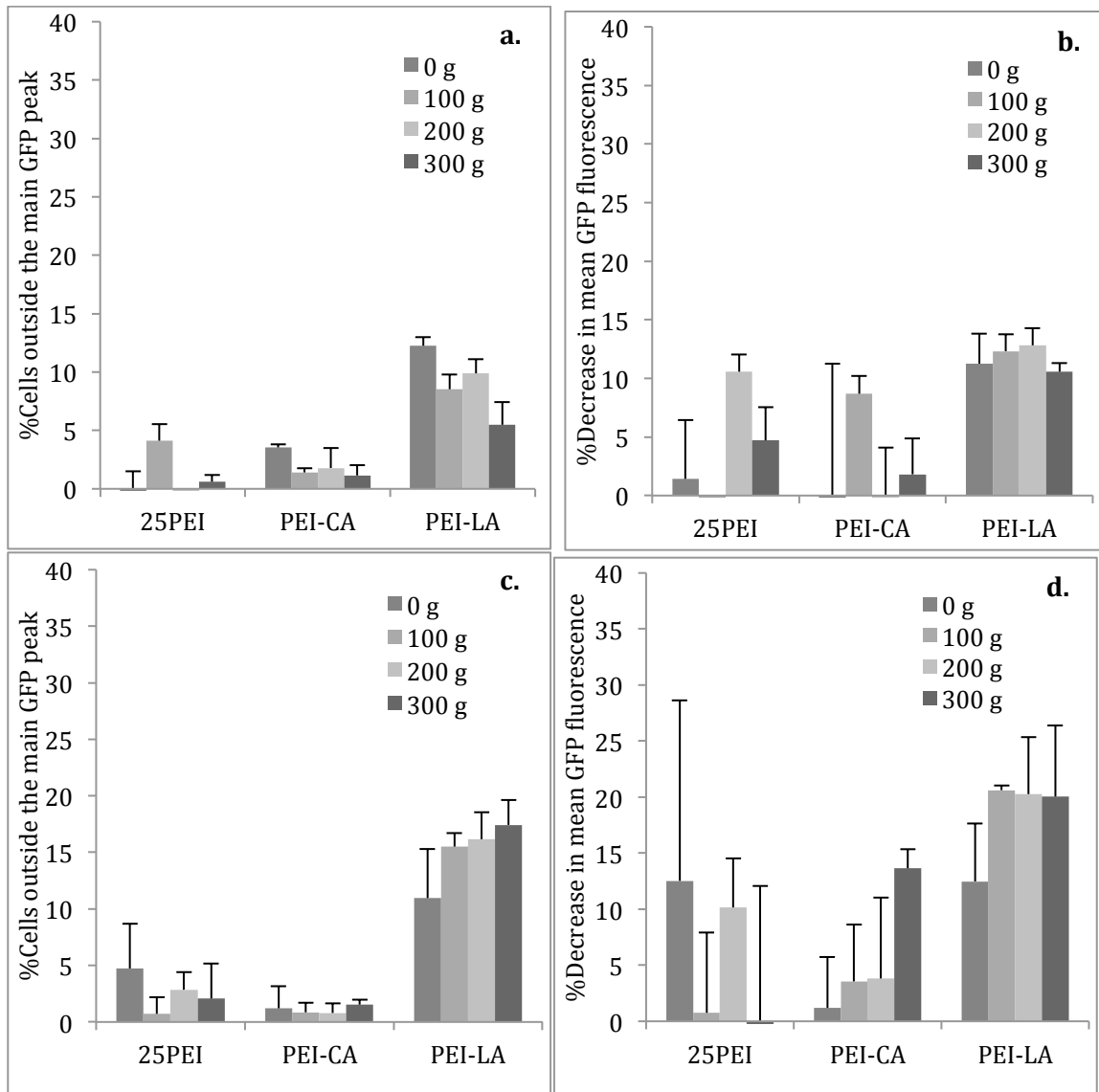


Figure 22 Effect of Centrifugation I: Percentage of Hut78 cells silenced (a,c) and percent GFP silencing (b,d) 72 hours after treatment with anti-GFP siRNA complexes at siRNA:polymer ratio 1:4. The cells were centrifuged before (a-b) and after (c-d) complex addition for 5 mins. The siRNA concentration in wells was 25 nM and polymer concentration in medium was 1.40 $\mu\text{g}/\text{mL}$ (1:4). GFP fluorescence was measured with flow cytometer 72 hours after the complex addition. The results were normalized to the control (scrambled siRNA treated) groups.

Based on the percentage of Hut78 cells silenced in **Figure 22a**, when the cells were centrifuged before the addition of complexes, there was no effect of the centrifugation in any of the polymers; PEI-LA was an effective polymer but centrifugation did not help the silencing efficiency even with this polymer. However, when the centrifugation was

performed after the complex addition (**Figure 22c**), while 25PEI and PEI-CA remained ineffective, the efficiency of PEI-LA slightly increased with increasing G-forces, but no significant difference was reached among the applied G-forces (0G: $11.0 \pm 4.4\%$, 100G: $15.5 \pm 1.2\%$, 200G: $16.1 \pm 2.4\%$, 300G: $17.4 \pm 2.2\%$). In terms of mean GFP silencing, there was no effect of centrifugation when the cells were centrifuged before complex addition (**Figure 22b**), even with the effective PEI-LA. When the cells were centrifuged after complex addition on the other hand, 25PEI remained ineffective, PEI-CA showed a significant increase in efficiency at the 300G (0G: $1.2 \pm 4.5\%$ vs. 300G: $13.7 \pm 1.7\%$), and PEI-LA showed increased efficiency that was equivalent for all G-values (0G: $12.5 \pm 5.2\%$, 100G: $20.6 \pm 0.4\%$, 200G: $20.2 \pm 5.1\%$, 300G: $20.0 \pm 6.3\%$; **Figure 22d**).

Based on this data, it can be concluded that (i) the applied G-force does have an enhancing effect on the efficiency of mainly PEI-LA, and (ii) the effect is due to complexes and cells being brought together with the centrifugation rather than cells settling down. This implies that there is an active physical force during centrifugation that forces the complexes into cells rather than a passive physical force that just brings the cells to the bottom where the added complexes can settle and interact. Although the enhancing effect of centrifugation in this experiment was not very substantial, it might be possible to optimize silencing by the magnitude of G-force and the duration of centrifugation. At low G-force/short duration it is possible that the cells settle but the complexes being much smaller in size do not. This was next investigated by centrifuging the cells for a controlled duration (0, 5, 10 and 15 minutes).

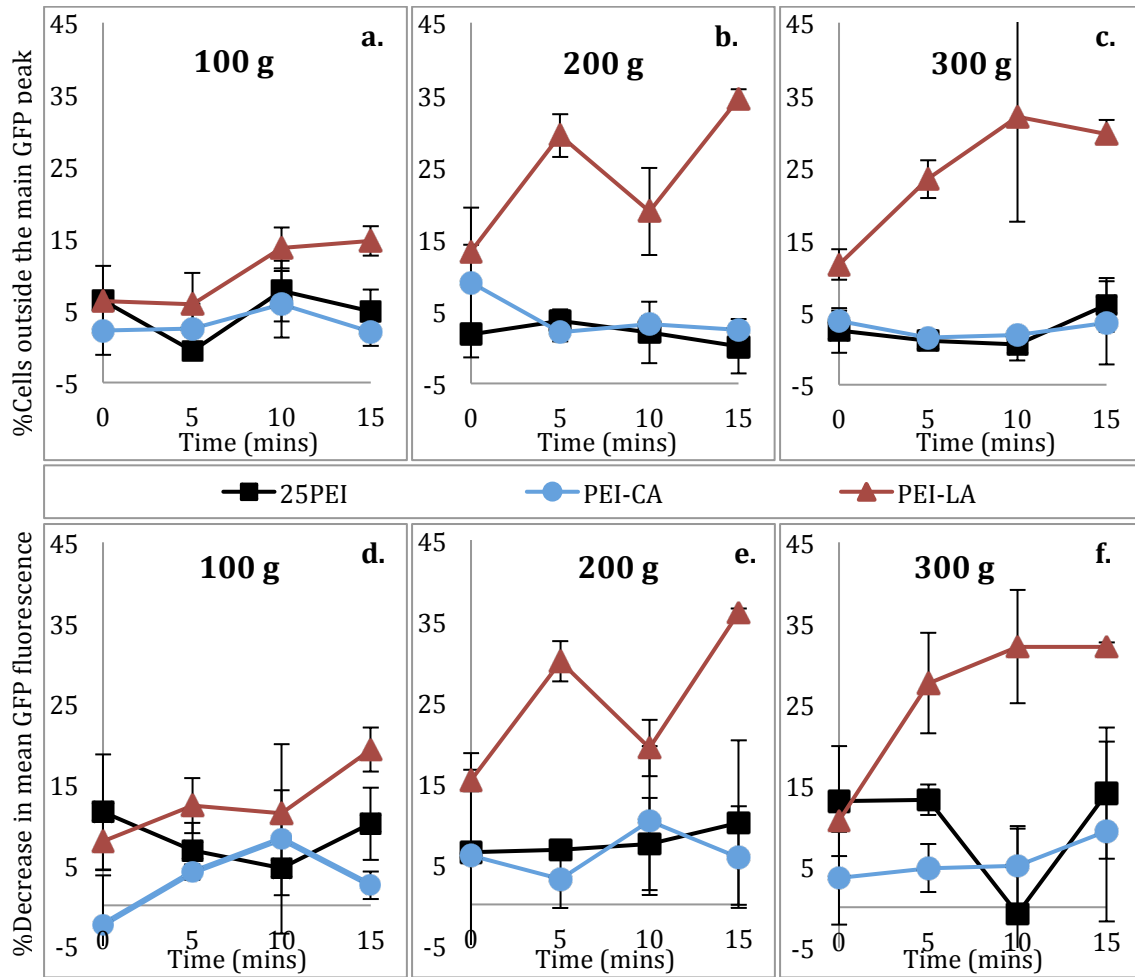


Figure 23 Effect of Centrifugation II: Percentage of Hut78 cells outside the main GFP peak (a-b-c) and percent decrease in mean GFP fluorescence (d-e-f) 72 hours after treatment with anti-GFP siRNA and lipid-modified PEI complexes at siRNA:polymer ratio 1:4 centrifuged at 100G (a,d), 200G (b,e) and 300G (c,f) for 0, 5, 10 and 15 mins after complex addition. The siRNA concentration in wells was 25 nM and polymer concentration in medium was 1.40 $\mu\text{g}/\text{mL}$ (1:4). GFP fluorescence was measured with flow cytometer 72 hours after the complex addition. The results were normalized to the control (scrambled siRNA treated) groups.

Based on percentage of cells silenced in **Figure 23**, 25PEI and PEI-CA have shown relatively constant siRNA silencing efficiencies that were independent of both the G-force applied and the duration of centrifugation. PEI-LA, on the other hand, has shown a slight increase with the duration of centrifugation at 100 g (0 min: $6.3 \pm 0.5\%$, 5 min: $5.8 \pm 4.4\%$, 10 min: $13.7 \pm 2.8\%$, and 15 min: $14.7 \pm 2.1\%$). At 200 g, PEI-LA showed a substantial increase in silencing efficiency at 5 mins ($29.4 \pm 3.0\%$), then decreased at 10

mins ($18.9\pm 6.1\%$) and increased again substantially at 15 mins to $34.4\pm 1.4\%$. The enhancing effect was also seen at 300 g at 5 and 10 min (0 min: $11.6\pm 2.1\%$, 5 min: $23.4\pm 2.6\%$ and 10 min: $32.0\pm 14.5\%$), which leveled off at the 15 min of centrifugation ($30.0\pm 2.0\%$).

In **Figure 23**, the mean GFP silencing data supported the data derived from cell percentage data.

Even though 25PEI and PEI-CA remained mostly unresponsive to the G-forces applied, PEI-LA showed a G- and duration-dependent response. The response to G-force started at 200 g value when applied for 5 min and it reached a plateau after 300 g value for 5 min. The effect of 200 g for 15 mins and 300 g for all time points were similar suggesting that either lower G-force for longer duration or higher G-force for shorter duration can have the same effect of enhancing the effect of the siRNA treatment.

For all the future studies, the cells were centrifuged immediately after complex addition at 300 g for 5 min to increase the efficiency of the treatments performed.

4.10. Effect of Extent of Lipid Substitution

After a better working mechanism for efficient silencing of GFP (i.e., application of G-force) was established, a more detailed study on PEI-CA and PEI-LA at different lipid-substitution ratios was performed to explore the effect of lipid substitution. Lipofectamine®2000 (Life Technologies, Burlington, ON) was included in the study to compare with the in-house prepared carriers. This commercial carrier is claimed to be an efficient commercial carrier for nucleic acids. GFP-positive Hut78 cells were treated with anti-GFP siRNA complexed with Lipofectamine®2000 (prepared exactly the same way as 25PEI in terms of complex formation volume and concentrations), 25PEI, 2PEI-CA4-2, 2PEI-CA1-3, 2PEI-CA1-4, 2PEI-LA4-3, 2PEI-LA4-4, 2PEI-LAVH, 2PEI-LA1-4 (given in increasing substitution rate as shown in **Table 7**) at siRNA:polymer weight ratio 1:4 and their efficiency was assessed at 72 hours after complex addition. The results are

summarized in **Figure 24**. Two sided t-test was used to determine the significance of the differences.

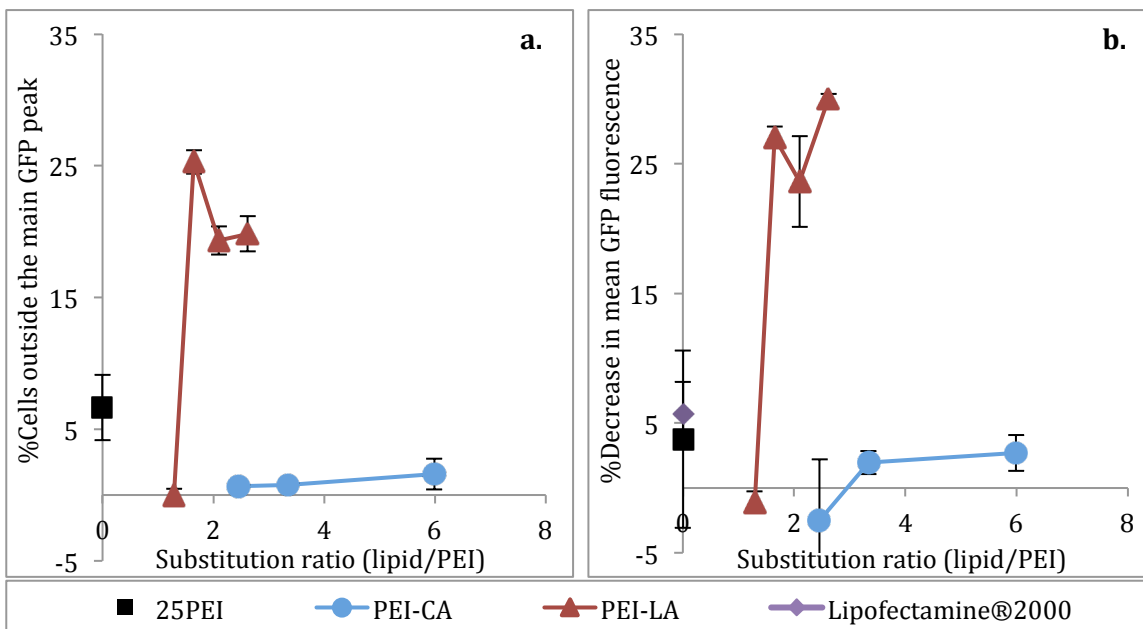


Figure 24 Effect of the Extent of Lipid Substitution: Percentage of Hut78 cells silenced (a) and percent GFP silencing (b) 72 hours after treatment with anti-GFP siRNA complexes at siRNA:polymer ratio 1:4. The cells were centrifuged at 300G for 5 mins after complex addition. The siRNA concentration in wells was 25 nM and polymer concentration in medium was 1.40 $\mu\text{g/mL}$. GFP fluorescence was measured by flow cytometry 72 hours after the complex addition. The results were normalized to the control (scrambled siRNA treated) groups.

Based on the percentage of cells silenced in **Figure 24**, 25PEI gave $6.6\pm 2.5\%$ silencing and Lipofectamine@2000 was found to be inefficient ($1.3\pm 0.8\%$). PEI-CA showed a minor increase with increasing substitution ratio but the efficiency was low (or insignificant) regardless of the substitution ratio. PEI-LA was inefficient at the lowest substitution ratio 1.29 LA/PEI, but was efficient at higher substitution ratios, the 1.65 being the most efficient ($25.3\pm 0.9\%$ silencing). The mean GFP silencing data was in line with these conclusions; however, the best result was seen at the PEI-LA with highest substitution ratio of 2.62 ($30.0\pm 0.4\%$).

It was shown that the in-house synthesized polymer, PEI-LA was significantly superior to Lipofectamine@2000, an efficient commercial transfection agent in Hut78 cells, which was inefficient in this cell line. Also surprisingly the effect of the rate of lipid substitution

did not show a dose response effect that would increase with increasing substitution, but rather showed a threshold like effect in which the polymer was effective after a threshold substitution ratio that did not change substantially.

4.11. Polymer Toxicity

In the previous sections, we have shown that lipid modified PEI is superior to both 25PEI and Lipofectamine®2000 in terms of efficiency to silence GFP. However, it cannot be concluded that the in-house carriers are superior without directly comparing the toxicities of the carriers. Scrambled control siRNA was complexed with Lipofectamine®RNAiMAX (very similar to Lipofectamine®2000, claimed to be more suitable for RNAi by the manufacturer), 25PEI, 2PEI-CA1-4 and 2PEI-LA1-4 as well as 2PEI that is shown to be non-toxic previously [52] and added to wild-type Hut78 cells to give 1, 2.5, 5 and 10 µg/mL final polymer concentration in medium. The toxicity of the carriers was measured using Trypan Blue staining and AlamarBlue® assay 72 hours after complex addition. The results are summarized in **Figure 25**.

Figure 25a shows that 2PEI was non-toxic on Hut78 cells up to 10 µg/mL (as expected) and the 25PEI was the most toxic with only 31.6±8.6% of the cells left viable at 10 µg/mL (based on trypan blue staining). PEI-CA and PEI-LA have very similar toxicities of up to 30% (min viability at 10 µg/mL CA: 70.3±9.3% and LA: 68.9±11.8%) that becomes significant after 5 µg/mL they are more toxic than 2PEI but significantly less toxic compared to 25PEI. Lipofectamine® RNAiMAX shows a very similar effect to 25PEI, significant toxicity starting at 5 µg/mL reaching up to 55% loss of viability at 10 µg/mL (44.0±13.5% viability).

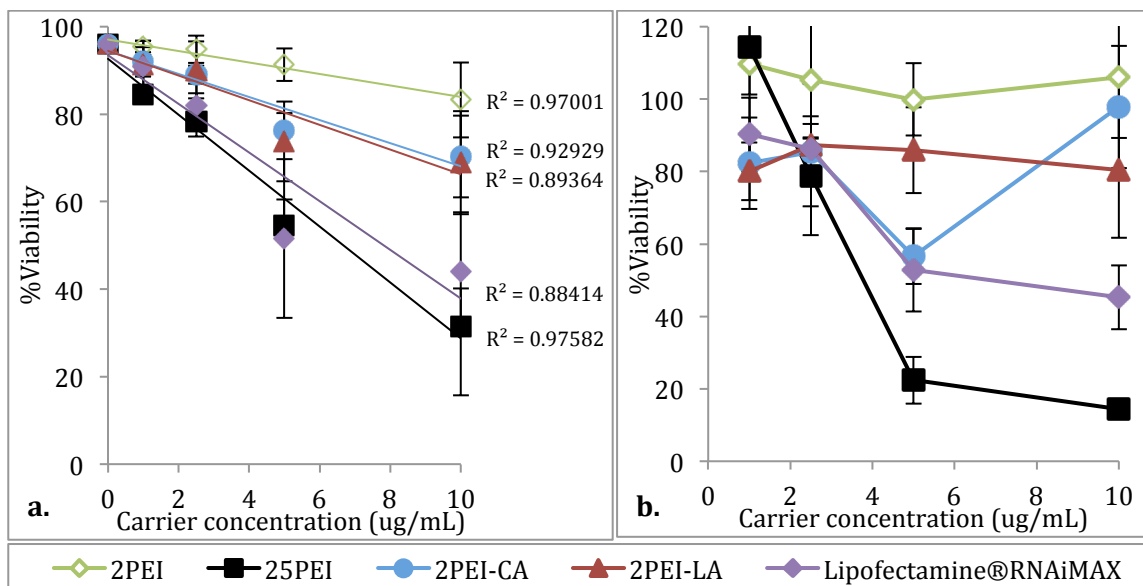


Figure 25 Polymer toxicity: Percentage of viable Hut78 cells via Trypan Blue counting (a) and AlamarBlue® (b) 72 hours after treatment with indicated scrambled siRNA complexes. Lipofectamine®RNAiMAX and polymers were complexed at siRNA:carrier ratio of 1:4, and centrifuged at 300G for 5 mins after complex addition to the cells. The siRNA concentration in wells varied between 18 to 180 nM and polymer concentrations were 1, 2.5, 5 and 10 µg/mL. The cell viability was measured 72 hours after the complex addition. The results were normalized to the untreated cells.

Figure 25b, where the viability was assessed by AlamarBlue® assay, also showed that 2PEI was not-toxic, while 25PEI was highly toxic. PEI-CA and PEI-LA were minimally toxic showing a similar trend except for the 5 µg/mL polymer concentration of PEI-CA (which gave some toxicity for no apparent reason). Lipofectamine® RNAiMAX was not as toxic as 25PEI in this assay but was still more toxic than the other carriers tested.

The results support the previous literature (and our expectations) that 2PEI is non-toxic on the cells and 25PEI is highly toxic, and the in-house carriers, that have been proven to be more efficient than both are minimally toxic making them suitable siRNA delivery agents. Also while it was not as efficient as the in-house CA- and LA- anchored carriers, (see **Figure 24** in **section 4.10.**) Lipofectamine®RNAiMAX was much more toxic than these carriers, giving toxicities almost as high as the 25PEI. This shows that the in-house carriers are superior to the commercial agent in Hut78 cell line from the toxicity perspective.

When the two methods of viability assessment, Trypan Blue staining and AlamarBlue® assay, were compared, it can be seen that Trypan Blue had superior specificity and linearity compared to AlamarBlue®. This is due to the fact that Trypan Blue is a more direct method of measuring cell viability while AlamarBlue® depends on the metabolic activity of the cell. Also it is possible that even though AlamarBlue® assay was suitable for suspension cells, it still can possess barriers that complicate the assay results. For example, the reagents could have decreased availability to the cells due to clamping of the cells or volume errors that can be encountered during handling due to very low amounts (as low as 5 µL) of reagents used. However, even though it may not be as clear as the Trypan Blue assay, AlamarBlue® results support the main deductions.

Part II: Endogenous Gene Silencing

4.12 Screening Select Targets for Silencing

As shown in previous sections, Linoleic acid when anchored to low MW (2 kDa) PEI had the ability to increase the efficiency of the polymer for silencing GFP while keeping the toxicity relatively low. It has been shown that PEI-LA has even superior efficiency to commercial agent Lipofectamine® (2000) in terms of GFP silencing as well as lower toxicity (RNAiMAX). However, GFP is an artificially introduced gene into the cells and it may not be a reliable measure of siRNA delivery efficiency when endogenous targets are considered. The artificial introduction of GFP might have undesired effects on cells, such as increasing its permeability to solutes (and nanoparticles), changes in proliferation rate or the GFP itself might be more prone to silencing due to its artificially introduced and/or over-expressed nature.

The silencing of an intrinsic and preferably pro-oncogenic gene can give a better measure of efficiency for the carriers. Hence, we targeted; (i) several cancer related genes due to their success to decrease cell viability upon siRNA treatment in other cell lines (KSP, CDK18, MAP, RPS, STK, PI3K,), as well as (ii) certain genes shown in the literature to induce apoptosis when depleted in Hut78 (STAT3, Bcl11b [69-71]). The goal was to determine their silencing effect on the viability of wild type Hut78 cells. More information on the selected targets is given in **Table 10**.

Table 10 Names, symbols and functions of the endogenous genes targeted in Hut78 cells.

Gene name	Symbol	Function
The kinesin spindle protein	KSP (KIF11)	A member of the kinesin superfamily of microtubule-based motors. Mediates centrosome separation and bipolar spindle assembly and maintenance during mitosis [66].
Cyclin-dependent kinase 18	CDK18 (PCTK3)	Cell cycle and cellular growth regulator. The specific function of this gene has not yet been determined [67].
Mitogen-activated protein kinase	MAP (ERK1-2)	Integration point for multiple biochemical signals. Involved in proliferation, differentiation, transcription regulation and development [68].
Ribosomal Protein S	RPS (RPS6KA5)	Encodes a ribosomal protein. Takes part in protein synthesis.
Fms-related tyrosine kinase 3	STK (FLT3)	Class III receptor tyrosine kinase that regulates hematopoiesis. Activates multiple cytoplasmic effector molecules in pathways involved in apoptosis, proliferation, and differentiation of hematopoietic cells in bone marrow.
Signal transducer and activator of transcription 3	STAT3	Transcription activator. Mediates the expression of a variety of genes in response to cell stimuli, and thus plays a key role in many cellular processes such as cell growth and apoptosis [69].
Phosphatidylinositol-4,5-bisphosphate 3-kinase	PI3K (PI3KCB)	Modulator of extracellular signals. Modulates cell growth, differentiation, survival, proliferation, migration and metabolism. Takes part in lymphocyte development, differentiation and activation. [70].
B-cell CLL/lymphoma 11B	Bcl11b	C2H2-type zinc finger protein. Closely related to BCL11A, whose translocation may be associated with B-cell malignancies. The specific function of this gene has not yet been determined [71].

4.12.1 Cell Viabilities Based on AlamarBlue® Assay

The siRNAs against the selected genes, KSP, STAT3 -4 different siRNA formulations were used, STAT3-1, STAT3-2, STAT3-7 and STAT3-8- (4 different siRNA formulations against STAT3 mRNA formulated to have complementary binding at different sites of the mRNA, numbered by the manufacturer for distinction), CDK18, Bcl11b, MAP, RPS, PI3K, STK were complexed with 2PEI-LA1-4, 2PEI-CA1-4 and Lipofectamine®RNAiMAX at siRNA:polymer weight ratio 1:4 and added to the cells to give the final siRNA concentration of 25, 50 and 100 nM in the medium. The cell viabilities were measured 72 hours after complex addition with AlamarBlue® assay. The results are summarized in **Figure 26**, mean, z score, one and two tailed t-tests were performed on the results and genes giving significant effect according to at least one test were considered hits in this assay (see appendix 3 for a table of hits relative to the statistical test performed).

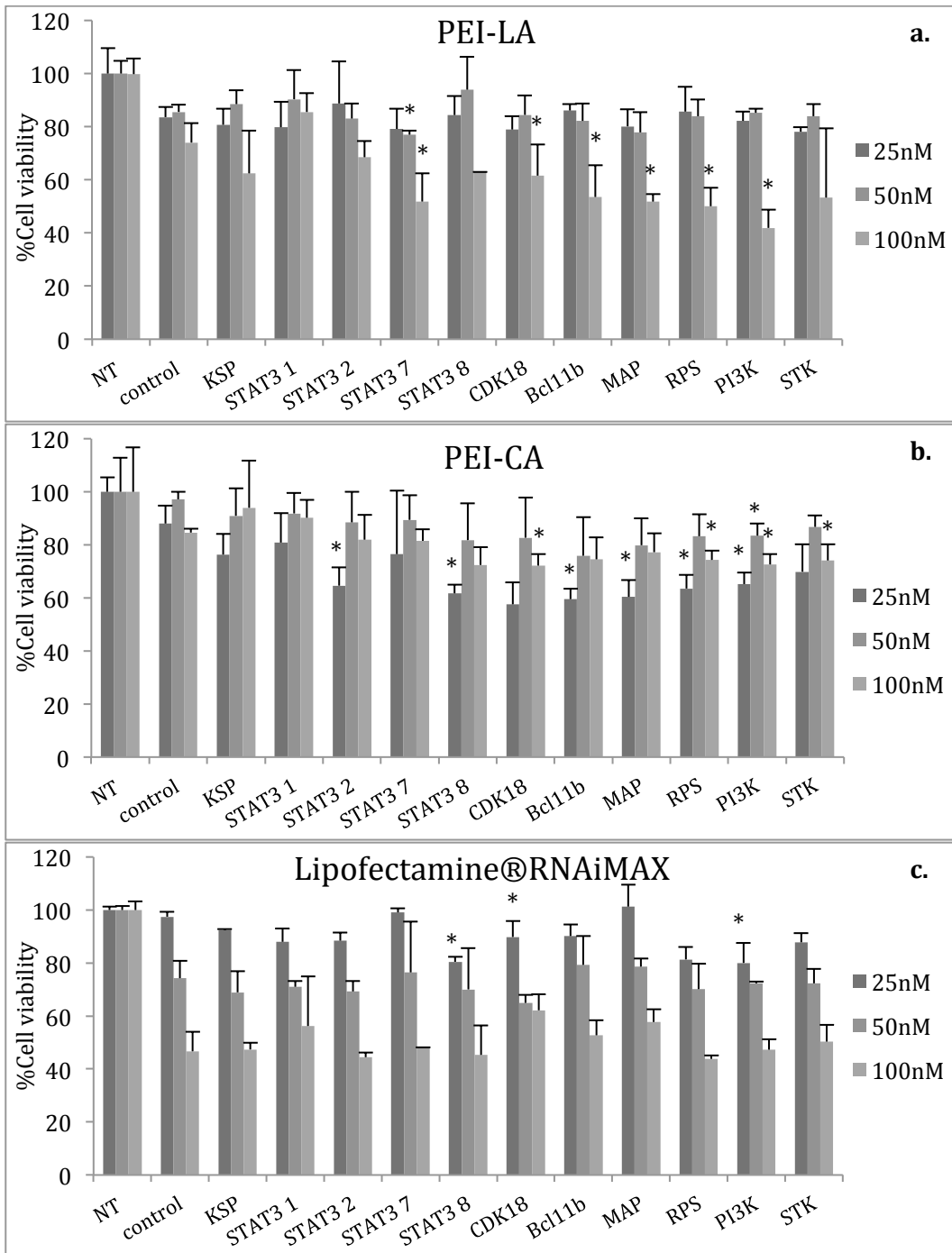


Figure 26 Percentage of viable Hut78 cells after treatment with selected siRNAs and 2PEI-LA1-4 (a), 2PEI-CA1-4 (b) and Lipofectamine®RNAiMAX (c) complexes at siRNA:carrier ratio 1:4. The siRNA concentration in wells was 25, 50 or 100 nM and polymer concentration was 1.40 µg/mL, 2.80 µg/mL and 5.60 respectively. The relative viability compared to untreated cells were analyzed with the AlamarBlue® after 72 hours of incubation with complexes and statistic analysis was performed against the control siRNA treated groups at respective doses.

Based on the data in **Figure 26a** where the siRNAs were complexed with PEI-LA, none of the siRNAs decreased the viability significantly at 25 nM siRNA dose. At 50 nM siRNA dose, only STAT3-7 had a significant effect on the viability of Hut78 cells. At 100 nM siRNA dose, STAT3-7, CDK18, Bcl11b, MAP, RPS, PI3K had significant effects on the viability of the cells.

Based on the data in **Figure 26b** where the siRNAs were complexed with PEI-CA, STAT3-2 and 8, Bcl11b, MAP, RPS, PI3K had significant effects on the viability of the cells at 25 nM siRNA dose. At 50 nM siRNA dose, only PI3K had a significant effect and at 100 nM siRNA dose CDK18, RPS, PI3K and STK had significant effects on the viability of the cells.

Based on the data in **Figure 26c** where the siRNAs were complexed with Lipofectamine® RNAiMAX, STAT3-8, CDK18 and PI3K had significant effects at 25 nM siRNA dose, while none of the siRNAs had any effect at higher doses.

PEI-LA showed the strongest effect at high siRNA dose with 6 hits, while it had 1 hit at medium and no hit at low siRNA dose implying the functional effect obtained could be enhanced with the dosage of siRNA. PEI-CA on the other hand, showed the strongest effect at low siRNA dose with 6 hits, at medium dose it had only 1 hit and at high dose it had 4 hits, the only consistent one being PI3K at all three doses. This can be explained with two possibilities; (i) some of the results might have been arbitrary (i.e., not a predictable dose-response) or (ii) some genes might show effects at low dose silencing but the cell might develop some kind of resistance at high doses (typical of non-specific cytotoxic effects at high doses). In the case of Lipofectamine® RNAiMAX, all 3 hits were at the low siRNA dose as the carrier was very toxic, reducing the viability for over 50% at high siRNA dose based on the control siRNA treated group's viability when complexed with scrambled control siRNA.

Considering all carriers and doses used, the strongest effect was seen with CDK18 and PI3K silencing, which was most effective in decreasing the viability. STAT3 was also effective but the effective siRNA formulations (versions 1, 2, 7 and 8) were different with different polymers so this result was approached skeptically.

4.12.2 Cell Viabilities Based on Trypan Blue Assay

AlamarBlue® assay showed high variation in the siRNA hits delivered by different carriers, and this could be due to the interactions between carriers and siRNA changing depending on the siRNA or due to the sensitivity of the assay being low to reveal all the hits. To support the results obtained, a second assay, Trypan Blue assay was used to determine the viability of the cells in a repeat experiment.

siRNAs against the same genes, (KSP, STAT3 - 4 different siRNA were mixed to give one anti-STAT3 consisting of 4 siRNA formulations-, CDK18, Bcl11b, MAP, RPS, PI3K, STK) were complexed with 2PEI-LA1-4 at siRNA:polymer weight ratio 1:4 and added to the cells to give the final siRNA concentration of 25, 50 and 100 nM in the medium. Cell viability was measured 72 hours after complex addition with Trypan Blue assay. The results are summarized in **Figure 27**, mean, z score, one and two tailed t-tests were performed on the results and siRNAs giving significant effect according to at least one test were considered hits (see appendix 4 for a table of hits relative to the statistical test performed).

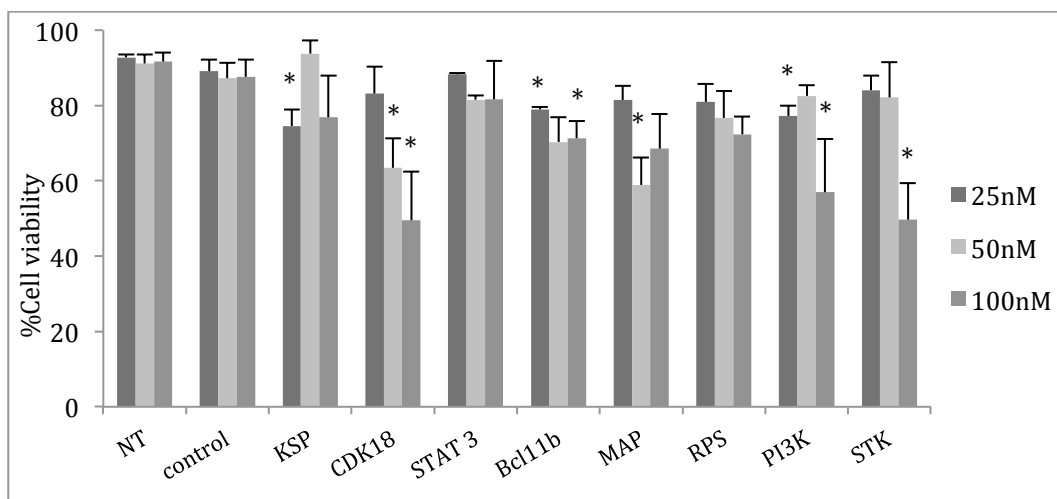


Figure 27 Percentage of viable Hut78 cells after treatment with selected siRNA complexes at siRNA:polymer ratio 1:4. The siRNA concentration in wells was 25, 50 or 100 nM and polymer concentration was 1.40 µg/mL (25 nM), 2.80 µg/mL (50 nM) and 5.60 (100 nM). The relative viability was expressed against untreated cells with Trypan Blue assay after 72 hours of incubation with the complexes and statistic analysis was performed against control siRNA treated groups.

As summarized in **Figure 27**, KSP, Bcl11b and PI3K at 25 nM siRNA concentration CDK18 and MAP at 50 nM siRNA concentration and CDK18, Bcl11b, PI3K and STK at 100 nM siRNA concentration had significant effects on the viability of the cells.

While KSP was only effective at low dose and MAP was only effective at medium dose suggesting an ‘artificial’ hit, CDK18 had a good dose response relationship, its effect appearing at medium dose and intensifying at high dose. Bcl11b and PI3K were effective at low and high doses but their effect was lost at medium dose and they did not show a functional effect increasing with the siRNA concentration. STAT3 has lost all its effect seen in the previous assay, which might be due to the mixing of the 4-siRNA formulations decreasing the effect of the treatment.

The best effect was seen with CDK18 siRNA unlike the other siRNAs, which was also effective in decreasing the viability of the cells in the previous experiment (section 4.12.1.). In addition, PI3K was found to be effective in decreasing cell viabilities supporting the previous study (section 4.12.1.), even though its effect was not seen as a dose response in this case. Thus, CDK18 and PI3K were chosen for further investigation with dose response studies as well as apoptosis assays.

4.13 PI3K dose response

As PI3K was effective in the initial siRNA screens, a more detailed dose response study was performed with this target. Wild type Hut78 cells were treated with siRNAs against PI3K complexed with 2PEI-LA1-4, 2PEI-CA1-4 and Lipofectamine® RNAiMAX at siRNA:polymer weight ratio 1:4 to give the final siRNA concentrations of 25, 50 and 100 nM in the medium, and cell viability was measured 72 hours after complex addition with Trypan Blue assay. The results are summarized in **Figure 28**.

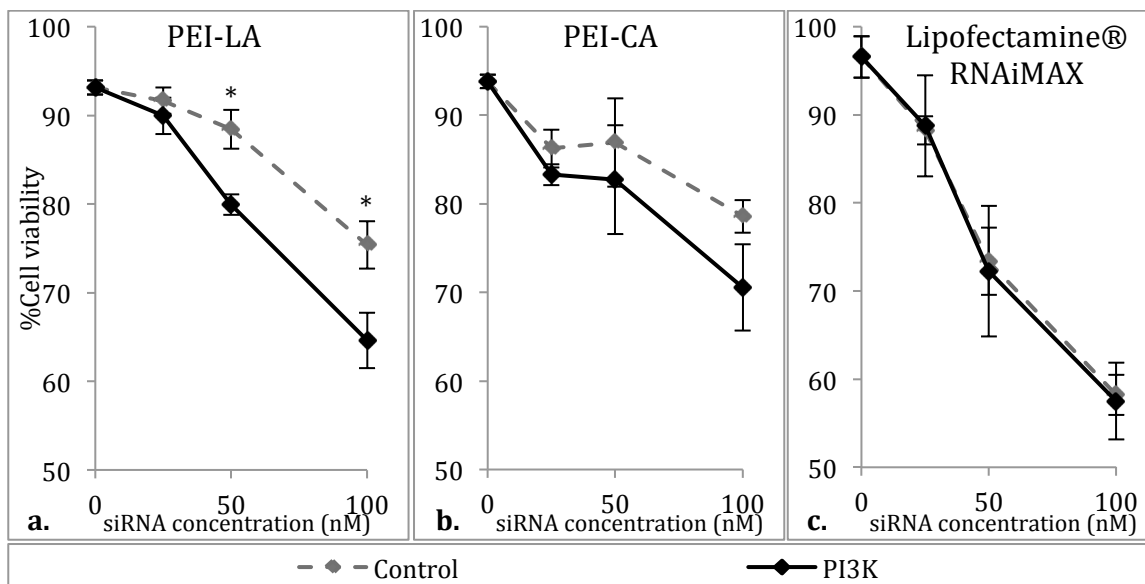


Figure 28 Percentage of viable Hut78 cells after treatment with PI3K siRNA and 2PEI-LA1-4 (a), 2PEI-CA1-4 (b) and Lipofectamine®RNAiMAX (c) complexes at siRNA:carrier ratio 1:4. The siRNA concentration in wells was 25, 50 or 100 nM and polymer concentration was 1.40 µg/mL (25 nM), 2.80 µg/mL (50 nM) and 5.60 (100 nM). The percent cell viability was analyzed with Trypan Blue assay after 72 hours of incubation with the complexes and student's t-test was performed against control siRNA treated groups to determine the significance of the results.

Based on the results in **Figure 28a** where PI3K siRNA was complexed with PEI-LA, there is a minor (insignificant) decrease in viability compared to control at 25 nM siRNA dose. A significant decrease in viability was evident at both 50 and 100 nM siRNA concentration (8.5% and 10.8% respectively).

Based on the results in **Figure 28b** where PI3K siRNA was complexed with PEI-CA, a difference in viability between the control and PI3K siRNA treated groups was evident at high siRNA concentrations, but the differences were not significant at the concentrations tested.

Based on the results in **Figure 28c** where PI3K siRNA was complexed with Lipofectamine® RNAiMAX, there was no significant difference between the control and PI3K groups, but there was a very sharp decrease in cell viability in both control and PI3K siRNA treatment groups.

It can be deduced that silencing PI3K had an effect on the viability of Hut78 cells and the effect was best seen in PEI-LA starting from the medium dose. While PEI-CA was not as effective as the PEI-LA, a slight effect can be seen in this polymer too. Lipofectamine®RNAiMAX, on the other hand, is overly toxic, decreasing the viability almost 50% at the high dose masking the effect of the PI3K even if the silencing was successful.

In the first part of the results, it was reported that PEI-LA can achieve up to 30-35% silencing of GFP expression; however, when PI3K is delivered, the functional effect is not as pronounced. There are several possible reasons for this phenomenon, first of all the effect of anti-GFP treatment was measured at the protein level via the fluorescence measurements in flow cytometry, while in the case of anti-PI3K treatment, the outcome measured was a functional effect, as the decrease in cell viability due to presumed decrease in the protein level. This introduces another variable to the effect, as it is possible that even if the level of PI3K decreases (to equivalent levels of GFP silencing) the level of decrease might not be toxic to the cells or the cell might switch to another survival mechanism independent of PI3K. Secondly, as GFP is introduced into the cells artificially, the transfection process might have an effect on the cells increasing the permeability or responsivity to the treatment, while the wild type cells used in functional assays are not as permeable or responsive to siRNA treatment.

4.14 Silencing PI3K for Apoptosis Induction

To further investigate the effect of anti-PI3K siRNA on Hut78 cells, silencing induced apoptosis was investigated by using Trevigen's FlowTACS™ Apoptosis Detection Kit for further insight. Wild-type Hut78 cells were treated with siRNAs against PI3K complexed with 2PEI-LA1-4 at siRNA:polymer weight ratio 1:4 to give the final siRNA concentrations of 12.5, 25, 50 and 100 nM in the medium. The results are summarized in **Figure 29**, and student's t-test was performed on the results to compare PI3K treatment groups with scrambled siRNA treatment groups

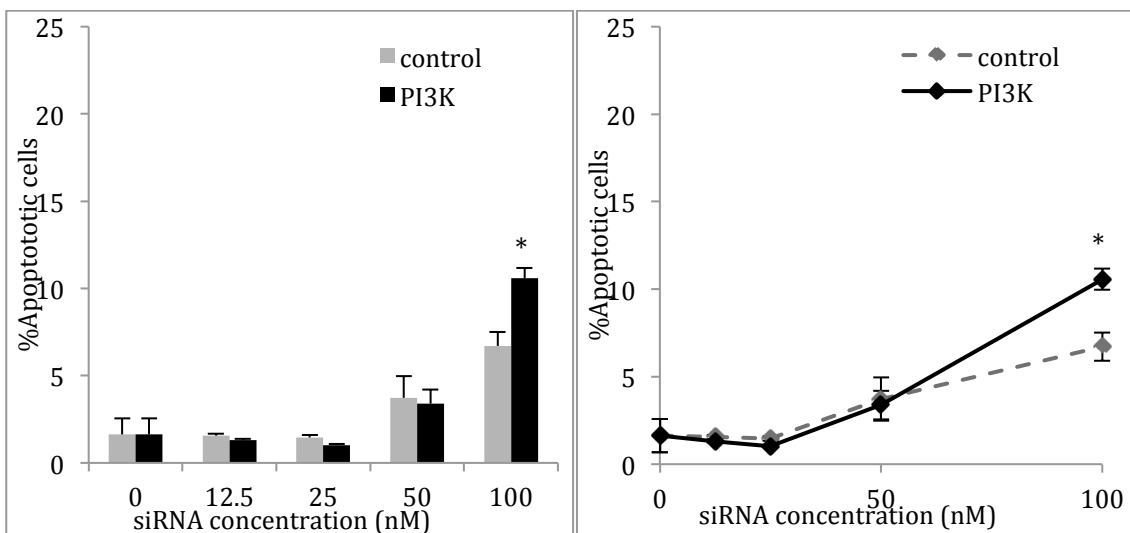


Figure 29 Percentage of apoptotic Hut78 cells after treatment with PI3K siRNA and 2PEI-LA1-4 at siRNA:polymer ratio 1:4. The siRNA concentration was 12.5, 25, 50 or 100 nM and polymer concentration was 0.70 $\mu\text{g}/\text{mL}$ (12.5 nM) 1.40 $\mu\text{g}/\text{mL}$ (25 nM), 2.80 $\mu\text{g}/\text{mL}$ (50 nM) and 5.60 (100 nM). The apoptosis was analyzed with FlowTACS™ Apoptosis Detection Kit after 72 hours of incubation with the complexes and student's t-test was performed against control siRNA treated groups to determine the significance of the results. The results were graphed as both bar and line graphs for visual clarity.

Based on the data in **Figure 29**, there is no clear apoptosis in cell population at 0, 12.5 and 25 nM siRNA while, at 50 nM siRNA, there is minimal apoptosis that is equal in both control and PI3K siRNA treatment groups. At 100 nM siRNA, there is a significant difference in apoptosis between the two groups (3.9%).

It can be deduced that, at 12.5 and 25 nM siRNA doses, there is no apoptosis caused by the treatment either due to the toxicity of the polymer or due to the anti-PI3K treatment as they are all equivalent to no treatment group. The toxicity of the polymer becomes apparent at 50 nM (2.80 $\mu\text{g}/\text{mL}$) but is still minimal as previously reported in **section 4.7**. At 100 nM siRNA dose, the control and anti-PI3K treatments show a difference of around 4%, which is statistically significant. However, as the viability difference was reported to be only 10% in section 4.13, the result was reasonable. Whether this difference is sufficient to observe a functional effect in the long run (and especially in an animal model) remains to be investigated. We alternatively explored CDK18 silencing as a possible target.

4.15 Silencing CDK18 Over 9 Days

CDK18, which was also effective in the siRNA screens along with PI3K, was subjected to a more detailed dose response study. Wild-type Hut78 cells were treated with siRNAs against CDK18 complexed with 2PEI-LA1-4 at siRNA:polymer weight ratio 1:4 to give the final siRNA concentrations of 25, 50, 75 and 100 nM. Cell viability was measured with Trypan Blue assay 3, 6 and 9 days after complex addition, the treatment was re-applied at 3rd and 6th days after subculturing the cells in the latter 2 assessment time points. The results are summarized in **Figure 30**, student's t-test was performed on the results to compare CDK18 treatment groups with scrambled siRNA treatment groups.

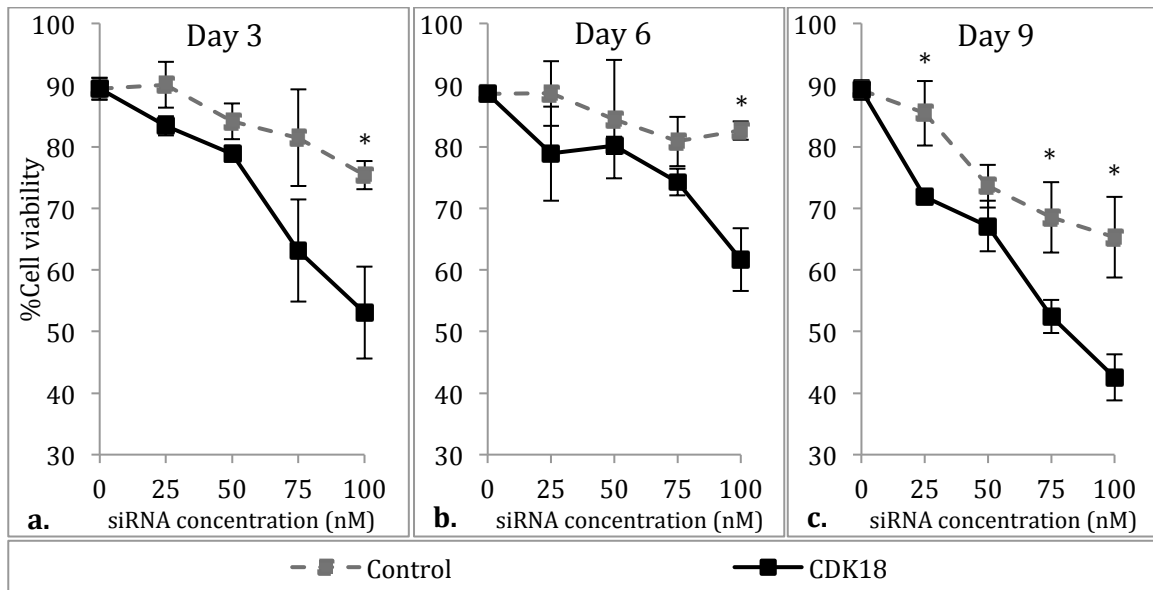


Figure 30 Percentage of viable Hut78 cells after treatment with CDK18 siRNA complexes at siRNA:polymer ratio 1:4 at days 3 (a), 6 (b) and 9 (c). The siRNA concentration was 25, 50, 75 or 100 nM and polymer concentration was 1.40 $\mu\text{g}/\text{mL}$ (25 nM), 2.80 $\mu\text{g}/\text{mL}$ (50 nM), 4.20 (75 nM) and 5.60 (100 nM). The percent cell viability was analyzed with the Trypan Blue assay and student's t-test was performed against control siRNA treated groups to determine the significance of the results.

On day 3 (**Figure 30a**), the decrease in cell viability was small and similar at 25 and 50 nM siRNA doses. At 75 nM, the difference between the control and CDK18 groups was more pronounced but it was not significant due to high variances. At 100 nM, the difference between the two groups (22.4%) became significant. On day 6 (**Figure 30b**), the decrease in cell viability was similar at 25, 50 and 75 nM siRNA doses, while the

difference (21.0%) became significant at 100 nM dose. On day 9 (**Figure 30c**), all anti-CDK18 siRNA doses except for the 50 nM had a significant effect on the viability of Hut78 cells compared to the control siRNA treatment.

At all 3 time points, even though the viabilities of the treatment groups changed, the anti-CDK18 siRNA gave ~20% lower cell viability (22.4%, 21.0%, 22.8% respectively) than the control siRNA treated cells at 100 nM. This implies that, as reported in section 4.4 in the case of GFP silencing, the effect is not additive, but unlike the GFP, the effect of CDK18 is preserved through the time points, when repetitive doses are applied.

Also the decrease is mostly insignificant in the control groups compared to no-treatment groups except for the 9th day, where the treatment seems to be more toxic. The increase in toxicity of both groups on day 9 may be explained by the effect of polymer accumulation in the cells. Even though the medium was changed every 3 days prior to new complex addition, it is possible that the remaining polymer that was in the cells, and hence was not washed off, had accumulated and caused the increase in the toxicity.

Overall, the treatment seems effective -more effective compared to PI3K- but further studies are needed for better understanding of the results.

4.16 CDK18 silencing over 3 days and apoptosis

To have a better insight to the effect of the CDK18 on Hut78 cells, the effect on viability was measured at 1st, 2nd and 3rd days of the treatment and apoptosis was also measured for further understanding of the nature of the effect. Wild-type Hut78 cells were treated with siRNAs against CDK18 complexed with 2PEI-LA1-4 at siRNA:polymer weight ratio 1:4 to give the final siRNA concentrations of 50 and 100 nM in the medium. Cell viability was measured with Trypan Blue assay and apoptosis was measured with BD Pharmingen's FITC Annexin V Apoptosis Detection kit (an apoptosis assay more suitable to suspension cells) 1, 2 and 3 days after complex addition. This was used as an alternative assay to measure apoptosis due to unsatisfactory results generated using the Trevigen's FlowTACSTM Apoptosis Detection Kit. The results are summarized in

Figures 31 and 32, student's t-test was performed on the results to compare CDK18 treatment groups with scrambled siRNA treatment groups.

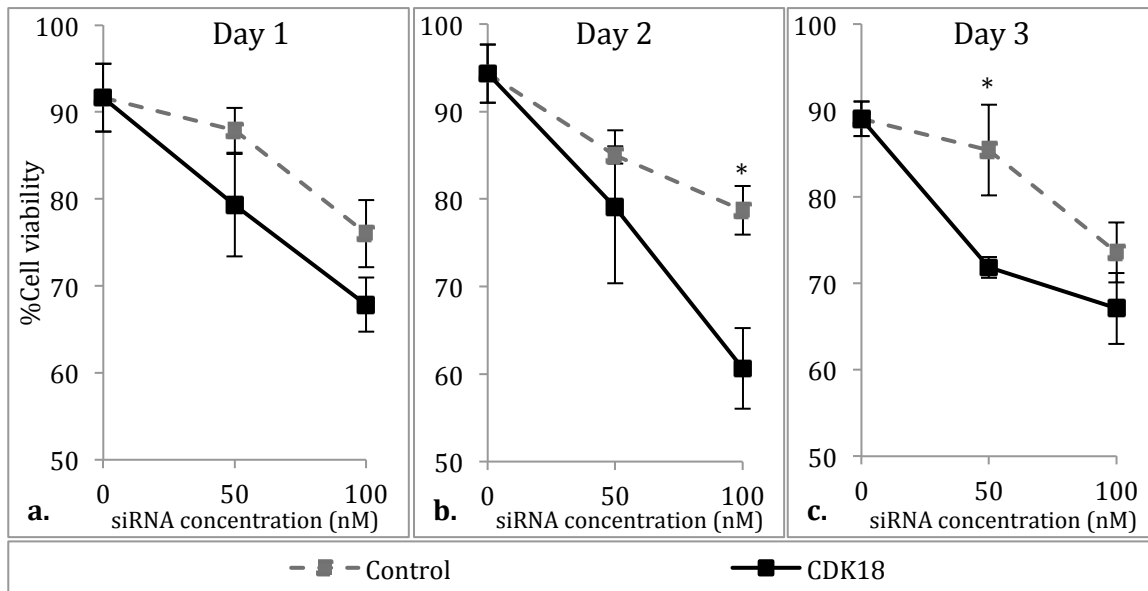


Figure 31 Percentage of viable Hut78 cells after treatment with CDK18 siRNA complexes at siRNA:polymer ratio 1:4 at days 1 (a), 2 (b) and 3 (c). The siRNA concentration was 50 or 100 nM and polymer concentration was 2.80 $\mu\text{g}/\text{mL}$ (50 nM) and 5.60 (100 nM). The percent cell viability was analyzed with Trypan Blue assay after 1, 2 and 3 days of incubation with the complexes and student's t-test was performed against control siRNA treated groups to determine the significance of the results.

Based on the data in **Figure 31** on day 1, the cell viability was lower at anti-CDK18 siRNA treated groups at both 50 and 100 nM siRNA concentrations; however, the differences were not significant. On day 2, although the cell viabilities were similar at 50 nM concentration, the cell viability of the 100 nM anti-CDK18 siRNA treated groups was significantly lower than that of the control groups (18.1%). On day 3, the viability of CDK18 group was significantly lower than that of control at 50 nM concentration (13.5%) but the effect is lost at the 100 nM siRNA concentration.

It can be seen that the viability of the control groups stays constant through the 3 days implying that the toxic effect of the carriers is immediate. The effect of the anti-CDK18 treatment on the other hand, increases slowly (but not significantly) resulting in

significant difference between the groups, except for the 100 nM point of the 3rd day that is assumed to be an experimental error.

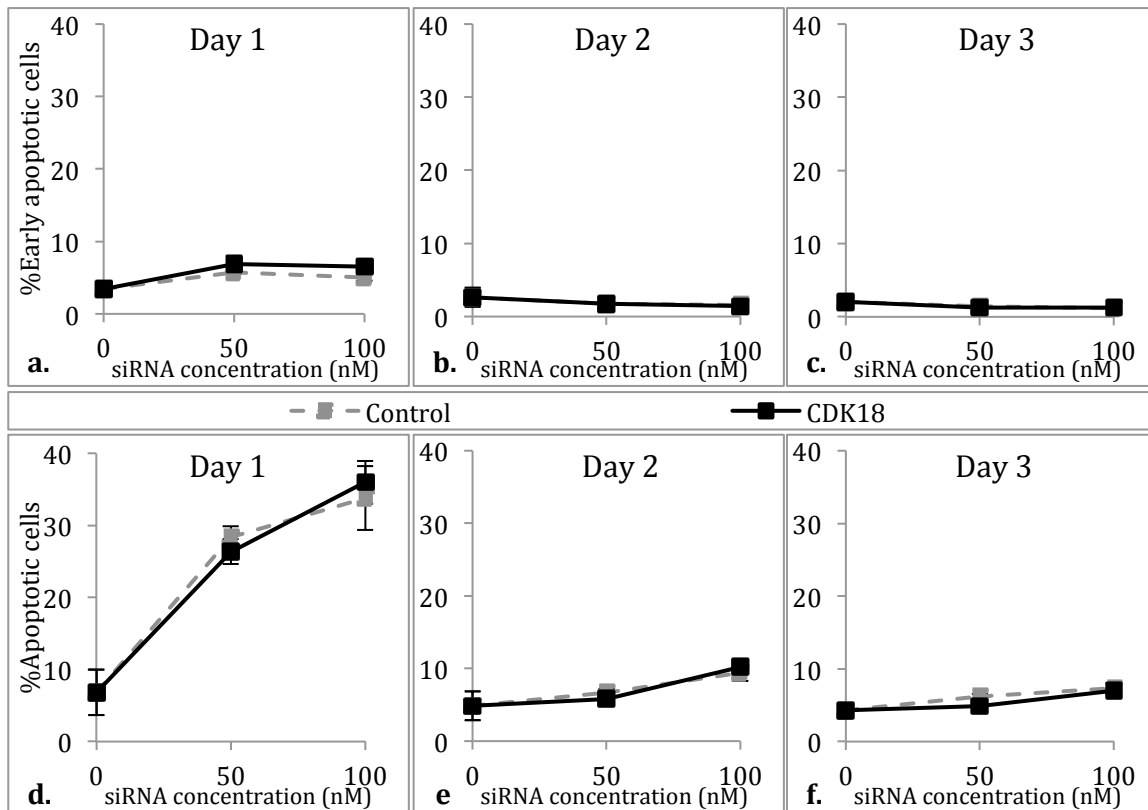


Figure 32 Percentage of early apoptotic (a-b-c) and apoptotic (d-e-f) Hut78 cells after treatment with CDK18 siRNA complexes at siRNA:polymer ratio 1:4 at days 1 (a-d), 2 (b-e) and 3 (c-f). The siRNA concentration was 50 or 100 nM and polymer concentration in medium was 2.80 $\mu\text{g}/\text{mL}$ (50 nM) and 5.60 (100 nM). The percent apoptosis was analyzed with FITC Annexin V Apoptosis Detection kit and student's t-test was performed against control siRNA treated groups to determine the significance of the results.

Based on the data in **Figure 32**, there is a slight (insignificant) amount of early apoptotic cells on the first day (a), which are lost in the following days (b-c). On day 1 (d), there is a significant amount of total apoptotic cells at both siRNA concentration of 50 (control siRNA: $28.4 \pm 1.6\%$ and CDK18 siRNA: $26.4 \pm 1.7\%$) and 100 nM (control siRNA: $33.8 \pm 4.4\%$ and CDK18 siRNA: $36.0 \pm 3.0\%$), which increases with the amount of siRNA in both control and CDK18 groups. On days 2 and 3 (e-f), the amounts of apoptotic cells are around the baseline level (un-treated samples), there is a slight increase in both groups on day 2 at 100 nM siRNA dose, but it is not significant.

The fact that the control and CDK18 groups had the same amount of apoptosis means that the apoptosis on the first day was due to the toxicity of the carrier rather than the effect of anti-CDK18 siRNA treatment. As there is apoptosis only on the first day, it can be deduced that the toxicity of the carriers are immediate. It is possible that the apoptosis due to CDK18 silencing manifested itself later than the third day. It is also probable that as the dynamics of the apoptosis assay gives a very short time interval for the detection of Annexin V, the time points selected did not capture that time interval that apoptosis could be detected, and the assay failed. However, as the effect of the anti-CDK18 siRNA on the viability of Hut78 cells compared to control siRNA is seen earlier than that, it is more probable that the mode of action of CDK18 silencing is not causing apoptosis but rather decreasing or diminishing the rate of proliferation. This also explains the minimal increase of the effect on 6th and 9th days in the previous section, if the cells have *decreased proliferation rate* due to the effect of CDK18 silencing rather than apoptosis. In other words, the cells do not undergo apoptosis, which would cause a much stronger effect when repetitive doses are given, but they just stop or slow down the proliferation causing the effect to be constant or minimal over the days.

The difference between the results of two experiments for apoptosis in sections 4.14 and 4.16 might be due to the different working principles of the apoptosis detection assays. For section 4.14, the FlowTACS™ apoptosis detection kit that measures DNA fragmentation was used, while for section 4.16 the FITC Annexin V apoptosis detection kit that measures the translocation of membrane phospholipid phosphatidylserine (PS) from inner to outer membrane. The FlowTACS™ detects DNA fragmentation that also happens in other forms of cell death than apoptosis, while PS relocation is more specific to apoptosis, resulting in overestimation of apoptosis in the former. Moreover, the first assay (FlowTACS™) is designed for use in attachment dependent cells rather than suspension cells like Hut78. It involves several centrifugation steps that might have caused disruption of fragile cells due to the treatment, and thus overestimation of apoptosis, while the second assay (FITC Annexin V) involves much less centrifugation introducing less strain on the cells. The involvement of several centrifugation steps also introduces variation at each step decreasing the viability of the assay. Finally, the targets

silenced with siRNA are different in Section 4.14 (PI3K) and Section 4.16 (CDK18) so that a differential apoptotic response is also expected.

It is known that PI3Ks have important roles in lymphocyte development and differentiation, regulate cell growth, differentiation, survival, proliferation, migration and metabolism. Although it is known unrestrained PI3K signalling contributes to autoimmunity and leukaemia [96] and PI3K/Akt activation is common in T cell acute lymphoblastic leukemia (T-ALL) [97], PI3K hasn't been studied in siRNA induced silencing in lymphoma. Although there are studies targeting PI3K/Akt pathway, in the leukemia and lymphoma field no extensive progress has been made through this pathway [98].

CDK18 on the other hand, has never been studied in the field of cancer, and even though for being a cyclin dependent kinase it is thought to have a role in cell cycle and growth, its role hasn't been defined precisely. Also it hasn't been explored for its role or the consequences of its silencing in leukemia and lymphoma.

5. Conclusions and Future

To summarize the main points of this thesis work, for the first part of this thesis, a polymer-based approach for anti-GFP siRNA delivery to GFP expressing Hut78 cells was investigated.

First, the most appropriate lipid-anchored PEI for this cell line were chosen out of a select library of 2 kDa PEI engineered by covalent addition of several fatty acids at a variety of substitution ratios. The most successful lipid substitution for siRNA mediated silencing in Hut78 cells was found to be LA considering all the studies conducted for this thesis. Second, the selected polymers, PEI-CA and PEI-LA, were investigated for the dynamics of GFP silencing by time to further the information about the silencing process, which was found to be dynamic but not additive.

Moreover, the method was tried on a similar cell line, Jurkat, to define the universal applicability of the method. While Jurkat cells were found unresponsive to treatment by this method, several courses of treatment were applied to increase the efficiency of the method. Constant shaking and alternate complexation conditions have failed to increase the efficiency of the method while centrifugation of the cells with complexes had a substantial effect on the efficiency of the treatment.

The in-house carriers were also tested for the effect of the extension of lipid substitutions and against a commercial agent, Lipofectamine®2000, which was found to behave similarly to that of 25PEI and was inefficient for siRNA delivery to Hut78 cells. It was also found that after a threshold value of substitution rate, the efficiency of the polymers did not increase.

Lastly, the in-house polymers, PEI-CA and PEI-LA, were tested for their toxicity against the native form of the polymer, 2PEI, the efficient but toxic 25PEI and the commercial agent Lipofectamine®RNAiMAX. It was found that the in-house polymers had toxicities slightly higher than non-toxic 2PEI, but substantially lower than that of 25PEI. Lipofectamine®RNAiMAX was found to be almost as toxic as 25PEI.

For the second part of the thesis, after construction of a working and efficient method of silencing on the model system of artificially GFP-expressing Hut78 cells, several endogenous targets were examined for their ability to decrease the viability of the wild type Hut78 cells and induce apoptosis.

First, several cancer related genes that has been successful on other cell lines in Uludag Lab and genes shown in the literature to induce apoptosis in Hut78 were screened for their ability to decrease the viability of Hut78 cells. Two of the most consistent and effective targets, PI3K and CDK18, were chosen for further investigation of their effects on Hut78 cells.

PI3K, the first possible target has shown significantly decreased viability with PEI-LA, while PEI-CA had a less pronounced effect and Lipofectamine®RNAiMAX was inefficient. It was decided that PEI-CA and Lipofectamine®RNAiMAX was not promising and the apoptosis was performed with PEI-LA only. When the apoptosis caused by the silencing of PI3K was measured, it was observed that the amount of apoptosis was lower than the decrease in cell viability, which is expected due to the dynamics of each process, cell viability being a cumulative measure while apoptosis is a snap shot.

CDK18, the second possible target has also shown decreased viability that was the most pronounced on the second day for high and on the third day for low dose of siRNA. When repetitive doses of anti-CDK18 treatment were applied, the effect was not cumulative, but it was preserved accompanied with increasing toxicity due to the carrier. However, when the apoptosis was measured, it was observed that there was no difference between the control siRNA treated samples and the anti-CDK18 siRNA treated samples.

Although doses as low as 25 nM were enough for significant silencing of GFP in GFP positive Hut78 cells, the effective dose was found to be 100 nM (5.6 µg/mL polymer) for PI3K and CDK18 silencing in wild type Hut78 cells. When considered in the context of literature, it is seen that the most widely used reagent Lipofectamine®2000 (see **Table 6**) has a wide range of effective doses. The effective dose can be 30-50 nM siRNA [74] or

the effective dose of the reagent can be around 5 µg/mL [73] both of which is comparable with the work in this thesis.

To conclude;

- (i) lipid-modified PEI has higher efficiency and lower toxicity than 25PEI as well as commercial carrier Lipofectamine®RNAiMAX for GFP silencing in engineered Hut78 cells, and the best results are seen in PEI-LA –Linoleic acid modified PEI,
- (ii) the in-house carriers are not as efficient in Jurkat cell line as in Hut78 cells for GFP silencing,
- (iii) centrifugation of the cells with the complexes increases the efficiency of the treatment significantly,
- (iv) it is possible to decrease the viability of wild-type Hut78 cells using selected cytotoxic siRNA.
- (v) the amount of apoptosis is lower than the decrease in the viability, pointing toward alternative routes of effect for the selected siRNAs.

For future purposes, several possible routes can be taken to improve the siRNA delivery method. One of the possible approaches include preparation of lipid-modified PEI constructs with higher efficiency for cell membrane interactions, as it was shown that the interaction between the cell and the complexes is a limiting factor via the centrifugation experiments. Another approach involves modification of siRNA using hydrophobic moieties or moieties that would stabilize the polymer-siRNA complex such as cholesterol or lipids. This would increase the stability of the complexes due to the presence of hydrophobic groups on both sides –polymer and siRNA-, giving them more time to be taken up by the cells.

For the second part, it would be beneficial to perform siRNA library screenings to identify potent targets whose silencing would induce apoptosis specifically in these cells [99], and try dual silencing [100]. The dual silencing has the potential to have a cumulative effect of the two siRNAs [101] or cause synthetic lethality [102] as cancer

cell usually depend on more than one pathway to sustain the state of uncontrolled proliferation. For the cumulative effect, there are several studies that aim to increase the effect of a chemotherapy drug or reverse the effect of drug resistance in specific types of cancers [103]. However, there are few that aim to silence two targets, both using RNAi mechanism [101]. While the first approach is quite powerful, the second one has the potential to be more specific and less toxic if the barriers of delivery are overcome. In the context of synthetic lethality, by concept it already is quite specific to cancer cells [102], meaning the toxic effect of the drug on normal tissue is already minimized. However, by delivering two siRNAs at the same time (i.e. with a single carrier) has the potential to ensure the silencing of both targets at the same time, intensifying the effect.

6. References:

- [1] Sell S, Stem cell origin of cancer and differentiation therapy, *Critical Reviews in Oncology/Hematology*, 2004;51:1-28
- [2] Passegué E, Jamieson CHM, Ailles LE, Weissman IL, Normal and leukemic hematopoiesis: Are leukemia a stem cell disorder or a reacquisition of stem cell characteristics?, *PNAS*, 2003;100(S1):11842–11849
- [3] Rowley JD, The role of chromosomal translocations in leukemo-genesis, *Seminars in Hematology*, 1999;36:59–72
- [4] Schmidt CA, Przybylski GK., What we can learn from leukemia as for the process of lineage commitment in hematopoiesis?, *International Reviews in Immunology*, 2001;20:107–15
- [5] Küppers R, Engert A, Hansmann ML, Hodgkin lymphoma, *Journal of Clinical Investigations*, 2012;122(10):3439-47
- [6] Raab MS, Podar K, Breitkreutz I, Richardson PG, Anderson KC, Multiple myeloma, *Lancet* 2009; 374(9686): 324–339
- [7] Harris NL, Jaffe ES, Stein H, Banks PM, Chan JKC, Cleary M, A revised European-American classification of lymphoid neoplasms: a proposal from the International Lymphoma Study Group, *Blood*, 1994;84:1361–1392.
- [8] Dave JB, Nelson M, Sanger WG, Lymphoma Cytogenetics, *Clinical Laboratory of Medicine*, 2011;31:725–761
- [9] Wright DH, Pathology of Extra-nodal non Hodgkin Lymphomas, *Clinical Oncology*, 2012;24:319-328
- [10] Mao X, Lillington DM, Czepulkowski B, Russell-Jones R, Young BD, Whittaker S, Molecular cytogenetic characterization of Sézary syndrome, *Genes Chromosomes Cancer*, 2003;36(3):250-60.
- [11] Facts 2012, Leukemia and Lymphoma Society, 2012;p3-6
- [12] Wollina U, Cutaneous T cell lymphoma: update on treatment, *International Journal of Dermatology*, 2012;51(9):1019-1036
- [13] Batista DA, Vonderheid EC, Hawkins A, Morsberger L, Long P, Murphy KM, Griffin CA, Multicolor fluorescence in situ hybridization (SKY) in mycosis fungoides and Sézary syndrome: search for recurrent chromosome abnormalities, *Genes Chromosomes Cancer*, 2006;45(4):383-91.
- [14] Mao X, Lillington D, Scarisbrick JJ, Mitchell T, Czepulkowski B, Russell-Jones R, Young B, Whittaker SJ, Molecular cytogenetic analysis of cutaneous T-cell lymphomas:

- identification of common genetic alterations in Sézary syndrome and mycosis fungoides, *British Journal of Dermatology*, 2002;147(3):464-475.
- [15] Zackheim HS, Kashani-Sabet M, Amin S, Topical corticosteroids for mycosis fungoides. Experience in 79 patients, *Arch Dermatology*, 1998;134(8):949-54.
- [16] Ysebaert L, Truc G, Dalac S, Lambert D, Petrella T, Barillot I, Naudy S, Horiot JC, Maingon P, Ultimate results of radiation therapy for T1–T2 mycosis fungoides (including reirradiation), *International Journal of Radiation Oncology, Biology, Physics*, 2004;58:1128–1134.
- [17] National Cancer Institute. (2010, February 18). Mycosis Fungoides and the Sézary Syndrome Treatment (PDQ®) Health Professional Version. Bethesda, MD: National Cancer Institute.
- [18] Nihal M, Stutz N, Schmit T, Ahmad N, Wood GS, Polo-like kinase 1 (Plk1) is expressed by cutaneous T-cell lymphomas (CTCLs), and its downregulation promotes cell cycle arrest and apoptosis, *Cell Cycle*, 2011;10(8):1303-1311.
- [19] Zhang C, Hazarika P, Ni X, Weidner DA, Duvic M, Induction of apoptosis by bexarotene in cutaneous T-cell lymphoma cells: relevance to mechanism of therapeutic action, *Clinical Cancer Research*, 2002;8(5):1234-1240.
- [20] Kaltoft K, Bisballe S, Dyrberg T, Boel E, Rasmussen PB, Thestrup-Pedersen K, Establishment of two continuous T-cell strains from a single plaque of a patient with mycosis fungoides, *In Vitro Cell Dev Biol*. 1992;A(3 Pt 1):161-167.
- [21] Kaltoft K, Bisballe S, Rasmussen HF, Thestrup-Pedersen K, Thomsen K, Sterry W, A continuous T-cell line from a patient with Sézary syndrome, *Arch Dermatology Research*, 1987;279(5):293-298.
- [22] Starkebaum G, Loughran TP Jr, Waters CA, Ruscetti FW, Establishment of an IL-2 independent, human T-cell line possessing only the p70 IL-2 receptor, *International Journal of Cancer*, 1991;49(2):246-253.
- [23] Poszepczynska E, Bagot M, Echchakir H, Martinvalet D, Ramez M, Charue D, Boumsell L, Bensussan A, Functional characterization of an IL-7-dependent CD4(+)CD8alphaalpha(+) Th3-type malignant cell line derived from a patient with a cutaneous T-cell lymphoma, *Blood*, 2000;96(3):1056-1063.
- [24] Abrams JT, Lessin S, Ghosh SK, Ju W, Vonderheid EC, Nowell P, Murphy G, Elfenbein B, DeFreitas E, A clonal CD4-positive T-cell line established from the blood of a patient with Sézary syndrome, *Journal of Investigative Dermatology*, 1991;96(1):31-37.
- [25] Popovic M, Sarin PS, Robert-Gurroff M, Kalyanaraman VS, Mann D, Minowada J, Gallo

- RC, Isolation and transmission of human retrovirus (human t-cell leukemia virus), *Science*, 1983;219(4586):856-859.
- [26] Gazdar AF, Carney DN, Bunn PA, Russell EK, Jaffe ES, Schechter GP, Guccion JG, Mitogen requirements for the in vitro propagation of cutaneous T-cell lymphomas, *Blood*, 1980;55: 409-417.
- [27] Schneider U, Schwenk HU, Bornkamm G, Characterization of EBV-genome negative "null" and "T" cell lines derived from children with acute lymphoblastic leukemia and leukemic transformed non-Hodgkin lymphoma, *International Journal of Cancer*, 1977;19(5):621-626.
- [28] Stevenson M, Therapeutic Potential of RNA Interference, *New England Journal of Medicine*, 2004;351:1772-1777.
- [29] Miele E, Spinelli GP, Miele E, Di Fabrizio E, Ferretti E, Tomao S, Gulino A, Nanoparticle-based delivery of small interfering RNA: challenges for cancer therapy, *International Journal of Nanomedicine*, 2012;7:3637-3657.
- [30] Ali HM, Urbinati G, Raouane M, Massaad-Massade L, Significance and applications of nanoparticles in siRNA delivery for cancer therapy, *Expert Review of Clinical Pharmacology*, 2012;5(4):403-412
- [31] Aliabadi HM, Mahdipoor P, Uludağ H, Polymeric delivery of siRNA for dual silencing of Mcl-1 and P-glycoprotein and apoptosis induction in drug-resistant breast cancer cells, *Cancer Gene Therapy*, 2013;20(3):169-177.
- [32] Pecot CV, Calin GA, Coleman RL, Lopez-Berestein G, Sood AK, RNA interference in the clinic: challenges and future directions, *Nature Reviews Cancer*, 2011;11:59–67.
- [33] Zhao X, Pan F, Holt CM, Lewis AL, Lu JR, Controlled delivery of antisense oligonucleotides: a brief review of current strategies, *Expert Opinions in Drug Delivery*, 2009;6:673–686. 649.
- [34] Whitehead KA, Langer R, Anderson DG, Knocking down barriers: advances in siRNA delivery, *Nature Reviews Drug Discovery*, 2009;2:129–138.
- [35] Kim DH, Rossi JJ, Strategies for silencing human disease using RNA interference, *Nature Reviews Genetics*, 2007;3:173–184.
- [36] Oliveira S, van Rooy I, Kranenburg O, Storm G, Schiffelers R, Fusogenic peptides enhance endosomal escape improving siRNA- induced silencing of oncogenes, *International Journal of Pharmacology*, 2007;331:211–214.
- [37] Rozema DB, Lewis DL, siRNA delivery technologies for mammalian systems, *Targets*, 2003;2(6):253-260
- [38] Mishra S, Heidel JD, Webster P, Davis ME, Imidazole groups on a linear, cyclodextrin-

- containing polycation produce enhanced gene delivery via multiple processes, *Journal of Controlled Release*, 2006;116:179-191.
- [39] Bartlett DW, Davis ME, Physicochemical and biological characterization of targeted, nucleic acid-containing nanoparticles, *Bioconjugate Chemistry*, 2007;18:456-468.
- [40] Schmidt-Wolf GD, Schmidt-Wolf IG, Non-viral and hybrid vectors in human gene therapy: an update, *Trends in Molecular Medicine*, 2003;9(2):67-72.
- [41] Zhang S, Zhi D, Huang L, Lipid-based vectors for siRNA delivery, *Journal of Drug Targeting*, 2012;20(9):724-735.
- [42] Ozpolat B, Sood AK, Lopez-Berestein G, Nanomedicine based approaches for the delivery of siRNA in cancer, *Journal of International Medicine*, 2010;267:44–53.
- [43] Storm G, Crommelin DJA, Liposomes: quo vadis?, *PSTT*, 1998;1(1):19-31.
- [44] Nguyen J, Szoka FC, Nucleic acid delivery: the missing pieces of the puzzle?, *Accounts of Chemical Research*, 2012;45(7):1153-1162
- [45] Yoo JW, Irvine DJ, Discher DE, Mitragotri S, Bio-inspired, bioengineered and biomimetic drug delivery carriers, *Nature Reviews Drug Discovery*, 2011;10(7):521-535
- [46] Singha K, Namgung R, Kim WJ, Polymers in small-interfering RNA delivery, *Nucleic Acid Therapeutics*, 2011;21(3):133-147.
- [47] Merkel OM, Zheng M, Debus H, Kissel T, Pulmonary gene delivery using polymeric nonviral vectors, *Bioconjugate Chemistry*, 2012;18;23(1):3-20.
- [48] Hassani Z, Lemkine GF, Erbacher P, Palmier K, Alfama G, Giovannangeli C, Behr JP, Demeneix BA, Lipid-mediated siRNA delivery down-regulates exogenous gene expression in the mouse brain at picomolar levels, *Journal of Gene Medicine*, 2005;7(2):198-207.
- [49] Grayson AC, Doody AM, Putnam D, Biophysical and structural characterization of polyethylenimine-mediated siRNA delivery in vitro, *Pharmaceutical Research*, 2006;23(8):1868-1876.
- [50] Moghimi SM, Symonds P, Murray JC, Hunter AC, Debska G, Szewczyk A, A two-stage poly(ethylenimine)-mediated cytotoxicity: implications for gene transfer/therapy, *Molecular Therapy*, 2005;11(6):990-995.
- [51] Boussif O, Lezoualc'h F, Zanta MA, Mergny MD, Scherman D, Demeneix B, Behr JP, A versatile vector for gene and oligonucleotide transfer into cells in culture and in vivo: polyethylenimine, *PNAS*, 1995;92(16):7297-7301.
- [52] Neamark A, Suwanton O, Bahadur RK, Hsu CY, Supaphol P, Uludağ H, Aliphatic lipid substitution on 2 kDa polyethylenimine improves plasmid delivery and transgene expression, *Molecular Pharmacology*, 2009;6(6):1798-815.

- [53] Bahadur KC, Landry B, Aliabadi HM, Lavasanifar A, Uludağ H, Lipid substitution on low molecular weight (0.6-2.0 kDa) polyethylenimine leads to a higher zeta potential of plasmid DNA and enhances transgene expression, *Acta Biomaterialia*, 2011;7(5):2209-2217.
- [54] Stepanenko OV, Verkhusha VV, Kuznetsova IM, Uversky VN, Turoverov KK, Fluorescent proteins as biomarkers and biosensors: throwing color lights on molecular and cellular processes, *Current Protein and Peptide Science*, 2008;9(4):338-369.
- [55] Zhang Y, Hatse S, De Clercq E, Schols D., CXC-chemokine receptor 4 is not a coreceptor for human herpesvirus 7 entry into CD4(+) T cells, *Journal of Virology*, 2000;74(4):2011-2016.
- [56] Gootenberg JE, Ruscetti FW, Mier JW, Gazdar A, Gallo A.C., Human cutaneous T cell lymphoma and leukemia cell lines produce and respond to T cell growth factor, *Journal of Experimental Medicine*, 1981;154: 1403-1418.
- [57] Maeda Y, Yusa K, Nakano Y, Harada S., Involvement of inhibitory factors in the inefficient entry of HIV-1 into the human CD4 positive HUT78 cell line, *Virus Research*, 2011;155(1):368-371.
- [58] Mirandola L, Chiriva-Internati M, Montagna D, Locatelli F, Zecca M, Ranzani M, Basile A, Locati M, Cobos E, Kast WM, Asselta R, Paraboschi EM, Comi P, Chiaramonte R., Notch1 regulates chemotaxis and proliferation by controlling the CC-chemokine receptors 5 and 9 in T cell acute lymphoblastic leukaemia, *Journal of Pathology*, 2012;226(5):713-22.
- [59] Samstag Y, Nebl G, Ras initiates phosphatidylinositol-3-kinase (PI3K)/PKB mediated signalling pathways in untransformed human peripheral blood T lymphocytes, *Advanced Enzyme Regulation*, 2005;45:52-62.
- [60] Basiouni S, Fuhrmann H, Schumann J, High-efficiency transfection of suspension cell lines, *Biotechniques*, 2012;0(0):1-4
- [61] Sun C, Tang T, Uludag H, A Molecular Dynamics Simulation Study on the effect of Lipid Substitution on Polyethylenimine Mediated siRNA Complexation, *Biomaterials*, 2013;34(11):2822-2833
- [62] Malo N, Hanley JJ, Cerquozzi S, Pelletier J, Nadon R, Statistical practice in high-throughput screening data analysis, *Nature Biotechnology*, 2006;24(2):167-175
- [63] Zimmerman DW, A Note on Interpretation of the Paired-Samples t Test. *Journal of Educational and Behavioral Statistics*, 1997;22(3):349–360.
- [64] Marra E, Palombo F, Ciliberto G, Aurisicchio L, Kinesin spindle protein SiRNA slows tumor progression, *Journal of Cell Physiology*, 2013;228(1):58-64.
- [65] Hsu CY, Uludağ H, A simple and rapid nonviral approach to efficiently transfect primary

- tissue-derived cells using polyethylenimine, *Nature Protocols*, 2012;19;7(5):935-45.
- [66] Valladares A, Hernández NG, Gómez FS, Curiel-Quezada E, Madrigal-Bujaidar E, Vergara MD, Martínez MS, Arenas Aranda DJ, Genetic expression profiles and chromosomal alterations in sporadic breast cancer in Mexican women, *Cancer Genetics and Cytogenetics*, 2006;170(2):147-51.
- [67] Garcia-Rodriguez S, Callejas-Rubio JL, Ortego-Centeno N, Zumaquero E, Rios-Fernandez R, Arias-Santiago S, Navarro P, Sancho J, Zubiaur M., Altered AKT1 and MAPK1 gene expression on peripheral blood mononuclear cells and correlation with T-helper-transcription factors in systemic lupus erythematosus patients, *Mediators of Inflammation*, 2012;2012:495934.
- [68] Bressanin D, Evangelisti C, Ricci F, Tabellini G, Chiarini F, Tazzari PL, Melchionda F, Buontempo F, Pagliaro P, Pession A, McCubrey JA, Martelli AM, Harnessing the PI3K/Akt/mTOR pathway in T-cell acute lymphoblastic leukemia: Eliminating activity by targeting at different levels, *Oncotarget* 2012; 3: 811-823
- [69] Grabarczyk P, Przybylski GK, Depke M, Völker U, Bahr J, Assmus K, Bröker BM, Walther R, Schmidt CA., Inhibition of BCL11B expression leads to apoptosis of malignant but not normal mature T cells, *Oncogene*, 2007; 26(26):3797-810
- [70] Verma NK, Davies AM, Long A, Kelleher D, Volkov Y., STAT3 knockdown by siRNA induces apoptosis in human cutaneous T-cell lymphoma line Hut78 via downregulation of Bcl-xL, *Cell Molecular Biology Letters*, 2010;15(2):342-55
- [71] Landry B, Aliabadi HM, Samuel A, Gul-Uludag H, Jiang X, Kutsch O, Uludag H, Effective Non-Viral Delivery of siRNA to Acute Myeloid Leukemia Cells with Lipid-Substituted Polyethylenimines, *PLoSone*, 2012;7(8);e44197
- [72] Congmin G, Mu Z, Yihui M, Hanliang L, Survivin--an attractive target for RNAi in non-Hodgkin's lymphoma, Daudi cell line as a model, *Leukemia & Lymphoma*, 2006;47(9):1941-1948.
- [73] Mei YP, Zhu XF, Zhou JM, Huang H, Deng R, Zeng YX, siRNA targeting LMP1-induced apoptosis in EBV-positive lymphoma cells is associated with inhibition of telomerase activity and expression, *Cancer Letters*, 2006;232(2):189-198.
- [74] Glienke W, Maute L, Koehl U, Esser R, Milz E, Bergmann L, Effective treatment of leukemic cell lines with wt1 siRNA, *Leukemia*, 2007;21(10):2164-2170.
- [75] Zhao Y, Mannhalter B, Hong H, Welsh JS, Mechanical properties of epoxy nanocomposites reinforced with very low content of amino-functionalized single-walled carbon nanotubes, *Journal of Nanoscience and Nanotechnology*, 2010;10(9):5776-5782.

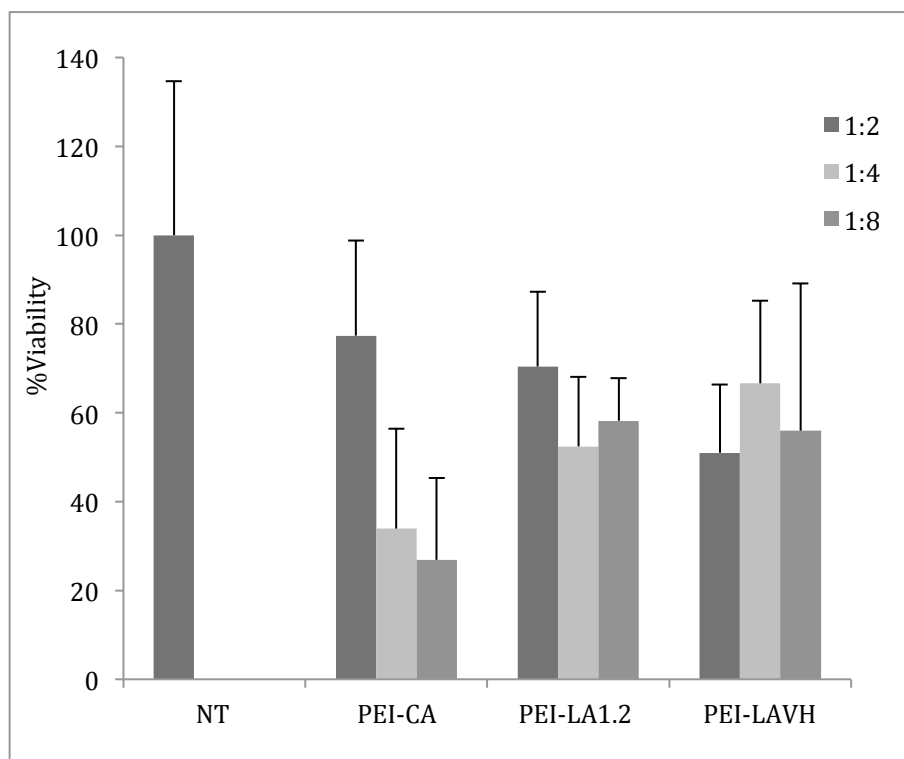
- [76] Ma LD, Zhou M, Wen SH, Ni C, Jiang LJ, Fan J, Xia L, Effects of STAT3 silencing on fate of chronic myelogenous leukemia K562 cells, *Leukemia & Lymphoma*, 2010;51(7):1326-1336.
- [77] Choudhury A, Derkow K, Daneshmanesh AH, Mikaelsson E, Kiaii S, Kokhaei P, Osterborg A, Mellstedt H, Silencing of ROR1 and FMOD with siRNA results in apoptosis of CLL cells, *British Journal of Haematology*, 2010;151(4):327-335.
- [78] Wang CM, Sheng GY, Lu J, Xie L, Bai ST, Xu XJ, Liu YF, Effect of small interfering RNA targeting wild-type FLT3 in acute myeloid leukaemia cells in vitro and in vivo, *Journal of International Medicine Research*, 2011;39(5):1661-1674.
- [79] Zhao N, Bagaria HG, Wong MS, Zu Y, A nanocomplex that is both tumor cell-selective and cancer gene-specific for anaplastic large cell lymphoma, *Journal of Nanobiotechnology*, 2011;9:2.
- [80] Naoghare PK, Tak YK, Kim MJ, Han E, Song JM, Knock-down of argonaute 2 (AGO2) induces apoptosis in myeloid leukaemia cells and inhibits siRNA-mediated silencing of transfected oncogenes in HEK-293 cells, *Basic Clinical Pharmacology and Toxicology*, 2011;109(4):274-282.
- [81] Xiang J, Ouyang Y, Cui Y, Lin F, Ren J, Long M, Chen X, Wei J, Zhang H, Silencing of Notch3 Using shRNA driven by survivin promoter inhibits growth and promotes apoptosis of human T-cell acute lymphoblastic leukemia cells, *Clinical Lymphoma, Myeloma & Leukemia*, 2012;12(1):59-65.
- [82] Kardava L, Yang Q, St Leger A, Foon KA, Lentzsch S, Vallejo AN, Milcarek C, Borghesi L, The B lineage transcription factor E2A regulates apoptosis in chronic lymphocytic leukemia (CLL) cells, *International Immunology*, 2011;23(6):375-384.
- [83] Buglio D, Palakurthi S, Byth K, Vega F, Toader D, Saeh J, Neelapu SS, Younes A, Essential role of TAK1 in regulating mantle cell lymphoma survival, *Blood*, 2012;120(2):347-355.
- [84] Chen J, Li J, Han Q, Sun Z, Wang J, Wang S, Zhao RC, Enhancer of zeste homolog 2 is overexpressed and contributes to epigenetic inactivation of p21 and phosphatase and tensin homolog in B-cell acute lymphoblastic leukemia, *Experimental Biology and Medicine*, 2012;237(9):1110-1116.
- [85] Kang SH, Jeong SJ, Kim SH, Kim JH, Jung JH, Koh W, Kim JH, Kim DK, Chen CY, Kim SH, Icariside II induces apoptosis in U937 acute myeloid leukemia cells: role of inactivation of STAT3-related signaling, *PLoS One*, 2012;7(4):e28706.
- [86] Kaymaz BT, Selvi N, Gündüz C, Aktan C, Dalmızrak A, Saydam G, Kosova B, Repression of STAT3, STAT5A, and STAT5B expressions in chronic myelogenous leukemia cell line K-

- 562 with unmodified or chemically modified siRNAs and induction of apoptosis, *Annual Hematology*, 2013;92(2):151-162.
- [87] Brien G, Trescol-Biemont MC, Bonnefoy-Bérard N, Downregulation of Bfl-1 protein expression sensitizes malignant B cells to apoptosis, *Oncogene*, 2007;26(39):5828-5832.
- [88] Zhu N, Gu L, Li F, Zhou M, Inhibition of the Akt/survivin pathway synergizes the antileukemia effect of nutlin-3 in acute lymphoblastic leukemia cells, *Molecular Cancer Therapy*, 2008;7(5):1101-1109.
- [89] Fenouille N, Puissant A, Dufies M, Robert G, Jacquel A, Ohanna M, Deckert M, Pasquet JM, Mahon FX, Cassuto JP, Raynaud S, Tartare-Deckert S, Auberger P, Persistent activation of the Fyn/ERK kinase signaling axis mediates imatinib resistance in chronic myelogenous leukemia cells through upregulation of intracellular SPARC, *Cancer Research*, 2010;70(23):9659-9670.
- [90] Cheong JW, Jung HI, Eom JI, Kim SJ, Jeung HK, Min YH, Aurora-A kinase inhibition enhances the cytosine arabinoside-induced cell death in leukemia cells through apoptosis and mitotic catastrophe, *Cancer Letters*, 2010;297(2):171-181.
- [91] Koldehoff M, Kordelas L, Beelen DW, Elmaagacli AH, Small interfering RNA against BCR-ABL transcripts sensitize mutated T315I cells to nilotinib, *Haematologica*, 2010;95(3):388-397.
- [92] Touzeau C, Dousset C, Bodet L, Gomez-Bougie P, Bonnaud S, Moreau A, Moreau P, Pellat-Deceunynck C, Amiot M, Le Gouill S, ABT-737 induces apoptosis in mantle cell lymphoma cells with a Bcl-2high/Mcl-1low profile and synergizes with other antineoplastic agents, *Clinical Cancer Research*, 2011;17(18):5973-5981.
- [93] Tyner JW, Jemal AM, Thayer M, Druker BJ, Chang BH, Targeting survivin and p53 in pediatric acute lymphoblastic leukemia, *Leukemia*, 2012;26(4):623-632.
- [94] Hou Y, Wang HQ, Ba Y, Effects of CDC7 gene silencing and Rituximab on apoptosis in diffuse large B cell lymphoma cells, *Journal of Cancer Research and Clinical Oncology*. 2012;138(12):2027-2034.
- [95] Ottosson-Wadlund A, Ceder R, Preta G, Pokrovskaja K, Grafström RC, Heyman M, Söderhäll S, Grandér D, Hedenfalk I, Robertson JD, Fadeel B, Requirement of apoptotic protease-activating factor-1 for bortezomib-induced apoptosis but not for Fas-mediated apoptosis in human leukemic cells, *Molecular Pharmacology*, 2013;83(1):245-255.
- [96] Okkenhaug K, Vanhaesebroeck B, PI3K in lymphocyte development, differentiation and activation, *Nature Reviews Immunology*, 2003;3(4):317-330.

- [97] Subramaniam PS, Whye DW, Efimenko E, Chen J, Tosello V, De Keersmaecker K, Kashishian A, Thompson MA, Castillo M, Cordon-Cardo C, Davé UP, Ferrando A, Lannutti BJ, Diacovo TG, Targeting nonclassical oncogenes for therapy in T-ALL, *Cancer Cell*, 2012;21(4):459-472.
- [98] Khan S, Kaur R, Shah BA, Malik F, Kumar A, Bhushan S, Jain SK, Taneja SC, Singh J, A novel cyano derivative of 11-keto- β -boswellic acid causes apoptotic death by disrupting PI3K/AKT/Hsp-90 cascade, mitochondrial integrity, and other cell survival signaling events in HL-60 cells, *Molecular Carcinogenesis*, 2012;51(9):679-695.
- [99] Krueger U, Bergauer T, Kaufmann B, Wolter I, Pilk S, Heider-Fabian M, Kirch S, Artz-Oppitz C, Isselhorst M, Konrad J, Insights into effective RNAi gained from large-scale siRNA validation screening, *Oligonucleotides*, 2007;17(2):237-250.
- [100] Kaelin WG Jr, The concept of synthetic lethality in the context of anticancer therapy, *Nature Reviews Cancer*, 2005;5(9):689-698.
- [101] Aliabadi HM, Mahdipoor P, Uludağ H, Polymeric delivery of siRNA for dual silencing of Mcl-1 and P-glycoprotein and apoptosis induction in drug-resistant breast cancer cells, *Cancer Gene Therapy*, 2013;20(3):169-177.
- [102] Dai B, Fang B, Roth JA, RNAi-induced synthetic lethality in cancer therapy, *Cancer Biology & Therapy*, 2009;8(23):2314-2316.
- [103] Chen S, Liu X, Gong W, Yang H, Luo D, Zuo X, Li W, Wu P, Liu L, Xu Q, Ji, Combination therapy with VEGFR2 and EGFR siRNA enhances the antitumor effect of cisplatin in non-small cell lung cancer xenografts, *Oncology Rep*, 2013;29(1):260-268.

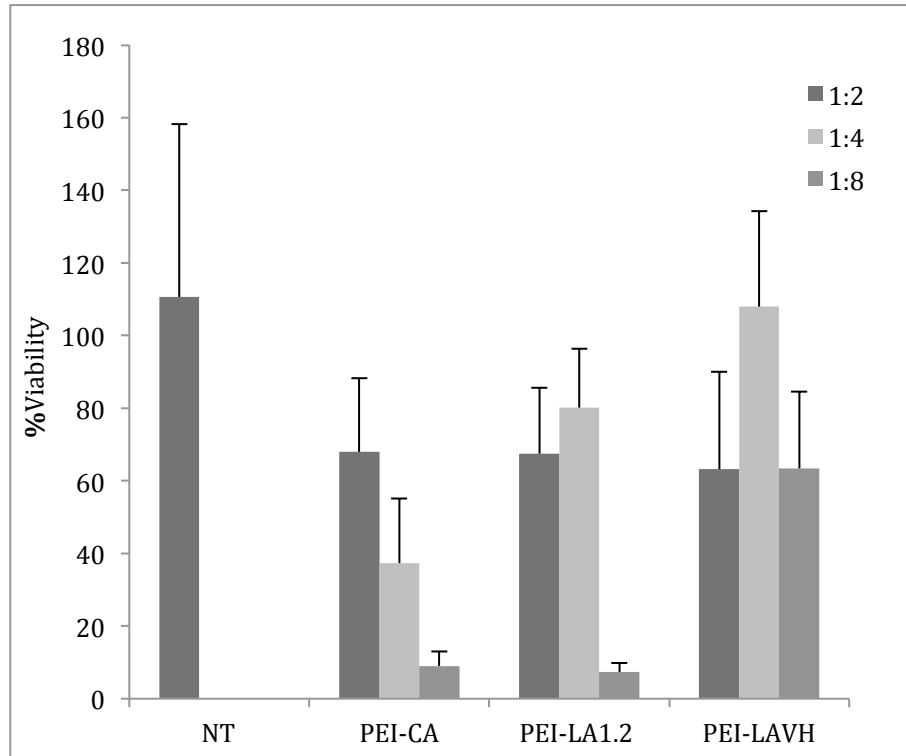
Appendix 1 FACS counts for Effect of complex formation volume

Below are the flow cytometry counts for the **section 4.7**.



Appendix 2 FACS counts for Effect of continuous shaking

Below are the flow cytometry counts for the **section 4.8**.



Appendix 3 Table of hits relative to the statistical test performed for screening select targets for silencing – AlamarBlue® Assay

Below is the table for the hits relative to the statistical tests performed on cell viabilities based on AlamarBlue® assay in **section 4.12.1**. M=POC (Percent of control), t= student's t-test (two sample), z= z-score, T= one sample t test. Hits are noted with an **X**.

PEI-LA												
Gene	25 nM				50 nM				100 nM			
	M	T	z	t	M	T	z	t	M	T	z	t
KSP												
STAT3 1												
STAT3 2									X			
STAT3 7					X			X				
STAT3 8												
CDK18									X			
Bcl11b									X			
MAP									X	X		X
RPS									X			
PIK									X			X
STK									X			
PEI-CA												
KSP												
STAT3 1												
STAT3 2	X											
STAT3 7												
STAT3 8	X	X										
CDK18	X			X								X
Bcl11b	X	X		X	X							
MAP	X			X								
RPS	X			X								X
PIK	X	X		X				X				X
STK	X			X								
Lipofectamine® RNAiMAX												
KSP		X		X								
STAT3 1												
STAT3 2												
STAT3 7												
STAT3 8		X	X									
CDK18				X								
Bcl11b												
MAP												
RPS												
PIK			X	X								
STK												

Appendix 4 Table of hits relative to the statistical test performed for screening select targets for silencing – Trypan Blue Assay

Below is the table for the hits relative to the statistical tests performed on cell viabilities based on Trypan Blue assay in **section 4.12.2**. M=mean test, t= student's t-test (two sample), z= z-score, T= one sample t test. Hits are noted with an **X**.

PEI-LA												
Gene	25 nM				50 nM				100 nM			
	M	T	z	t	M	T	z	t	M	T	z	t
KSP			X	X								
STAT3					X							
CDK18					X			X	X		X	X
Bcl11b		X		X								X
MAP					X		X	X				
RPS												
PIK				X					X			
STK					X				X			X